# A Proteomic Approach to Identification of Prodrug-Activating Serine Hydrolases: Activation of Valacyclovir

by

Vikram Shenoy

A dissertation submitted in partial fulfillment
of the requirements for the degree of
Doctor of Philosophy
(Medicinal Chemistry)
in The University of Michigan
2020

Doctoral Committee:

Professor Gordon L. Amidon, Co-Chair
Professor George A. Garcia, Co-Chair
Professor Gregory E. Amidon
Assistant Professor Brent R. Martin
Associate Professor Andrew D. White

Vikram Shenoy

vpshenoy@umich.edu

ORCID iD: 0000-0001-7792-4912

## DEDICATION

To my wife, Shivali, for always giving me purpose
To my parents, Kumuda and Varadaraj, for being my guiding light
To my friends and family, for keeping me grounded

## ACKNOWLEDGEMENTS

This work would not have been possible without the support of many people in my life. Thanks to my wife, Shivali, who has been with me every step of this journey and kept me sane and happy, showering me with love and support even from three time zones away. Of course, to my parents, Kumuda and Varadaraj, I cannot begin to express how grateful I am for their love, support, and advice. They got me to where I am today, and hearing about their scientific graduate studies as a young child inspired me to take on this challenge in my life. Thanks to my brother and sister for always being there for me and making me feel like family was always close by. Thanks to my other parents, Shilpi and Sandeep, for their love and support and giving me another home. To my other family members who have been part of my tribe, thank you.

To my advisor, Gordon, under whom it has been a consummate pleasure to work, it was a blessing to have stumbled into his lab over four years ago, and the connection with him, the colleagues, and the project were felt immediately. I am grateful for his guidance and mentorship and his steady hand and big-picture outlook that counterbalanced my own tendencies. Heartfelt thanks to Gail, who helped with so many logistical and procurement hurdles and made sure things were running smoothly behind the scenes every single day. I would be remiss not to thank my top-notch collaborators, Dr. Jian Shi and Brian Thompson, both of whom helped me achieve my goals and did so not simply out of obligation but with

a whole-hearted interest in solving the same scientific problems as I. Their helpful discussions and invaluable technical skills bolstered the impact of my work, and their friendship never failed to brighten my days of toil. I must also thank their advisors, Drs. Hao-Jie Zhu and David Smith, who provided material and financial support and helpful advice and also trusted me enough to take up some of their students' time and energy.

Thanks to my former colleagues: Dr. Yasuhiro Tsume, for teaching me many skills that I used throughout my project and sharing many jokes that I probably cannot use anywhere else in life; Dr. Longsheng Lai, for helping me with learning the background of my project and providing privileged insight on experimental work, writing, and presentations; Dr. Hao Xu, for helping me get set up in lab and start my initial chemistry and biology experiments and otherwise sharing useful knowledge gained from his own doctoral experience; Dr. Yongjun Hu, for sharing vital equipment and materials with me and performing valuable technical work for me in the process while making it look so easy; and Drs. Patrick Sinko, Marival Bermejo, and Bart Hens, for your friendship, camaraderie, and encouragement throughout the years.

I need to also thank my committee, Drs. George Garcia, Andy White, and Brent Martin, for their critical suggestions, their technical expertise, their constructive feedback and, most importantly, for letting me pass all my examinations to date. To those handling administrative, operational, safety, and IT matters, Sarah Lloyd, Antoinette Hopper, Pat Greeley, L.D. Hieber, Drs. Rod Sorenson, Nicole Crandall, and the IT and custodial staff, I am extremely grateful.

I also would like to gratefully acknowledge my funding sources, namely the National Institutes of Health, Grant #1R01GM115481-01, Rackham Graduate School, and the Lyons Fellowship from the College of Pharmacy.

To anyone who provided any help during this time of my life or otherwise, large or small, thank you. I am lucky to have had every person I've listed here on my team and they should all take some of the credit for the most important achievement of my life so far. In PhDs more so than anywhere else, it really does take a village.

## TABLE OF CONTENTS

## LIST OF FIGURES

FIGURE

## LIST OF TABLES

TABLE

## LIST OF SCHEMES

SCHEME

## LIST OF ABBREVIATIONS

ABP – activity-based probe

ABPP – activity-based protein profiling

ACV – acyclovir

AEBSF – 4-(2-aminoethyl)benzenesulfonyl fluoride

AMB – 4-(aminomethyl)benzyl alcohol

AMB-FP – 4-(aminomethyl)benzyl-fluorophosphonate probe

BPHL – biphenyl hydrolase-like protein

cABPP – competitive activity-based protein profiling

CES – carboxylesterase

Da - dalton

DCM – dichloromethane

DIEA – *N*,*N*-diisopropylethylamine

DMEM – Dulbecco's Minimum Essential Medium

DMSO – dimethyl sulfoxide

FDA – U.S. Food and Drug Administration

FP – fluorophosphonate probe

GI – gastrointestinal

HPLC – high-performance liquid chromatography

HRMS – high-resolution mass spectrometry

kDa - kilodalton

KO – knockout (*Bphl*-knockout)

LC-MS/MS – liquid chromatography-tandem mass spectrometry

MS – mass spectrometry

NMR – nuclear magnetic resonance

PAE – prodrug-activating enzyme

PEG – polyethylene glycol

PK – pharmacokinetics

PPCE – prolyl oligopeptidase

PPME1 – protein phosphatase methylesterase 1

RBBP9 – retinoblastoma binding protein 9

SDS-PAGE – sodium dodecyl sulfate-polyacrylamide gel electrophoresis

SH – serine hydrolase

SILAC – stable isotope labeling of amino acids in cell culture

TCEP – tris(2-carboxethyl)phosphine

TFA – trifluoroacetic acid

THF – tetrahydrofuran

TLC – thin-layer chromatography

UV - ultraviolet

VACV – valacyclovir

WT – wildtype

## ABSTRACT

Prodrug discovery and development in the pharmaceutical industry have been hampered by a lack of knowledge on activation pathways. Such knowledge would de-risk prodrug campaigns by enabling proper selection of preclinical animal models, prediction of pharmacogenomic variability, and identification of drug-drug interactions. Technologies for annotation of activating enzymes have not kept pace with the growing need for it. Activity-based protein profiling (ABPP) has matured considerably in recent decades, leading to widespread use in drug discovery. Here, we report the extension of competitive ABPP to prodrug-activating enzyme (PAE) identification in SILAC cell lysates using a modified fluorophosphonate (FP) probe and MS-based identification. This was followed by characterization of the new PAE *in vitro*, as well as in mouse tissue lysates and by single-pass intestinal perfusions (SPIP).

Focusing on the ester prodrug valacyclovir (VACV), we modified the FP probe using an aminomethylbenzyl phosphonate ester structurally based on the serine protease inhibitor 4-(2-aminoethyl)benzenesulfonyl fluoride, which extinguishes VACV activation in Caco-2 cells, our proteome of interest, and inhibits BPHL, the only confirmed VACV PAE to date. The novel probe, AMB-FP, identified serine hydrolase RBBP9 as another activating enzyme in Caco-2 cells, which was validated via the selective inhibitor emetine. Selective concentrations of

emetine abolished VACV activation in Caco-2 lysates, suggesting that RBBP9, not BPHL, is the major presystemic VACV-activating enzyme.

Kinetic characterization of RBBP9 revealed a single-binding stoichiometry and a catalytic efficiency comparable to that of BPHL ($k_{cat}{\cdot}K_M^{-1}$ = 104 $mM^{-1}{\cdot}s^{-1}$). Emetine inhibition data from VACV hydrolysis assays in jejunum and liver soluble lysates of wildtype (WT) and *Bphl*-knockout (KO) mice revealed that RBBP9 and BPHL are co-equal mediators of VACV activation in the liver, but that RBBP9 is the predominant PAE in the jejunum. Furthermore, the data indicated that these two enzymes are likely the only major enzymes involved in VACV activation in these tissues. Finally, SPIP data from WT mice with and without emetine pre-perfusion confirmed the RBBP9-dependence of VACV presystemic activation as portal vein samples showed >50% increase in unactivated VACV in emetine-treated mice. Importantly, this was the first evidence of RBBP9 VACV activation in a more physiologically relevant system than lysates. Based on these results, we envision that others might use the cABPP approach in the future for global, rapid, and efficient discovery of prodrug-activating enzymes in situations where traditional solutions are inadequate or prohibitively inefficient.

# CHAPTER I

# Introduction

## The Prodrug Strategy

Today's lead compounds that emerge from medicinal chemistry and drug discovery efforts are often not optimizable for pharmacokinetic and pharmacodynamic performance, leading to deficiencies in one or more of these attributes as a result of this tradeoff. Many of the resulting new chemical entities (NCEs) with these deficiencies are halted during preclinical trials, but some survive to become investigational new drugs (INDs) and enter costly human clinical trials with a high risk of failure. Clinical-stage failures can translate to massive financial losses, leading to the consideration of salvage strategies at this point.

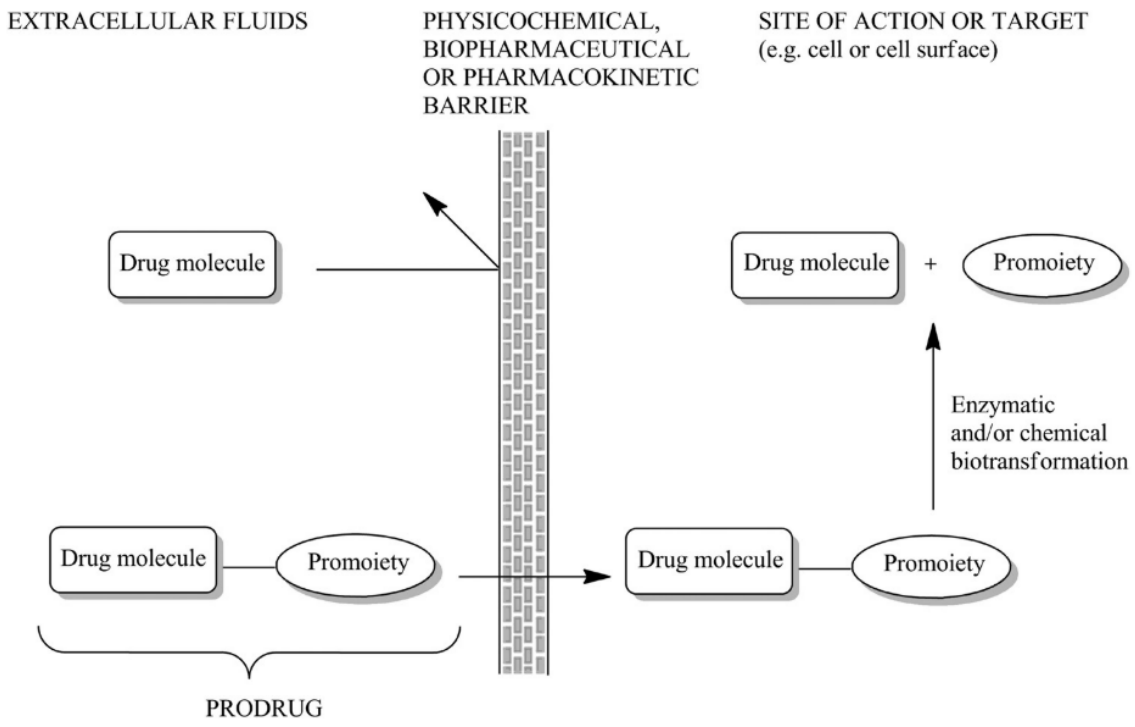


Figure 1.1. Schematic illustration of the prodrug strategy.[1]

Reproduced with permission from ref. 1.

Formulation approaches are typically attempted first but are best suited for issues of gastrointestinal stability or discomfort,[2] poor solubility,[3] poor organoleptic properties,[4] or excessive absorption rate.[5] When reformulation fails or is deemed inadvisable, a common alternative is a chemical approach known as the prodrug strategy, in which the IND is derivatized to an inactive form ("prodrug") devoid of the limiting deficiencies seen in the original ("parent") drug. At the appropriate time following administration, the prodrug reverts chemically and/or enzymatically to the parent drug (Figure 1.1). Though the reliance on prodrugs as a late-stage salvage strategy is still the norm, early-stage implementation is being recognized as a prudent way to avoid repeating expensive *in vivo* studies already carried out with the parent drug, with *de novo* prodrug development efforts becoming increasingly

feasible and cost-effective as a result of post-genomic era advances in technology and knowledge.[6]

From a U.S. regulatory perspective, prodrugs can be brought to market faster and at less cost since their New Drug Applications (NDAs) are fileable under section 505(b)(2) of the Federal Food, Drug, and Cosmetic Act, wherein the application "contains full reports of safety and effectiveness but where at least some of the information required for approval comes from studies not conducted by or for the applicant and for which the applicant has not obtained a right of reference."[7] Essentially, this permits the filing of prodrugs using some or all of the data provided in the filing of the active drug even if the applicant does not have the right to reference that data, thereby shortening the path to approval. Filed this way, prodrugs extend the patent exclusivity period of a previously approved drug by five years if the prodrug is not an ester, salt, or hydrate of an existing NCE, or otherwise by three years if one or more non-bioavailability/bioequivalence studies were required for approval and completed by the applicant. In some cases, this patent life extension can single-handedly justify the development of a prodrug.

The prodrug strategy has yielded blockbuster drugs spanning numerous drug classes, including antivirals (e.g. valacyclovir), antihyperlipidemics (e.g. simvastatin), and antihypertensives (e.g. enalapril), with 15% of the top selling drugs on the market in 2009 categorized as prodrugs.[8] Recent estimates place the prevalence of prodrugs worldwide at 10–14% of all approved drugs,[9] illustrating their importance in drug development today.

## Enzymatic Activation Pathways

A prodrug must be activated, i.e. reverted to the parent drug, *in vivo* prior to exerting its pharmacological effect(s). Thus, the site and rate of activation for a given prodrug can be strongly predictive of its clinical success. Recognizing the importance of prodrug activation, a 2009 publication by Dr. Kuei-Meng Wu at the U.S. Food and Drug Administration's Center for Drug Evaluation and Research (CDER) proposed a prodrug classification system with two main categories based on the site of activation: intracellularly and extracellularly activated agents are respectively designated Type I and Type II, each with further subdivisions (IA/IB and IIA/IIB/IIC) based on the specific tissue(s) or compartment(s) of activation.[10] While these classifications are only a framework, they emphasize the importance of considering activation to aid regulatory review and risk assessment of prodrugs.

In order to realize its full utility, a prodrug should only be activated once it has cleared all impediments to the parent drug's performance, as a parent drug liberated too soon or too rapidly from its prodrug may not be able to reach the site of action in sufficient quantity. Conversely, a parent drug that is liberated too late or too slowly may result in clearance of the prodrug before the drug can reach therapeutic levels at the site of action. Though a small percentage of prodrugs are thought to be activated chemically, i.e. spontaneously, most prodrugs rely on enzymatic catalysis for activation. Hence, identifying prodrug-activating enzymes (PAEs) is vital for the same reasons identifying drug-metabolizing enzymes is: it enables the discovery and prediction of (1) prodrug interactions with other drugs,[11] excipients,[12] foods, and disease states that can adversely impact prodrug efficacy

and safety; (2) interspecies differences in enzyme specificity, kinetics, and tissue distribution of PAEs that can better inform the selection of preclinical animal models; (3) pharmacogenomic variants that can predispose individuals to low efficacy or high toxicity when taking an average dose of a prodrug; and (4) new targeted prodrugs, structurally designed to be activated by a specific enzyme or set of enzymes.

## New Chemoproteomic Methods for Identification of PAEs

Exploratory studies for PAE identification *in vitro* are identical to those used in reaction phenotyping, the identification of drug-metabolizing enzymes (DMEs) and the quantitation of their relative contributions to the metabolized fraction, $f_m$, of a drug.[13,14] This involves the incubation of the prodrug with enzymes and inhibitors of interest, whose selection will depend on qualitative data or intuition about the expected routes and sites of biotransformation. Total hepatic lysate, produced by homogenization then sedimentation of cell debris at 9,000 *g* to yield the "S9" fraction, and/or microsomes and plasma are tested for most prodrugs, with intestinal S9 and/or microsomes also investigated in the case of oral prodrugs specifically. Pre-incubation with cofactors like nicotinamide adenine dinucleotide (NADH) or divalent metal cations/chelators and nonselective mechanism-based inhibitors (MBIs) like bis(4-nitrophenyl)phosphate (BNPP) or 1-aminobenzotriazole (ABT) helps to broadly identify classes of enzymes involved in the activation process. Once a class of PAE is identified, well-characterized specific inhibitors or antibodies and recombinantly overexpressed enzymes are used to confirm the identity of individual PAEs as needed. The main drawbacks of the preceding

methods are that the PAE must be characterized enough to be a candidate DME and must either be compatible with heterologous expression systems or have commercially available selective inhibitors or antibodies. If these conditions are not met, a more laborious approach is utilized: activity-guided fractionation. Here, the PAEs are purified from lysate by several rounds of fractionation, using prodrug activation assays as a readout and fold purification and in-gel visualization as an endpoint. After the active fractions are sufficiently purified, PAEs are unambiguously identified by N-terminal sequencing or, more recently, bottom-up mass spectrometry.[15] While this approach is well-established and tested, each round of purification and the ensuing assays is time-consuming, leaving much room for improvement.

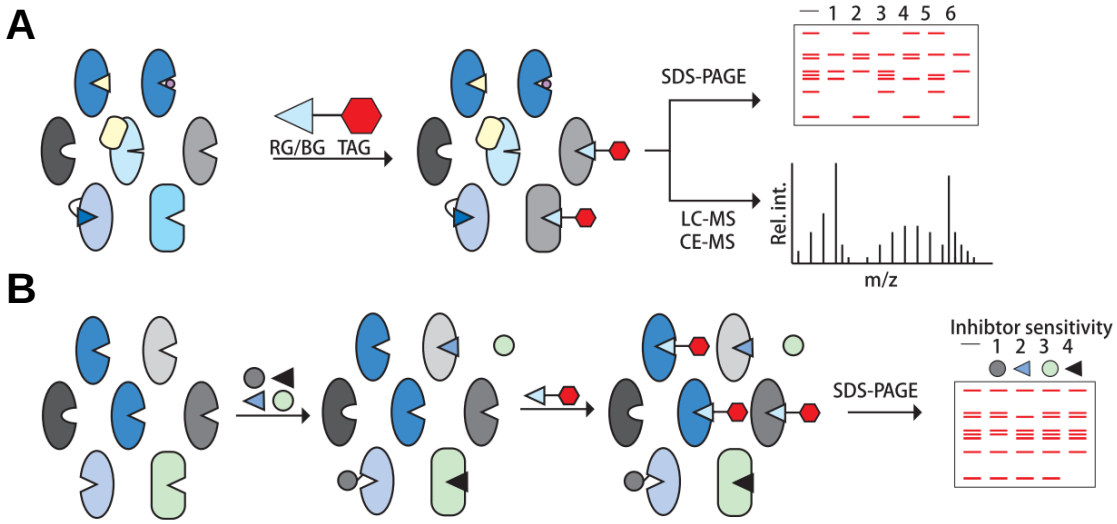


Figure 1.2. Schematic diagram of the central conceit and workflow of ABPP.[16]

(A) General ABPP scheme with both gel- and MS-based readout. Probes label enzyme subsets in complex proteomes, enabling visualization or purification and identification. RG, reactive group; BG, binding group; TAG, reporter group (e.g. rhodamine or biotin). (B) Competitive ABPP scheme with gel-based readout, illustrating inhibitor selectivity profiling. Reproduced with permission from ref. 16.

Since the turn of the century, a new streamlined approach for profiling protein activity in complex proteomes termed activity-based protein profiling (ABPP) has been pioneered and popularized by Dr. Benjamin Cravatt and colleagues.[17–19] The fundamental feature of ABPP is the chemical probes, bearing an MBI for active-site interrogation at one end and a reporter functionality, e.g. a fluorophore or affinity tag, at the other end for downstream enrichment and detection in gel or by mass spectrometry (MS). The MBI moiety covalently binds a nucleophilic catalytic residue, in effect, labeling the enzyme in proportion to its activity. Anything that affects a labeled enzyme's activity, and therefore its signal intensity, can be detected, such as active site occupants, e.g. substrates and competitive inhibitors, making this technique extremely promising for PAE identification and drug discovery (Figure 1.2).[20–22] Theoretically, one probe-prodrug competitive ABPP (cABPP) experiment with MS-based proteomic identification can identify all relevant PAEs for a prodrug in an enzyme preparation if they are all susceptible to the MBI. It follows that probes with wide reactivity profiles are ideal for this application as they can assay the active site occupancy of several enzymes in parallel, increasing throughput. Previously, our lab demonstrated proof of concept by confirming activation of ester prodrug oseltamivir by carboxylesterase 1 (CES1) in competitive labeling experiments with the pan-serine hydrolase MBI fluorophosphonate-polyethylene glycol-biotin (FP-PEG-biotin, Scheme 2.2).[23]

## The Need for Study of Ester PAEs

One of the primary factors contributing to prodrug activation kinetics is the type of chemical reaction required for activation. By far, the most common type is hydrolysis, with carboxylic acid esters encountered most. This functional group offers synthetic simplicity and strikes a fine balance between chemical stability and enzymatic susceptibility. Additionally, numerous drugs contain phenoxyl, carboxyl, and hydroxyl groups, making ester prodrugs highly accessible. The versatility of ester prodrugs is reflected in the structural diversity of promoieties that can be utilized, often increasing bioavailability via solubility and/or permeability depending on their physicochemical and stereoelectronic properties. For more than half a century, ester xenobiotics have been known to be metabolized by efficient and often broad-spectrum hydrolases enriched in the epithelia of drug-metabolizing organs as well as the bloodstream.[24] This made esters a very safe choice for prodrug derivatization, especially before the proliferation of genomic and structural data made target-based design possible. The effective guarantee of first-pass ester hydrolysis is a primary reason for the prevalence of esters in the prodrug space, especially for oral administration.

Despite the ubiquity of esters in prodrugs and drugs, mammalian and human esterases involved in xenobiotic metabolism remain poorly characterized, with the main exceptions being the carboxylesterase isoforms CES1 and CES2. Tissue-enriched respectively in the liver and small intestine, CES1 and CES2 hydrolyze a broad variety of esters, protectively converting xenobiotics to more polar and excretable metabolites. In addition to esters, these promiscuous serine

hydrolases (SHs) cleave amides, carbamates, and thioesters, and are important DMEs and PAEs of several bioactive agents[25,26] and prodrugs.[27–30] In nearly all instances CESs were reported to be PAEs, the publications came several years after prodrug approval, attesting to the sluggish state of PAE annotation in spite of the growing awareness of clinically significant CES genovariants.

**Valacyclovir and Valacyclovirase**

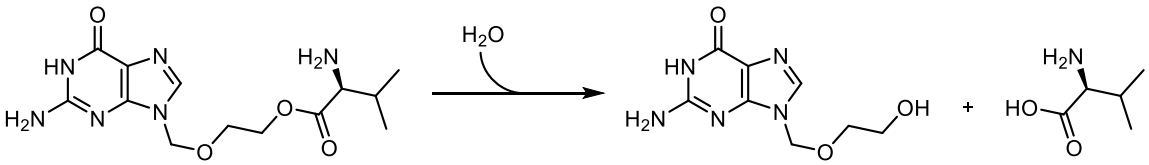


Scheme 1.1. Hydrolysis of valacyclovir to acyclovir and L-valine.

Outside the CES family, a few unique ester PAEs have been discovered—our lab identified a fascinating SH responsible for activation of the antiviral prodrug valacyclovir (VACV, Scheme 1.1), biphenyl hydrolase-like protein (BPHL).[31] VACV, the L-valyl ester of nucleoside mimetic acyclovir (ACV), itself a prodrug, was developed in the early 1990s,[32] 10 years before the discovery of BPHL. VACV had an oral bioavailability three to five times that of ACV but, peculiarly, had a slightly lower log P due to the α-amino group in valine, making increased passive permeability unlikely. This mystery was solved when VACV was shown to be the first non-peptidic substrate for intestinal oligopeptide transporter PepT1, an apically expressed, proton-dependent transporter of di- and tripeptides.[33,34] After PepT1-mediated uptake into enterocytes, VACV is thought to undergo first-pass hydrolysis by BPHL in both the gut and liver. BPHL is unique among SHs for its stringent specificity for primary α-amino acid esters of primary and secondary alcohols.[35–38] This made BPHL an attractive target for rational design of oral

prodrugs seeking increased absorption via uptake by PepT1 and presystemic activation by BPHL, termed the double-targeted prodrug strategy (Figure 1.3).[39,40]

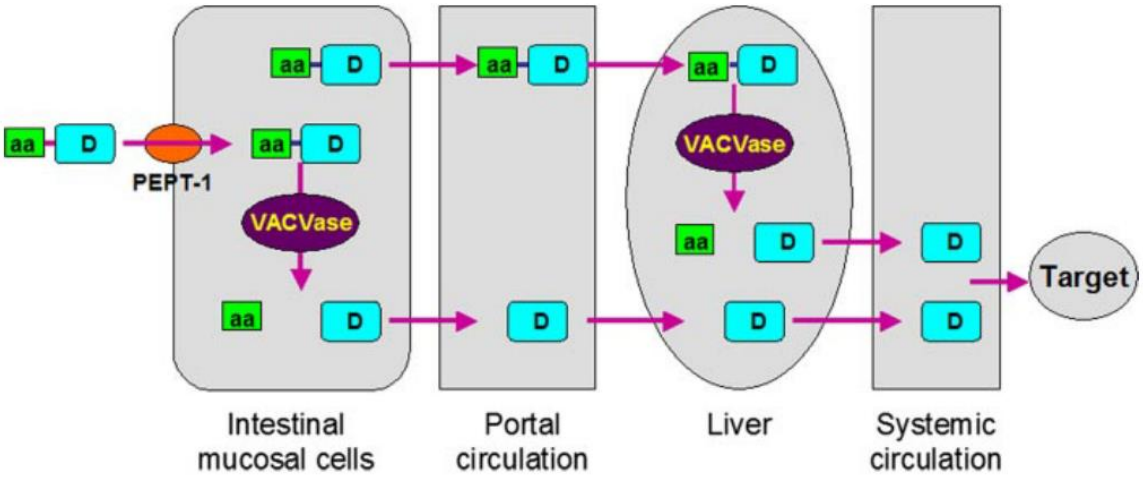


Figure 1.3. Schematic model of the double-targeted prodrug strategy.[35]

A schematized mechanism for the increased oral absorption of PEPT1- and BPHL-targeting (double-targeted) amino acid-ester prodrugs. D, drug; aa, amino acid; VACVase, BPHL. Reproduced with permission from ref. 35.

Though BPHL was considered to have the highest $f_m$ for VACV, there was considerable evidence of additional VACVases in the gut wall. After immunoprecipitation of BPHL from Caco-2 cell lysate, the cell line in which it was first identified as a VACVase, there was significant residual activity remaining.[41] Furthermore, *Bphl*-knockout (KO) mice showed no significant differences in PK parameters of VACV or ACV compared to wildtype (WT) after single-dose oral and IV studies.[42] Clearly, BPHL is not obligatory for presystemic or systemic activation of VACV, begging the question of what other PAEs could be involved.

## Specific Aims

For this dissertation project, the original goal was to use cABPP to identify the undiscovered VACVase(s) in Caco-2 cells. Given the near-total inhibition of VACVase activity in Caco-2 lysates by MBIs of SHs, we set out to use

commercially available FP activity-based probes (ABPs) to investigate. These probes did not inhibit Caco-2 VACVase activity, however, meaning that our first aim would be to synthesize a novel anti-VACVase FP ABP, validate its inhibitory activity, and visualize its unique targets. The second aim was to develop and optimize an MS-based cABPP protocol with the novel FP to identify the VACVase(s) in Caco-2 lysate. The final aim was to validate and characterize the discovered VACVase(s) *in vitro* and *in situ* to understand the clinical relevance of the findings.

Succeeding in these aims would represent the first documented application of ABPP to the MS-based determination of an unidentified PAE, paving the way for more widespread adoption in both industry and academia as a prodrug discovery and development tool. Given the relative maturation of ABPP as a field and numerous enzyme classes now boasting class-selective ABPs, we envision that this approach can take hold sooner rather than later in pharmaceutical R&D. Ultimately, a stronger knowledge of physiological factors affecting prodrug activation will more quickly lead us to the smarter prodrugs of tomorrow that are urgently needed today.

## References


1. Huttunen KM, Raunio H, Rautio J. Prodrugs--from Serendipity to Rational Design. *Pharmacol Rev*. 2011;63(3):750-771. doi:10.1124/pr.110.003459

2. Dammann HG, Burkhardt F, Wolf N. Enteric coating of aspirin significantly decreases gastroduodenal mucosal lesions. *Aliment Pharmacol Ther*. 1999;13(8):1109-1114. doi:10.1046/j.1365-2036.1999.00588.x

3. Gupta S, Kesarla R, Omri A. Formulation strategies to improve the bioavailability of poorly absorbed drugs with special emphasis on self-emulsifying systems. *ISRN Pharm*. 2013;2013:1-16. doi:10.1155/2013/848043

4. Sohi H, Sultana Y, Khar RK. Taste masking technologies in oral pharmaceuticals: recent developments and approaches. *Drug Dev Ind Pharm*. 2004;30(5):429-448. doi:10.1081/DDC-120037477

5. Ratnaparkhi P, Jyoti GP, Mukesh. Sustained release oral drug delivery system - an overview. *Int J Pharma Res Rev IJPRR*. 2013;2(23):11-21.

6. Rautio J, Meanwell NA, Di L, Hageman MJ. The expanding role of prodrugs in contemporary drug design and development. *Nat Rev Drug Discov*. 2018;17(8):559-587. doi:10.1038/nrd.2018.46

7. FDA F and DA. Guidance for Industry: Applications Covered by Section 505(b)(2). *Guidance*. 1999;505(October):1-12. http://www.fda.gov/cder/guidance/index.htm. Accessed August 18, 2019.

8. Clas S-D, Sanchez RI, Nofsinger R. Chemistry-enabled drug delivery (prodrugs): recent progress and challenges. *Drug Discov Today*. 2014;19(1):79-87. doi:10.1016/j.drudis.2013.08.014

9. Ram PR, Priyanka P, Shreekrishna L, Saroj S. Prodrug as a novel approach of drug delivery - a review. *J Drug Deliv Ther*. 2015;5(3):5-9.

10. Wu KM. A new classification of prodrugs: Regulatory perspectives. *Pharmaceuticals*. 2009;2(3):77-81. doi:10.3390/ph2030077

11. Tirkkonen T, Laine K. Drug interactions with the potential to prevent prodrug activation as a common source of irrational prescribing in hospital inpatients. *Clin Pharmacol Ther*. 2004;76(6):639-647. doi:10.1016/j.clpt.2004.08.017

12. Zhang C, Xu Y, Zhong Q, et al. In vitro evaluation of the inhibitory potential of pharmaceutical excipients on human carboxylesterase 1A and 2. *PLoS*

*One*. 2014;9(4). doi:10.1371/journal.pone.0093819

13. Harper TW, Brassil PJ. Reaction phenotyping: Current industry efforts to identify enzymes responsible for metabolizing drug candidates. *AAPS J*. 2008;10(1):200-207. doi:10.1208/s12248-008-9019-6

14. Di L. Reaction phenotyping to assess victim drug-drug interaction risks. *Expert Opin Drug Discov*. 2017;12(11):1105-1115. doi:10.1080/17460441.2017.1367280

15. Zhang Y, Fonslow BR, Shan B, Baek M-C, Yates JR. Protein Analysis by Shotgun/Bottom-up Proteomics. 2013. doi:10.1021/cr3003533

16. Saghatelian A, Cravatt BF. Assignment of protein function in the postgenomic era. *Nat Chem Biol*. 2005;1(3):129. doi:10.1038/nchembio0805-130

17. Cravatt BF, Wright AT, Kozarich JW. Activity-Based Protein Profiling: From Enzyme Chemistry to Proteomic Chemistry. *Annu Rev Biochem*. 2008;77(1):383-414. doi:10.1146/annurev.biochem.75.101304.124125

18. Liu Y, Patricelli MP, Cravatt BF. Activity-based protein profiling: The serine hydrolases. *Proc Natl Acad Sci*. 1999;96(26):14694-14699. doi:10.1073/pnas.96.26.14694

19. van Rooden EJ, Bakker AT, Overkleeft HS, van der Stelt M. Activity-Based Protein Profiling. *eLS*. 2018:1-9. doi:10.1002/9780470015902.a0023406

20. Wang K, Yang T, Wu Q, Zhao X, Nice EC, Huang C. Chemistry-based functional proteomics for drug target deconvolution. *Expert Rev Proteomics*. 2012;9(3):293-310. doi:10.1586/epr.12.19

21. Jeffery DA, Bogyo M. Chemical proteomics and its application to drug discovery. *Curr Opin Biotechnol*. 2003;14(1):87-95. doi:10.1016/S0958-1669(02)00010-1

22. Bantscheff M, Scholten A, Heck AJR. Revealing promiscuous drug-target interactions by chemical proteomics. *Drug Discov Today*. 2009;14(21-22):1021-1029. doi:10.1016/j.drudis.2009.07.001

23. Xu H, Majmudar JD, Davda D, et al. Substrate-Competitive Activity-Based Profiling of Ester Prodrug Activating Enzymes. *Mol Pharm*. 2015;12(9):3399-3407. doi:10.1021/acs.molpharmaceut.5b00414

24. Liederer BM, Borchardt RT. Enzymes involved in the bioconversion of ester-based prodrugs. *J Pharm Sci*. 2006;95(6):1177-1195. doi:10.1002/jps.20542

25. Sun Z, Murry DJ, Sanghani SP, et al. Methylphenidate is stereoselectively hydrolyzed by human carboxylesterase CES1A1. *J Pharmacol Exp Ther*. 2004;310(2):469-476. doi:10.1124/jpet.104.067116

26. Pindel E V., Kedishvili LNY, Abraham TL, et al. Purification and cloning of a human liver carboxylesterase that catalyzes the hydrolysis of cocaine and heroin. *FASEB J*. 1997;11(9):14769-14775.

27. Imai T, Ohura K. The Role of Intestinal Carboxylesterase in the Oral Absorption of Prodrugs. *Curr Drug Metab*. 2011;11(9):793-805. doi:10.2174/138920010794328904

28. Laizure SC, Parker RB, Herring VL, Hu ZY. Identification of carboxylesterase-dependent dabigatran etexilate hydrolysis. *Drug Metab Dispos*. 2014;42(2):201-206. doi:10.1124/dmd.113.054353

29. Shi D, Yang J, Yang D, et al. Anti-Influenza Prodrug Oseltamivir Is Activated by Carboxylesterase Human Carboxylesterase 1, and the Activation Is Inhibited by Antiplatelet Agent Clopidogrel. *J Pharmacol Exp Ther*. 2006;319(3):1477-1484. doi:10.1124/jpet.107.120030

30. Danks MK, Morton CL, Krull EJ, et al. Comparison of activation of CPT-11 by rabbit and human carboxylesterases for use in enzyme/prodrug therapy. *Clin Cancer Res*. 1999;5(4):917-924.

31. Kim I, Chu XY, Kim S, Provoda CJ, Lee KD, Amidon GL. Identification of a human valacyclovirase: Biphenyl hydrolase-like protein as valacyclovir hydrolase. *J Biol Chem*. 2003;278(28):25348-25356. doi:10.1074/jbc.M302055200

32. Beauchamp LM, Orr GF, De Miranda P, Burnette T, Krenitsky TA. Amino acid ester prodrugs of acyclovir. *Antivir Chem Chemother*. 1992;3(3):157-164. doi:10.1177/095632029200300305

33. Ganapathy ME, Huang W, Wang H, Ganapathy V, Leibach FH. Valacyclovir: A substrate for the intestinal and renal peptide transporters PEPT1 and PEPT2. *Biochem Biophys Res Commun*. 1998;246(2):470-475. doi:10.1006/bbrc.1998.8628

34. Balimane P V., Tamai I, Guo A, et al. Direct evidence for peptide transporter (PepT1)-mediated uptake of a nonpeptide prodrug, valacyclovir. *Biochem Biophys Res Commun*. 1998;250(2):246-251. doi:10.1006/bbrc.1998.9298

35. Lai L, Xu Z, Zhou J, Lee K-D, Amidon GL. Molecular Basis of Prodrug Activation by Human Valacyclovirase, an a-Amino Acid Ester Hydrolase. *J Biol Chem*. 2008;283(14):9318-9327. doi:10.1074/jbc.M709530200

36. Kim I, Song X, Vig BS, et al. A novel nucleoside prodrug-activating enzyme: substrate specificity of biphenyl hydrolase-like protein. *Mol Pharm*. 2004;1(2):117-127. doi:10.1021/mp0499757

37. Kim I, Crippen GM, Amidon GL. Structure and specificity of a human valacyclovir activating enzyme: a homology model of BPHL. *Mol Pharm*. 2004;1(6):434-446. doi:10.1021/mp049959+

38. Sun J, Dahan A, Walls ZF, Lai L, Lee KD, Amidon GL. Specificity of a prodrug-activating enzyme hVACVase: The leaving group effect. *Mol Pharm*. 2010;7(6):2362-2368. doi:10.1021/mp100300k

39. Sun J, Dahan A, Amidon GL. Enhancing the intestinal absorption of molecules containing the polar guanidino functionality: A double-targeted prodrug approach. *J Med Chem*. 2010;53(2):624-632. doi:10.1021/jm9011559

40. Dahan A, Khamis M, Agbaria R, Karaman R. Targeted prodrugs in oral drug delivery: the modern molecular biopharmaceutical approach. *Expert Opin Drug Deliv*. 2012;9(8):1001-1013. doi:10.1517/17425247.2012.697055

41. Kim I. A Novel Prodrug Activating Enzyme: Identification and Characterization of BPHL. *Dr Thesis*. 2004. doi:10.1016/B978-012397720-5.50034-7

42. Hu Y, Epling D, Shi J, et al. Effect of biphenyl hydrolase-like (BPHL) gene disruption on the intestinal stability, permeability and absorption of valacyclovir in wildtype and Bphl knockout mice. *Biochem Pharmacol*. 2018;156(August):147-156. doi:10.1016/j.bcp.2018.08.018

43. Patricelli MP, Giang DK, Stamp LM, Burbaum JJ. Direct visualization of serine hydrolase activities in complex proteomes using fluorescent active site-directed probes. *Proteomics*. 2001;1(9):1067-1071. doi:10.1002/1615-9861(200109)1:9<1067::AID-PROT1067>3.0.CO;2-4

44. Bachovchin DA, Ji T, Li W, et al. Superfamily-wide portrait of serine hydrolase inhibition achieved by library-versus-library screening. *Proc Natl Acad Sci U S A*. 2010;107(49):20941-20946. doi:10.1073/pnas.1011663107

45. Lai L. Structure and Function of a Prodrug Activating Enzyme Valacyclovir Hydrolase. *Dr Thesis*. 2006. doi:10.1017/S0165115300023299

46. Middleton WJ. New Fluorinating Reagents. Dialkylaminosulfur Fluorides. *J Org Chem*. 1975;40(5):574-578. doi:10.1021/jo00893a007

47. Burger A, Anderson JJ. Monoesters and Ester-amidates of Aromatic Phosphonic Acids. *J Am Chem Soc*. 1957;79(13):3575-3579. doi:10.1021/ja01570a073

48. Xu H, Sabit H, Amidon GL, Showalter HDH. An improved synthesis of a fluorophosphonate-polyethylene glycol-biotin probe and its use against competitive substrates. *Beilstein J Org Chem*. 2013;9:89-96. doi:10.3762/bjoc.9.12

49. McKenna CE, Higa MT, Cheung NH, McKenna MC. The facile dealkylation of phosphonic acid dialkyl esters by bromotrimethylsilane. *Tetrahedron Lett*. 1977;18(2):155-158. doi:10.1016/S0040-4039(01)92575-4

50. Kidd D, Liu Y, Cravatt BF. Profiling serine hydrolase activities in complex proteomes. *Biochemistry*. 2001;40(13):4005-4015. doi:10.1021/bi002579j

51. Strelow JM. A Perspective on the Kinetics of Covalent and Irreversible Inhibition. *J Biomol Screen*. 2017;22(1):3-20. doi:10.1177/1087057116671509

52. Worek F, Thiermann H, Szinicz L, Eyer P. Kinetic analysis of interactions between human acetylcholinesterase, structurally different organophosphorus compounds and oximes. *Biochem Pharmacol*. 2004;68(11):2237-2248. doi:10.1016/j.bcp.2004.07.038

53. Adibekian A, Martin BR, Chang JW, et al. Confirming target engagement for reversible inhibitors in vivo by kinetically tuned activity-based probes. *J Am Chem Soc*. 2012;134(25):10345-10348. doi:10.1021/ja303400u

54. Sharman J, Pennick M. Lisdexamfetamine prodrug activation by peptidase-mediated hydrolysis in the cytosol of red blood cells. *Neuropsychiatr Dis Treat*. 2014;10:2275-2280. doi:10.2147/NDT.S70382

55. Speers AE, Cravatt BF. Profiling enzyme activities in vivo using click chemistry methods. *Chem Biol*. 2004;11(4):535-546. doi:10.1016/j.chembiol.2004.03.012

56. Harsha HC, Molina H, Pandey A. Quantitative proteomics using stable isotope labeling with amino acids in cell culture. *Nat Protoc*. 2008;3(3):505-516. doi:10.1038/nprot.2008.2

57. Yang Y, Yang X, Verhelst SHL. Comparative analysis of click chemistry mediated activity-based protein profiling in cell lysates. *Molecules*. 2013;18(10):12599-12608. doi:10.3390/molecules181012599

58. Bachovchin DA, Brown SJ, Rosen H, Cravatt BF. Identification of selective inhibitors of uncharacterized enzymes by high-throughput screening with fluorescent activity-based probes. *Nat Biotechnol*. 2009;27(4):387-394. doi:10.1038/nbt.1531

59. Bachovchin DA, Koblan LW, Wu W, et al. A high-throughput, multiplexed assay for superfamily-wide profiling of enzyme activity. *Nat Chem Biol*. 2014;10(8):656-663. doi:10.1038/nchembio.1578

60. Bachovchin DA, Mohr JT, Speers AE, et al. Academic cross-fertilization by public screening yields a remarkable class of protein phosphatase methylesterase-1 inhibitors. *Proc Natl Acad Sci U S A*. 2011;108(17):6811-6816. doi:10.1073/pnas.1015248108

61. Wilk S, Orlowski M. Inhibition of Rabbit Brain Prolyl Endopeptidase by N-Benzyloxycarbonyl-Prolyl-Prolinal, a Transition State Aldehyde Inhibitor. *J Neurochem*. 1983;41(1):69-75. doi:10.1111/j.1471-4159.1983.tb11815.x

62. Hett EC, Xu H, Geoghegan KF, et al. Rational Targeting of Active-Site

Tyrosine Residues Using Sulfonyl Fluoride Probes. 2015. doi:10.1021/cb5009475

63. M. Vorobiev S, Janet Huang Y, Seetharaman J, et al. Human Retinoblastoma Binding Protein 9, a Serine Hydrolase Implicated in Pancreatic Cancers. *Protein Pept Lett*. 2012;19(2):194-197. doi:10.2174/092986612799080356

64. Woitach JT, Zhang M, Niu CH, Thorgeirsson SS. A retinoblastoma-binding protein that affects cell-cycle control and confers transforming ability. *Nat Genet*. 1998;19(4):371-374. doi:10.1038/1258

65. Shields DJ, Niessen S, Murphy EA, et al. RBBP9: A tumor-associated serine hydrolase activity required for pancreatic neoplasia. *Proc Natl Acad Sci*. 2010;107(5):2189-2194. doi:10.1073/pnas.0911646107

66. Vorobiev SM, Su M, Seetharaman J, et al. Crystal structure of human retinoblastoma binding protein 9. *Proteins Struct Funct Bioinforma*. 2009;74(2):526-529. doi:10.1002/prot.22278

67. Simon GM, Cravatt BF. Activity-based proteomics of enzyme superfamilies: Serine hydrolases as a case study. *J Biol Chem*. 2010;285(15):11051-11055. doi:10.1074/jbc.R109.097600

68. Hidalgo IJ, Li J. Carrier-mediated transport and efflux mechanisms of Caco-2 cells. *Adv Drug Deliv Rev*. 1996;22(1-2):53-66. doi:10.1016/S0169-409X(96)00414-0

69. Sambuy Y, De Angelis I, Ranaldi G, Scarino ML, Stammati A, Zucco F. The Caco-2 cell line as a model of the intestinal barrier: influence of cell and culture-related factors on Caco-2 cell functional characteristics. *Cell Biol Toxicol*. 2005;21(1):1-26. doi:10.1007/s10565-005-0085-6

70. Imai, Teruko; Masumi, Imoto; Sakamoto, Hisae; Hashimoto M. Identification of esterases expressed in Caco-2 cells and effects of their hydrolyzing activity in predicting human intestinal absorption. *Drug Metab Dispos*. 2005;33(8):1185-1190. doi:10.1124/dmd.105.004226.tion

71. Imai T, Taketani M, Shii M, Hosokawa M, Chiba K. Substrate specificity of carboxylesterase isozymes and their contribution to hydrolase activity in human liver and small intestine. *Drug Metab Dispos*. 2006;34(10):1734-1741. doi:10.1124/dmd.106.009381

72. Hosokawa M. Structure and catalytic properties of carboxylesterase isozymes involved in metabolic activation of prodrugs. *Molecules*. 2008;13(2):412-431. doi:10.3390/molecules13020412

73. Bar-Even A, Noor E, Savir Y, et al. The moderately efficient enzyme: Evolutionary and physicochemical trends shaping enzyme parameters. *Biochemistry*. 2011;50(21):4402-4410. doi:10.1021/bi2002289

74. Yang B, Hu Y, Smith DE. Impact of peptide transporter 1 on the intestinal

absorption and pharmacokinetics of valacyclovir after oral dose escalation in wild-type and PepT1 knockout mice. *Drug Metab Dispos*. 2013;41(10):1867-1874. doi:10.1124/dmd.113.052597

75. Hidalgo IJ, Raub TJ, Borchardt RT. Characterization of the Human Colon Carcinoma Cell Line (Caco-2) as a Model System for Intestinal Epithelial Permeability. *Gastroenterology*. 1989;96(2):736-749. doi:10.1016/S0016-5085(89)80072-1

76. Inoue M, Morikawa M, Tsuboi M, Sugiura M. Species Difference and Characterization of Intestinal Esterase on the Hydrolizing Activity of Ester-Type Drugs. *Jpn J Pharmacol*. 1979;29(1):9-16. doi:10.1254/jjp.29.9

77. Taketani M, Shii M, Ohura K, Ninomiya S, Imai T. Carboxylesterase in the liver and small intestine of experimental animals and human. *Life Sci*. 2007;81(11):924-932. doi:10.1016/j.lfs.2007.07.026

78. Puente XS, Lopez-Otin C. Cloning and Expression Analysis of a Novel Human Serine Hydrolase with Sequence Similarity to Prokaryotic Enzymes Involved in the Degradation of Aromatic Compounds. *J Biol Chem*. 1995;270(21):12926-12932. doi:10.1074/jbc.270.21.12926

79. Debbage PL, Griebel J, Ried M, Gneiting T, DeVries A, Hutzler P. Lectin intravital perfusion studies in tumor-bearing mice: Micrometer- resolution, wide-area mapping of microvascular labeling, distinguishing efficiently and inefficiently perfused microregions in the tumor. *J Histochem Cytochem*. 1998;46(5):627-639. doi:10.1177/002215549804600508

# CHAPTER II

## Synthesis and Validation of Novel Fluorophosphonate Probes Targeting VACV PAEs

### Introduction

The serine hydrolase (SH) enzyme superfamily, which includes BPHL and roughly one percent of the human proteome, is exceptionally large for an enzyme class. Though they are diverse in function, SHs are named for their common conserved feature: a catalytic Ser nucleophile that attacks the carbonyl electrophile of its typical substrates. The enhanced nucleophilicity of Ser distinguishes it from all other Ser sidechains in proteins and makes the subclass ideal for probing by activity-based protein profiling (ABPP), especially fluorophosphonate (FP) activity-based probes (ABPs).[18,43] Structurally inspired by toxic organophosphorus nerve agents like sarin and diisopropyl fluorophosphate, FPs combine phosphonate transition state analogs of carboxylic acid ester substrates with the well-tuned electrophilicity of the fluoride leaving group for selective inactivation of the catalytic Ser nucleophile, thus irreversibly inhibiting SHs by forming a highly stable phosphonylated adduct via addition-elimination. As countless studies over the years have demonstrated, FP ABPs are remarkably selective for SHs at working concentrations, not binding appreciably to noncatalytic Ser residues or other endogenous nucleophiles, such as Cys and Lys residues. Within the SH family,

however, FP ABPs are much less discerning since they lack structural features necessary to bias their reactivity towards a smaller set of SHs.

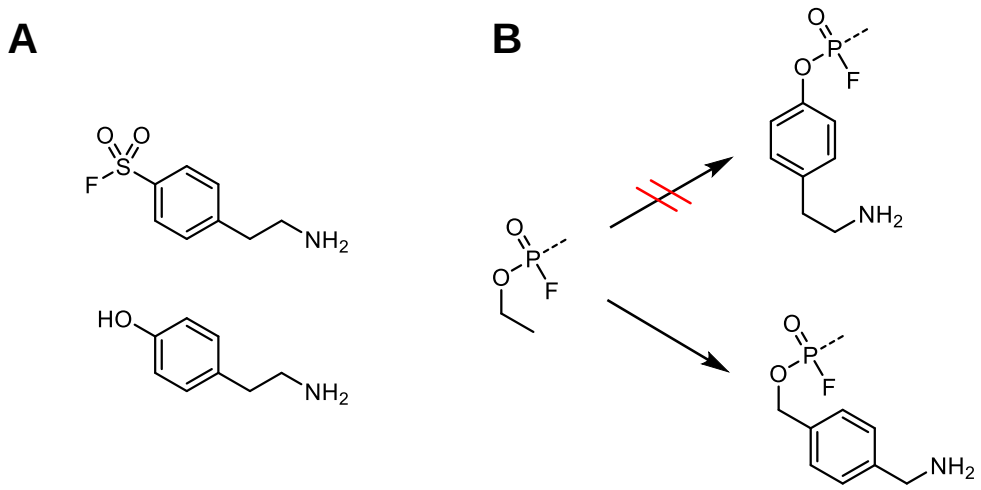


Scheme 2.1. Structures of AEBSF and probe modifications.

(A) Structure of AEBSF and its alcohol analog, tyramine. (B) Tyramine was not amenable to phosphonate esterification (*top*), leading to the use of the more nucleophilic isobaric isomer 4-(aminomethyl)benzyl alcohol.

While class-wide probe promiscuity is generally useful, with estimates of SH coverage by FP-biotin in mouse tissue lysates at 80–85%,[44] hBPHL, the only known valacyclovir (VACV) PAE prior to this work, is among the 15–20% not labeled by FP ABPs under typical conditions. To generate a useful probe of VACVases, we sought to replace the ethyl group in the commercially available FP with a moiety that would lead to inhibition of BPHL. Pan-serine protease inhibitor 4-(2-aminoethyl)benzenesulfonyl fluoride (AEBSF, Scheme 2.1) which sulfonylates the active Ser in BPHL and has been crystallographically characterized in this complex,[45] was chosen as this moiety because it also extinguishes all VACVase activity in Caco-2 lysate (Figure 2.1). The amino group of AEBSF makes a critical electrostatic contact with Asp155,[45] which we thought

could be harnessed in an FP ABP to label BPHL and other hypothetical VACV PAEs with localized anionic regions within their active sites.

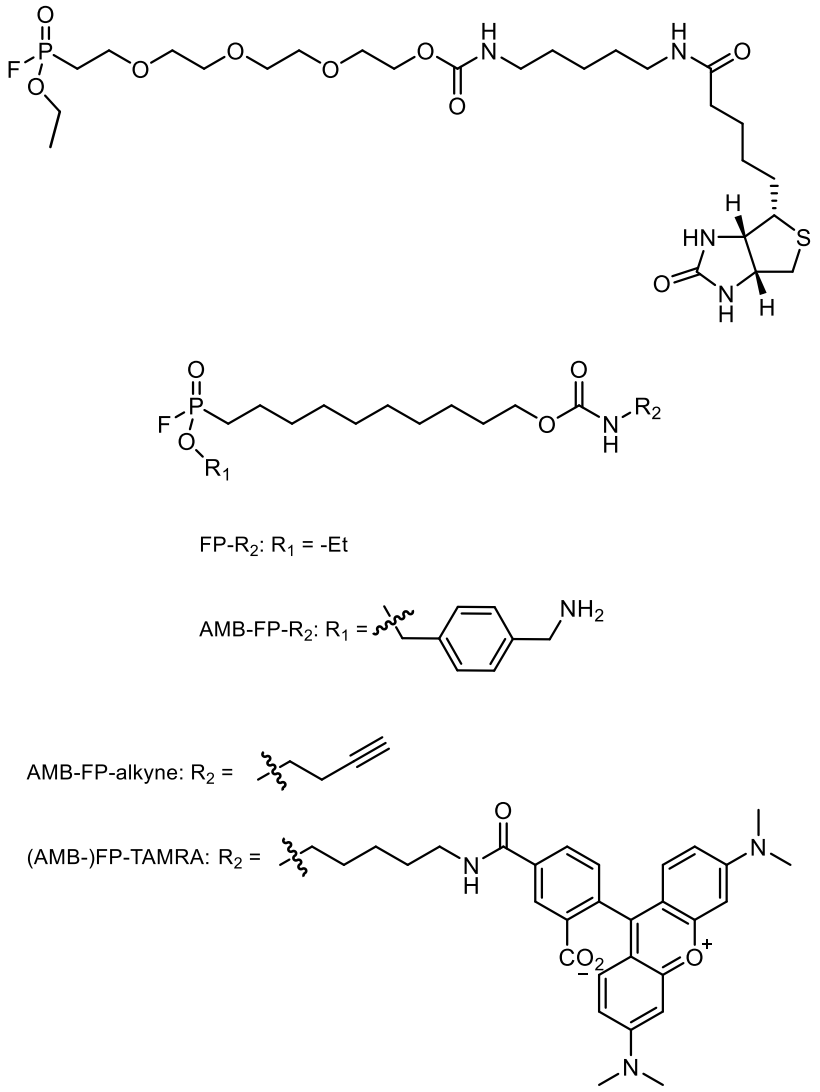


Scheme 2.2. Probe structures.

Structures of FP-PEG-biotin (*top*), FP-TAMRA, AMB-FP-TAMRA, and AMB-FP-alkyne (*bottom*).

Esterification of the phosphonate group with tyramine, the alcohol analog of AEBSF, into the basic FP probe structure was ultimately infeasible due to the phenol's lack of nucleophilicity. An isobaric alcohol with more nucleophilicity, 4-(aminomethyl)benzyl alcohol (AMB), in which a methylene group adjacent to the amino group in tyramine is shifted to between the phenyl ring and hydroxyl group,

was used instead to preserve the size of the moiety. Thus was generated a novel aminomethylbenzyl-FP (AMB-FP, Scheme 2.2), which, to our knowledge, is the first reported FP ABP with a primary amino group, and one of only a handful in which the ethyl substituent has been replaced by a specificity group. Two different probes were synthesized: one with a carboxytetramethylrhodamine group (AMB-FP-TAMRA) and one with a terminal alkyne (AMB-FP-alkyne) for “click chemistry” cycloaddition with an azide-functionalized biotin group. A directly biotinylated version of the probe was synthesized in small quantities but was too unstable for use.

The new AMB-FP inhibited VACV activation in Caco-2 lysate but did not inhibit rBPHL, suggesting that it was inhibiting one or more undiscovered VACV PAEs. Moreover, the novel probe inhibited VACV activation in Bphl-knockout (KO) mouse tissue lysates. In both these experiments, the commercial FP probe did not inhibit VACV activation. In-gel comparison of labeling profiles in various lysates demonstrated a large, shared target set with a minority of targets unique to each probe. Here we report the synthesis and validation of AMB-FP-TAMRA and AMB-FP-alkyne and their comparison to commercially available ethylated FP ABPs.

## Results

*Probe Synthesis*

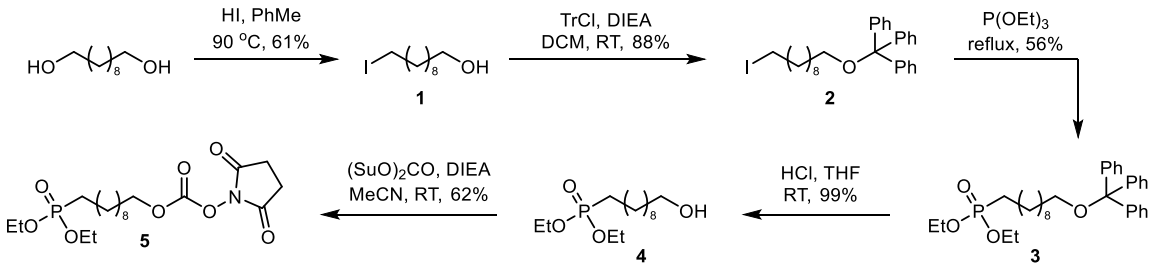


Scheme 2.3. Synthetic route from starting material to intermediate 5.

The synthetic routes to alkynylated probe **15** and fluorogenic probe **10**, outlined in Scheme 2.3, Scheme 2.4, and Scheme 2.5, were ten-step, linear syntheses with an overall yield of 2.2% and 0.8%, respectively. Starting with 1,10-decanediol, monoiodination in hot hydriodic acid gave **1** in 61% yield after purification. Protection of the remaining alcohol by a trityl group was accomplished with trityl chloride and *N*,*N*-diisopropylethylamine in dichloromethane, yielding iodoether **2** in 88% yield following purification. The phosphonate group was appended by a standard Arbuzov reaction in triethyl phosphite, generating diethyl phosphonate **3** in 56% yield. Hydrochloric acid in tetrahydrofuran (THF) was used to deprotect the trityl ether and provide **4** in 99% yield after purification, which was then activated to carbonate ester **5** by disuccinimidyl carbonate in acetonitrile in 62% yield following flash chromatography.

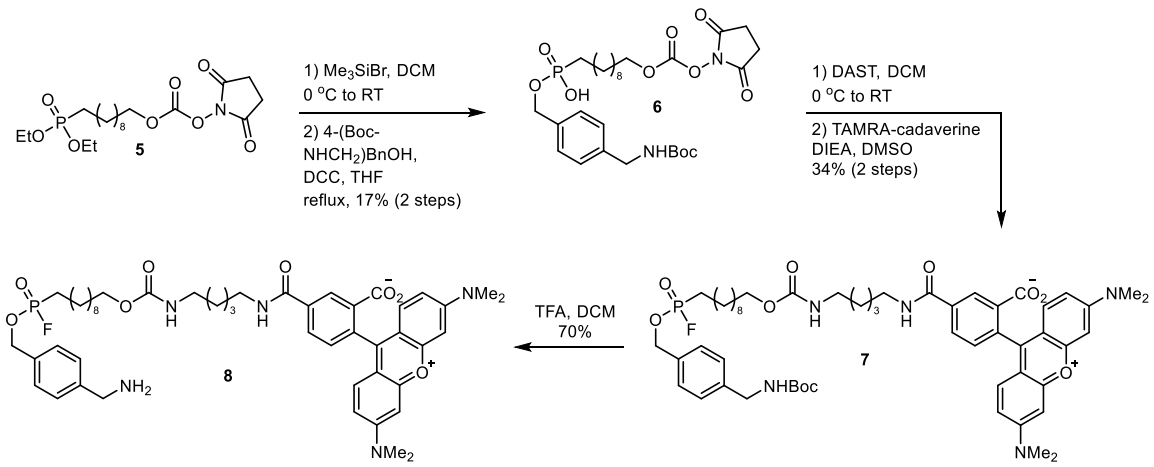


Scheme 2.4. Synthetic route from intermediate 5 to AMB-FP-TAMRA (8).

Only the 5-TAMRA isomer is shown, but an equimolar mixture of 5- and 6-TAMRA isomers was synthesized.

At this point, the syntheses diverge in the order of steps due to the cost of the TAMRA 5-amino-1-pentanamide reagent and its lability towards the fluorinating agent used to generate the fluorophosphonate. Specifically, the free carboxylate group on the phenyl ring can be converted to an electrophilic acyl fluoride in the presence of diethylaminosulfur trifluoride.[46] Thus, the route to TAMRA probe **8** required that the fluorophosphonate be generated prior to addition of the TAMRA moiety. The free phosphonic acid was generated by dealkylation of **5** via bromotrimethylsilane in dichloromethane and was carried forward without purification. Monoesterification to intermediate **6** was performed directly afterwards via a procedure adapted from Burger and Anderson,[47] in which dicyclohexylcarbodiimide (DCC) is used as a coupling agent in refluxing THF. DCC in THF was added to the reaction mixture dropwise over 2 h, providing **7** in 17% yield over two steps after purification by preparative LC. Next came installment of the fluorine-phosphorus bond by treatment with diethylaminosulfur trifluoride at 0°C, which gave the crude fluorophosphonate. TAMRA 5-amino-1-pentanamide

was appended in DMSO, replacing the succinimidyl group to generate the penultimate carbamate **7** after preparative LC purification in 34% yield over 2 steps. Removal of the Boc group with TFA in DCM gave the final TAMRA probe **8** in 70% yield (0.8% overall yield over ten steps) with purity determined by HPLC to be >95%.

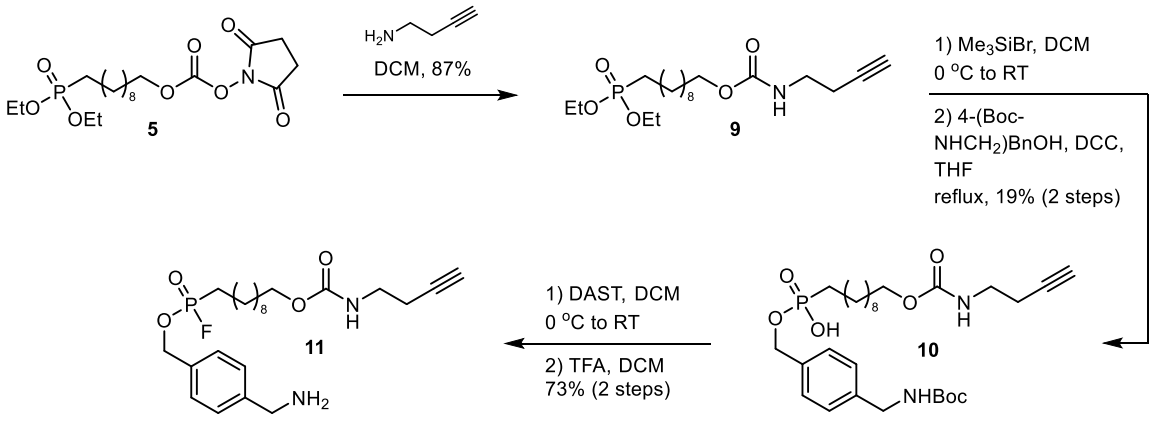


Scheme 2.5. Synthetic route from intermediate 5 to AMB-FP-alkyne (11).

The synthesis of alkynylated probe **11** from **5** begins with addition of 1-amino-3-butyne to the carbonate in acetonitrile to generate alkynylcarbamate **9** with a yield of 87% after flash chromatography. This was followed by the same steps used to synthesize probe **8**, generating compounds **10** and **11** by successive phosphonate dealkylation and monoesterification (19% over two steps), fluorination and Boc deprotection (73% over two steps). Compound **11** was synthesized with an overall yield of 2.2% over ten steps and >95% purity as determined by HPLC.

*VACV Activation Probe Inhibition Assay*

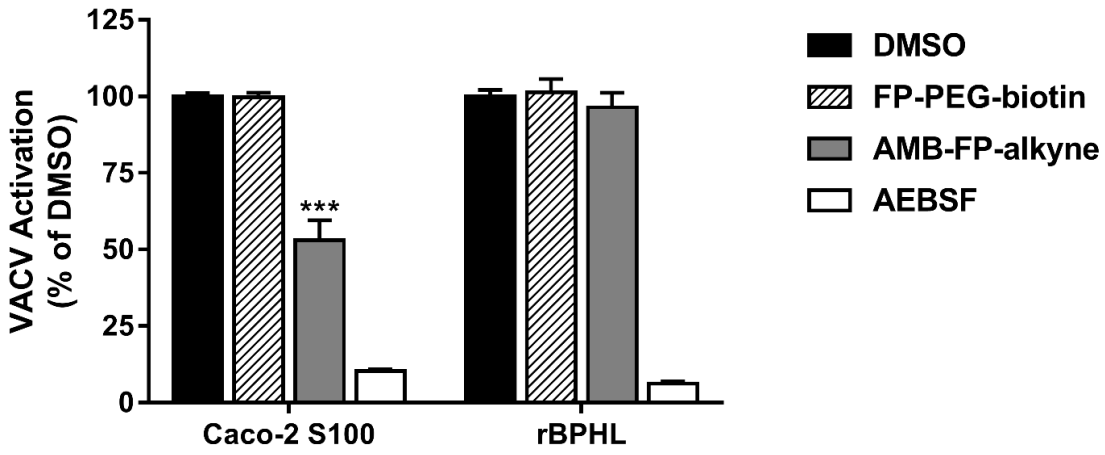


Figure 2.1. Inhibition of VACV activation in Caco-2 S100 and rBPHL.

Activation of VACV in Caco-2 S100 and rBPHL with the listed inhibitors. Both FP probes were incubated at 20 μM. AEBSF (500 μM) served as positive control. Results are shown as mean ± SD (n = 3). ****p* < .001 compared to DMSO control by unpaired *t*-test.

In Caco-2 cytosol at pH 7.4, AMB-FP-alkyne at 20 μM inhibited VACV hydrolysis to 55% of DMSO control (Figure 2.1). In contrast, 20 μM each of FP-PEG-biotin and FP-TAMRA did not appreciably inhibit VACV hydrolysis, even with incubation times up to an hour. With purified rBPHL, no inhibition was observed with any probe up to 20 μM. Finally, in Bphl-KO mouse jejunum and liver lysates, VACV activation was reduced to 66% and 71% of DMSO control, respectively, after incubation with 20 μM AMB-FP-alkyne (Figure 2.2). Taken together, these data suggest that AMB-FP-alkyne is inhibiting one or more unidentified VACV PAEs in Caco-2.

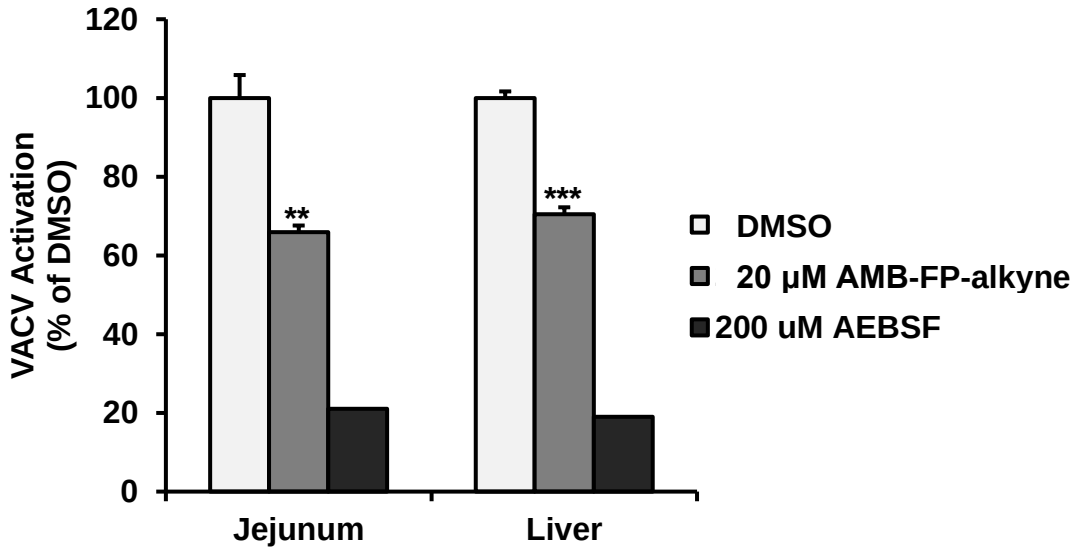


Figure 2.2. Inhibition of VACV activation in Bphl-KO mouse tissue S100.

Inhibition of VACV activation in both jejunum and liver S100 fractions by AMB-FP-alkyne (20 µM) shows roughly similar results in both tissues. ***p* < .01 and ****p* < .001 compared to DMSO control by unpaired *t*-test.

*Optimization of In-Gel Probe Labeling Conditions*

With 0.5 µM AMB-FP-TAMRA, the most abundant Caco-2 cytosolic proteins were detectably labeled (Figure 2.3). Many more targets were visibly labeled at 5 µM, as expected, though two or three bands showed a constant signal at all concentrations and timepoints (e.g. thin closed arrow), implying that with the stoichiometries employed at the 0.5 µM probe concentration, the labeling reaction proceeded to completion. Another set of bands showed a time-dependent, concentration-independent labeling profile, with constant labeling across probe concentrations but greater labeling at later timepoints (e.g. thick filled arrow). The labeling of these enzymes was rate-limited by insufficient binding affinity and/or reactivity specific to the enzyme-probe pair. Conversely, other enzymes showed a concentration-dependent, time-independent labeling profile, with constant labeling across timepoints but greater labeling at higher probe concentrations (e.g. thin

open arrow). Such enzymes react quickly with the probe such that labeling has plateaued at 2 min, likely meaning that the reaction is rate-limited by probe concentration. Finally, some enzymes show both time and concentration dependence (e.g. thick hollow arrow). At 5 μM, two bands show the highest intensities by a wide margin: one right below the 65 kDa marker, possibly CES1, and one just above the 23 kDa marker, possibly lysophospholipase A2 (LYPA2).

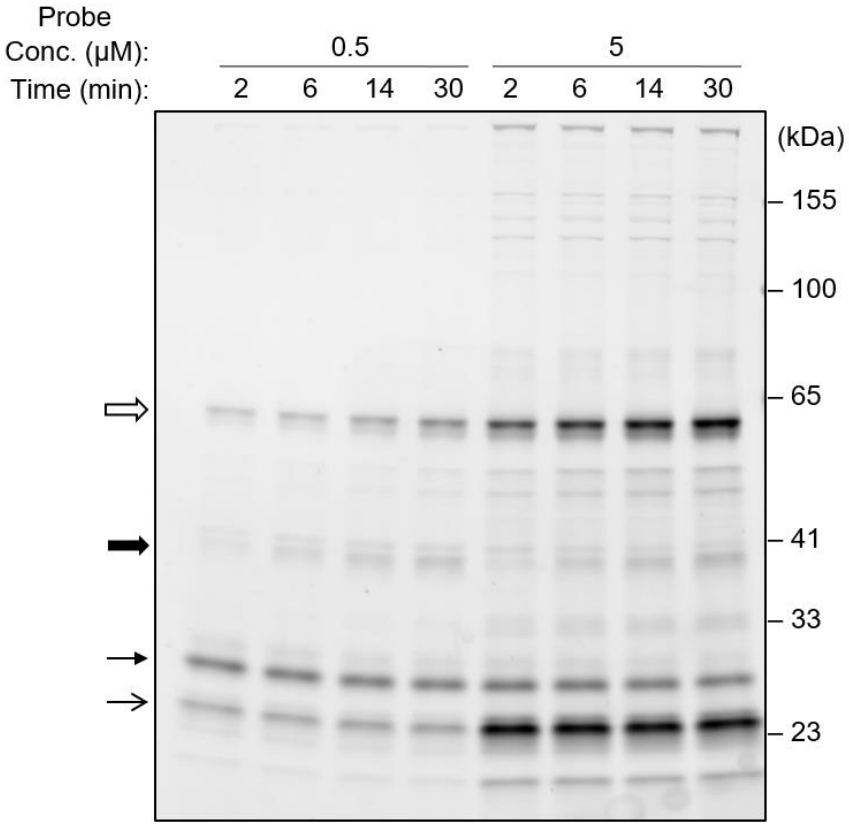


Figure 2.3. Time and concentration optimization of gel-based ABPP.

Optimization of labeling time and AMB-FP-TAMRA concentration for gel-based ABPP studies. Arrows of different styles indicate bands with one of the four representative concentration-based kinetic profiles.

*In-Gel Probe Target Comparison in Caco-2*

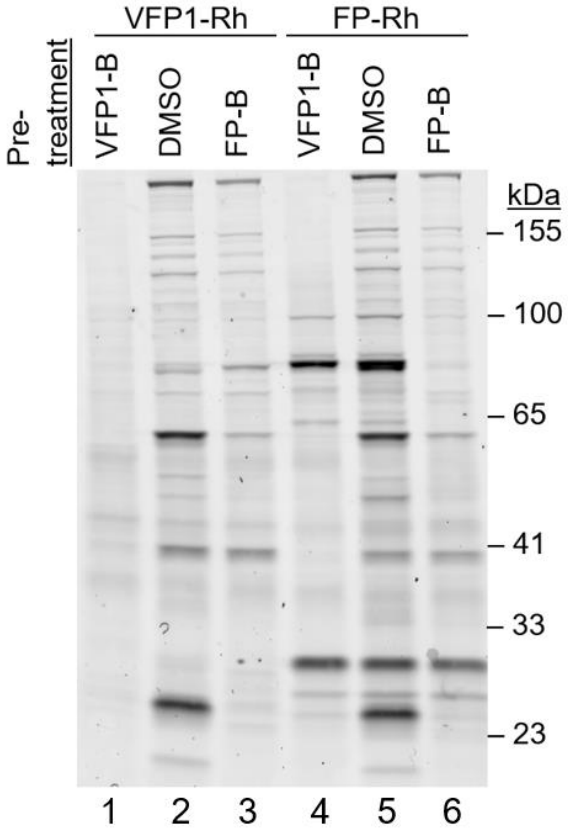


Figure 2.4. Comparison of probe targets in Caco-2 S100.

Targets of AMB-FP-TAMRA (VFP1-Rh, ) and FP-TAMRA (FP-Rh) in Caco-2 S100. Lanes 1 and 6 served as negative controls. Lanes 3 and 4 show targets unique to each probe. VFP1-B = AMB-FP-biotin; FP-B = FP-biotin.

The baseline labeling profiles of equimolar AMB-FP-TAMRA and FP-TAMRA are seen in lanes 2 and 5 (Figure 2.4). To visualize unique targets, these same reactions were also carried out with pre-treatment by the opposing probe (i.e. FP-PEG-biotin pre-treatment prior to labeling with AMB-FP-TAMRA and vice versa). These results are seen in lane 3 (AMB-FP-TAMRA) and lane 4 (FP-TAMRA), with a greater number of bands and higher band intensities seen with FP-TAMRA. Lanes 1 and 6 are control reactions with pre-treatment by the same probe used for labeling to ensure the non-fluorogenic probes block all labeling by

their fluorogenic counterparts. While AMB-FP-alkyne suitably blocked all AMB-FP-TAMRA labeling (lane 1), FP-PEG-biotin was not as effective in this regard. However, this may be due to the fact that the reporter group, contrary to intuition, can have a significant impact on probe reactivity profiles.

*In-Gel Probe Target Comparison in Cell/Tissue Lysates*

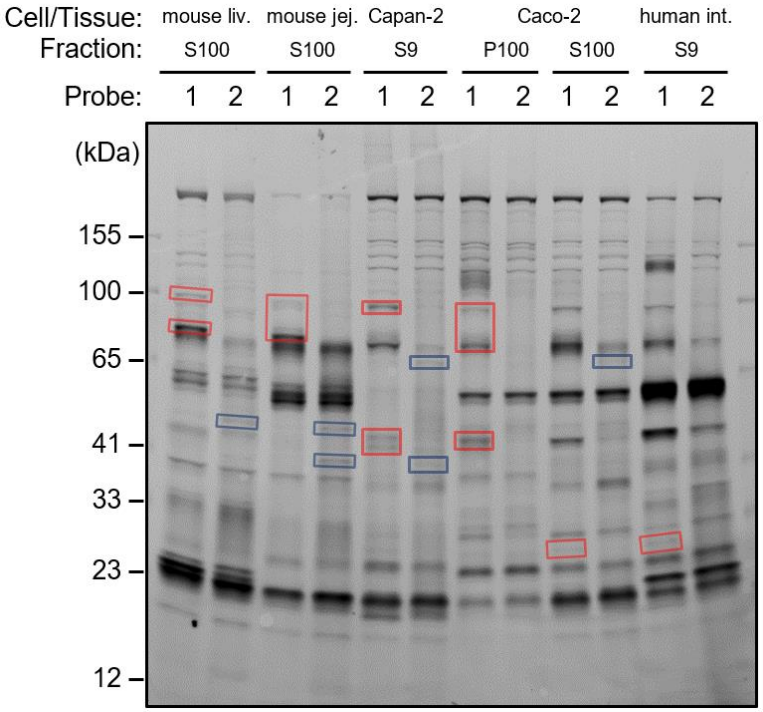


Figure 2.5. Comparison of probe targets in a panel of cell/tissue lysates.

Fluorescent gel scan of labeling of cell and tissue lysates to completion (30 min) with FP-TAMRA (5 μM) or AMB-FP-TAMRA (10 μM). Unique targets are boxed in red for FP-TAMRA or blue for AMB-FP-TAMRA.

To visualize the differences in labeling profiles in other proteomes, AMB-FP-TAMRA and FP-TAMRA were screened against a panel of cell and tissue lysates. AMB-FP-TAMRA was tested at twice the concentration used for FP-TAMRA (10 vs. 5 μM) to compensate for its slower labeling kinetics, likely due to increased steric bulk near the reactive center. The visible bands demonstrate that most targets are common to both probes (Figure 2.5). FP-TAMRA has more

unique bands, boxed in red, than does AMB-FP-TAMRA, which might be due to its smaller size, enabling access to more restrictive active sites. AMB-FP-TAMRA also labels unique targets, boxed in blue, though generally, the activity of these bands is lower than seen with the bands unique to FP-TAMRA.

## Discussion

As a tool in chemical biology, ABPs are highly versatile due to their structural modulability. FPs provide an ideal scaffold for diversification since the phosphonate group, compared to carbonyl (or other $sp^2$ carbon-based) electrophiles, has an extra substituent. In most FPs, including the original FP[18,43], this is an ethyl substituent as a result of synthetic convenience from the use of cheap and readily available triethyl phosphite to install the phosphonate group. To synthesize a novel AMB-FP probe with a 4-(aminomethyl)benzyl (AMB) ester in place of the ethyl group, we used a mostly conventional synthetic route adapted from the synthesis of FP-PEG-biotin by Xu et al.[48] Differences include (1) the initial use of hydriodic acid to monoiodinate the starting diol directly without protection, (2) the use of an acid-labile trityl protecting group on the iodoalcohol in place of the benzyl group, (3) the double dealkylation of the diethyl phosphonate by bromotrimethylsilane in lieu of monodealkylation by lithium azide, and (4) the obligatory inclusion of a phosphonate esterification step to install the AMB moiety.

The chemical transformation of one hydroxyl group on a symmetric diol is difficult to achieve selectively due to the chemical equivalence of the functionalities. Attempts to selectively protect one of the two alcohols in high yield were not fruitful. Failures notwithstanding, iodination in excess hot hydriodic acid was surprisingly selective over the timescales and stoichiometries employed, resulting in much less of the diiodide byproduct than would be expected purely entropically. The second adjustment, the use of an acid-labile trityl protecting group, yielded several advantages over the benzyl group, most notably the safety

and ease of deprotection. Hydrogenolysis, the preferred method of benzyl ether deprotection, carries significant risks of explosion and fire normally seen with pressurized hydrogen gas. In contrast, trityl ethers are cleanly and efficiently reverted to the alcohol in mild acid. The third change was the double dealkylation of the phosphonate using the well-known method of silylation and solvolysis pioneered by McKenna et al.[49] using bromotrimethylsilane followed by an aqueous solvent mixture. Finally, dicyclohexylcarbodiimide was used as a coupling agent for selective but low-yielding phosphonate monoesterification in a method first reported by Burger and Anderson.[47]

The modification of the commercial FP probe to the novel AMB-FP probe resulted in the inhibition of unannotated VACVase activity in Caco-2 cell lysate, as inferred from its simultaneous lack of rBPHL inhibition. We corroborated this conclusion by observing the same inhibition of VACV activation in Bphl-KO mouse jejunum and liver lysates, which are definitively devoid of Bphl. When figuring out the proper labeling conditions in Caco-2 S100 with the new probe, it was observed that Caco-2 S100 contained a proteome of diverse abundances and reactivities, featuring enzymes possessing any and all combinations of time- and probe concentration-dependent labeling profiles. Comparison of AMB-FP-TAMRA and FP-TAMRA labeling demonstrated that the commercial probe is more promiscuous and has faster kinetics, but AMB-FP-TAMRA has a few unique targets in both Caco-2 S100 and other lysates. The slower labeling kinetics, likely due in part to the bulky AMB group near the reactive electrophile, may be beneficial for observing competition. Altogether, these results illustrate the potential of semi-rational ABP

design for the synthesis of broad-spectrum probes with complementary reactivities when commercially available probes do not yield the desired results.

## Methods

*Synthetic Materials and Equipment*

All reagents were commercially available and used without further purification. $^{1}H$ and $^{13}C$ NMR spectra were obtained on Varian 400 or 500 MHz spectrometers and $^{31}P$ and $^{19}F$ spectra were obtained on a Varian 500 MHz spectrometer at the indicated frequencies in the indicated deuterated solvents. Chemical shifts are reported as δ (ppm) relative to either the residual solvent peak set to a reference value or to the tetramethylsilane internal standard peak set to 0.0 ppm. Mass spectrometric analysis was performed using an Agilent 6230 TOF HPLC-MS. Flash column chromatography was carried out on 240 mesh silica gel (Sigma-Aldrich). Preparative LC was performed on the Shimadzu LC-8A model with SCL-10A VP system controller, SPD-M20A Prominence diode array detector, FRC-10A fraction collector, and a 5-valve manual injection port equipped with a 10 mL sample loop. Thin-layer chromatography (TLC) was performed on 0.2 mm thickness silica gel plates with fluorescent indicator (Sigma-Aldrich). Developed TLC plates were visualized by UV illumination at 254 nm, phosphomolybdic acid staining, dimethylaminocinnamaldehyde staining, *p*-anisaldehyde staining, or iodine staining.

**10-Iodo-1-decanol (1)**

A solution of 1,10-decanediol (3 g) in toluene (40 mL) was heated to 90$^{o}$C and to it was added 57% HI solution (8 mL). The mixture was stirred at this temperature for 16 h, at which point was added saturated $NaHCO_3$ solution (20 mL) until no

bubbling was observed. Saturated $Na_2S_2O_3$ solution was then added (2 mL) and allowed to stir until the toluene phase was fully decolorized. After separating the organic and aqueous layers, the aqueous layer was extracted with $Et_2O$ (3 x 20 mL). Organic fractions were combined and washed with brine and dried over $Na_2SO_4$. The crude product was concentrated in vacuo and chromatographed on silica gel (5-50% EtOAc:hexanes) to give 3.01 g of a colorless oil (yield = 61%): **$^1$H NMR** (400 MHz, $CDCl_3$) δ 3.63 (t, *J* = 6 Hz, 2H), 3.18 (t, *J* = 8 Hz, 2H), 1.81 (quint, *J* = 8 Hz, 2H), 1.56 (quint, *J* = 7 Hz, 2H), 1.29–1.43 (br, 13H); **$^{13}$C NMR** (100 MHz, $CDCl_3$) δ 63.0, 33.5, 32.8, 30.5, 29.5, 29.4, 29.3, 28.5, 25.7, 7.4.

**10-Triphenylmethoxy-1-iododecane (2)**

To a solution of **1** (5.7 g) and N,N-diisopropylethylamine (DIEA, 3.8 mL) in DCM (80 mL) was added $Ph_3CCl$ (6.9 g) and 4-dimethylaminopyridine (50 mg), which were stirred together at RT for two days. The solvent was removed in vacuo and the residue was chromatographed on silica gel (100% hexanes-3% EtOAc:hexanes) to give 9.33 g of pale yellow oil (yield = 88%): **$^1$H NMR** (500 MHz, $CDCl_3$) δ 7.44 (d, *J* = 8.5 Hz, 6H), 7.28 (t, *J* = 7.8 Hz, 6H), 7.21 (t, *J* = 7.3 Hz, 3H), 3.17 (t, *J* = 7 Hz, 2H), 3.04 (t, *J* = 6.5 Hz, 2H), 1.80 (quint, *J* = 7.3 Hz, 2H), 1.61 (quint, *J* = 7 Hz, 2H), 1.35 (br, 4H), 1.26–1.40 (br, 10H); **$^{13}$C NMR** (125 MHz, $CDCl_3$) δ 144.6, 128.7, 127.7, 126.8, 86.3, 63.7, 33.6, 30.5, 30.1, 29.5, 29.4, 28.5, 26.3, 7.3.

**Diethyl 10-triphenylmethoxydecylphosphonate (3)**

A solution of **2** (9.33 g) in triethyl phosphite (7.5 mL) was brought to reflux at 165$^o$C and stirred overnight. The solvent was partially removed in vacuo and the mixture

was chromatographed on silica gel (33% EtOAc:hexanes-100% EtOAc) to give 5.3 g of a colorless oil (yield = 56%): **$^{1}$H NMR** (500 MHz, $(CD_3)_2CO$) δ 7.44 (d, *J* = 7.5 Hz, 6H), 7.28 (q, *J* = 6.8 Hz, 6H), 7.22 (t, *J* = 7.5 Hz, 3H), 4.03–4.15 (m, 5H), 3.03 (t, *J* = 6.5 Hz, 2H), 1.67–1.75 (m, 2H), 1.53–1.64 (m, 4H), 1.29–1.39 (m, 11H), 1.20–1.29 (m, 8H); **$^{13}$C NMR** (125 MHz, $CDCl_3$) δ 144.5, 128.7, 127.7, 126.8, 86.3, 63.7, 61.4, 61.3, 30.7, 30.6, 30.0. 29.5, 29.4, 29.1, 26.3, 25.1, 22.4, 16.5, 16.1

**Diethyl 10-hydroxydecylphosphonate (4)**

Compound **3** (2.3 g) was dissolved in THF (19 mL) and HCl (2 mL) and stirred overnight. The mixture was neutralized with 1 M $NaHCO_3$ and extracted with DCM (3 x 20 mL). The organic fractions were combined and washed with 1 M $NaHCO_3$ and brine and dried over $Na_2SO_4$. The solvent was removed in vacuo and the residue chromatographed on silica gel (33% EtOAc:hexanes-100% EtOAc-10% MeOH:EtOAc) to give 1.25 g of a colorless oil (yield = 99%): **$^{1}$H NMR** (500 MHz, $CD_3OD$) δ 4.08 (quint, *J* = 5.6 Hz, 4H), 3.54 (t, *J* = 7.5, 2H), 1.79 (sextuplet, *J* = 7 Hz, 2H), 1.54 (br, 4H), 1.29–1.43 (br, 18H).

**10-Diethoxyphosphonodecyl (2,5-dioxopyrrolidin-1-yl)carbonate (5)**

To a solution of **4** (547.6 mg) and DIEA (365 uL) in $CH_3CN$ (10.5 mL) was added disuccinimidyl carbonate (1011.1 mg). After stirring for 24 h at RT, the solvent was removed in vacuo. The residue was dissolved in EtOAc (10 mL) and washed with 5% HCl (8 mL), $dH_2O$ (8 mL), and brine (10 mL). The washes were back-extracted with EtOAc (5 mL) and organic layers were combined before drying over $Na_2SO_4$. The solvent was removed in vacuo and the residue chromatographed on silica gel (50% EtOAc:hexanes-100% EtOAc-5% MeOH:EtOAc) to give 503 mg of a

colorless oil (yield = 62%): **$^{1}$H NMR** (400 MHz, $CDCl_3$) δ 4.32 (t, *J* = 7.2 Hz, 2H), 4.09 (octuplet, *J* = 8 Hz, 4H), 2.84 (s, 4H), 1.74 (m, 4H), 1.60 (m, 2H), 1.29–1.43 (m br, 18H); **$^{13}$C NMR** (100 MHz, $CDCl_3$) δ 168.7, 151.6, 71.6, 61.4, 61.3, 30.6, 30.5, 29.3, 29.2, 29.0, 28.3, 26.2, 25.4, 25.3, 25.1, 22.4, 22.3, 16.5, 16.4.

**10-((((2,5-Dioxopyrrolidin-1-yl)oxy)carbonyl)oxy)decyl)phosphonic acid**

A solution of **5** (841 mg) in DCM (10 mL) was cooled to 0$^{o}$C. To this was added bromotrimethylsilane (1 mL) with stirring for 15 min, at which point the mixture was warmed to RT and allowed to stir overnight. The solvent was removed in vacuo and the oily residue was dissolved in 1:1 $H_2O$/acetone (15 mL) and stirred for 4 h. The mixture was extracted with DCM (3 x 10 mL). Organic fractions were combined, washed with brine, and dried over $Na_2SO_4$. The solvent was removed in vacuo to give 578 mg of white solid that was used without further purification: **HRMS** $[M+H]^+$ *m/z* 380.1469 (calcd.), 380.1470 (found).

***tert*-Butyl (4-((((10-((((2,5-dioxopyrrolidin-1-yl)oxy)carbonyl)oxy)decyl)(hydroxy)phosphonyl)oxy)methyl)benzyl)carbamate (6)**

A solution of 10-((((2,5-Dioxopyrrolidin-1-yl)oxy)carbonyl)oxy)decyl)phosphonic acid (578 mg) and 4-(Boc-aminomethyl)benzyl alcohol (402 mg) in tetrahydrofuran (5 mL) was heated to reflux at 75$^{o}$C. To this was added a solution of N,N'-dicyclohexyl carbodiimide (360 mg) in tetrahydrofuran (4 mL) over a period of 2 h. This was stirred for 24 hours, after which point the reaction was cooled to RT and filtered through a celite pad to remove the insoluble urea byproduct. The filtrate was directly purified by preparative LC (0.2–90% MeCN:$H_2O$ gradient, 254 nm

detection) to give 155 mg of a colorless oil (yield = 17% over two steps): **$^{1}$H NMR** (500 MHz, $CD_3OD$) δ 7.32 (d, *J* = 8 Hz, 2H), 7.26 (d, *J* = 4.5 Hz, 2H), 4.98 (d, *J* = 9 Hz, 2H), 4.31 (m, 4H), 2.82 (s, 4H), 1.73 (m, 4H), 1.60 (m, 2H), 1.45 (s, 9H), 1.30–1.40 (br, 4H), 1.23–1.30 (br, 9H); **$^{13}$C NMR** (125 MHz, $CDCl_3$) δ 168.7, 151.6, 139.1, 135.5, 135.4, 128.0, 127.5, 71.6, 66.1, 66.0, 44.3, 30.5, 30.4, 29.3, 29.2, 29.0, 28.4, 28.3, 26.5, 25.4, 25.3, 22.2, 22.1;

***tert*-butyl (4-((((10-((((2,5-dioxopyrrolidin-1-yl)oxy)carbonyl)oxy)decyl)fluorophosphonyl)oxy)methyl)benzyl)carbamate**

A solution of **7** (20.9 mg) in DCM (0.5 mL) was cooled to 0$^{o}$C and to it was added diethylaminosulfur trifluoride (14 uL). The reaction was stirred for 15 min at 0$^{o}$C and 30 min at RT. Then was added ice-cold 1 M $NaHCO_3$ (0.15 mL) and the two phases were stirred for 5 min at RT. The phases were separated, and the organic layer was washed with brine and dried over $Na_2SO_4$. The solvent was removed in vacuo to give 21 mg of a colorless oil which was used without further purification: **HRMS** $[M+Na]^+$ *m/z* 623.2510 (calcd.), 623.2505 (found).

**5-((5-((((10-(((4-(((*tert*-Butoxycarbonyl)amino)methyl)benzyl)oxy)fluorophosphonyl)decyl)oxy)carbonyl)amino)pentyl)carbamoyl)-2-(6-(dimethylamino)-3-(dimethyliminio)-3H-xanthen-9-yl)benzoate (7)**

To solution of **8** (21 mg) and DIEA (8 uL) in DMSO (0.35 mL) was added 5/6 mixed isomer TAMRA-cadaverine conjugate (20 mg, Biotium). After stirring at RT overnight, the reaction was diluted in MeCN and purified by preparative LC (0.2–90% MeCN:$H_2O$ gradient, 500 nm detection). Solvent was removed by

lyophilization to yield 12 mg of pink oil (yield = 34% over two steps): **$^{1}$H NMR** (500 MHz, $CD_3OD$) δ 8.66 (s, 0.5H due to mixed-isomer preparation), 8.28 (d, *J* = 8 Hz, 0.5H due to mixed-isomer preparation), 7.83 (m, 0.5H due to mixed-isomer preparation), 7.35 (m, 1H), 7.30 (m, 1H), 7.26 (s, 4H), 7.17 (d, *J* = 9.5 Hz, 1H), 6.85 (dd, *J* = 2.5, 9.5 Hz, 1H), 6.73 (m, 1H), 5.15 (m, 2H), 4.92 (br, 2H), 4.32 (br, 1H), 4.02 (br, 1H), 3.52 (m, 1H), 3.26 (d, *J* = 12.5 Hz, 6H), 3.17 (br, 2H), 2.66–2.99 (br, 12H), 2.35 (t, *J* = 7.5, 1H), 1.89 (m, 1H), 1.71 (m, 2H), 1.52–1.66 (br, 4H), 1.40–1.50 (br, 6H), 1.15–1.40 (br, 13H), 0.78–0.92 (m, 2H); **$^{31}$P NMR** (125 MHz, $CD_3OD$) δ 35.2, 29.8; **$^{19}$F NMR** (125 MHz, $CD_3OD$) δ -75.7; **HRMS** $[M+H]^+$ *m/z* 1000.5006 (calcd.), 1000.4990 (found).

**5-((5-((((10-(((4-(aminomethyl)benzyl)oxy)fluorophosphonyl)decyl)oxy)carbonyl)amino)pentyl)carbamoyl)-2-(6-(dimethylamino)-3-(dimethyliminio)-3H-xanthen-9-yl)benzoate (8)**

Compound **7** (2 mg) was added to a solution of 25% TFA in DCM and stirred for 4 h at RT. The reaction was diluted in MeCN and purified by preparative LC (0.2–90% MeCN:$H_2O$ gradient, 500 nm detection). The solvent was subsequently removed by lyophilization to yield 1.4 mg of pink oil (yield = 70%): **HRMS** $[M+H]^+$ *m/z* 900.4471 (calcd.), 900.4462 (found).

**10-(Diethoxyphosphoryl)decyl but-3-yn-1-ylcarbamate (9)**

To solution of **5** (790 mg) and DIEA (0.35 mL) in $Et_2O$ (10 mL) was added 1-amino-3-butyne (0.165 mL), leading to rapid precipitation of *N*-hydroxysuccinimide as a white solid. After stirring at RT overnight, the solvent was removed at low pressure.

The crude product was dissolved in 1:1 EtOAc:hexanes (3 mL) and chromatographed on silica gel (50–100% EtOAc:hexanes) to yield 615 mg of colorless oil (yield = 87%): **$^1$H NMR** (500 MHz, $CDCl_3$) δ 4.87 (s, 1H), 4.04–4.13 (m, 6H), 3.29 (q, *J* = 5 Hz, 2H), 2.25 (td, *J* = 10, 5 Hz, 2H), 1.98 (t, *J* = 1.7 Hz, 1H), 1.68–1.76 (m, 4H), 1.44–1.66 (br, 4H), 1.25–1.41 (br, 18H)

**(10-((But-3-yn-1-ylcarbamoyl)oxy)decyl)phosphonic acid**

A solution of **9** (223 mg) in DCM (5 mL) was cooled to 0$^o$C. To this was added bromotrimethylsilane (0.3 mL) with stirring for 15 min, at which point the mixture was warmed to RT and allowed to stir overnight. The solvent was removed in vacuo and the oily residue was dissolved in 1:1 $H_2O$:acetone (10 mL) and stirred for 4 h. The mixture was extracted with DCM (3 x 5 mL). Organic fractions were combined, washed with brine, and dried over $Na_2SO_4$. The solvent was removed in vacuo to give 214 mg of white solid that was used without further purification: **HRMS** $[M+H]^+$ *m/z* 334.1778 (calcd.), 334.1779 (found).

**10-(((4-(((*tert*-Butoxycarbonyl)amino)methyl)benzyl)oxy)(hydroxy)phosphoryl)decyl but-3-yn-1-ylcarbamate (10)**

A solution of (10-((But-3-yn-1-ylcarbamoyl)oxy)decyl)phosphonic acid (214 mg) and 4-(Boc-aminomethyl)benzyl alcohol (172 mg) in tetrahydrofuran (1 mL) was heated to reflux at 75$^o$C. To this was added a solution of *N*,*N'*-dicyclohexyl carbodiimide (160 mg) in tetrahydrofuran (3 mL) over a period of 1.5 h. This was stirred for 24 h, after which point the reaction was cooled to RT and filtered through a celite pad to remove the insoluble urea byproduct. The filtrate was directly

purified by preparative LC (0.2–90% MeCN:$H_2O$ gradient, 254 nm detection) to give 67 mg of a colorless oil (yield = 19% over two steps): **$^1$H NMR** (500 MHz, $CDCl_3$) δ 7.32 (d, *J* = 8 Hz, 2H), 7.25 (d, *J* = 8 Hz, 3H), 4.99 (d, *J* = 7.5 Hz, 2H), 4.29 (s, 2H), 4.04 (m, 3H), 3.33 (t, J = 6.75 Hz, 2H), 2.40 (td, *J* = 3, 7 Hz, 2H), 2.00 (t, *J* = 2.5 Hz, 1H), 1.67–1.79 (m, 3H), 1.54–1.66 (m br, 5H), 1.46 (s, 9H), 1.21–1.39 (br, 15H); **$^{13}$C NMR** (125 MHz, $CDCl_3$) δ 156.6, 135.5, 128.0, 127.6, 69.9, 65.9, 65.8, 65.1, 30.5, 30.4, 29.4, 29.2, 29.2, 29.0, 28.4, 26.5, 25.8, 25.4, 22.2, 22.1, 19.9; **HRMS** $[M+H]^+$ *m/z* 553.3043 (calcd.), 553.3037 (found).

**10-(((4-(((*tert*-Butoxycarbonyl)amino)methyl)benzyl)oxy)fluorophosphoryl)decyl but-3-yn-1-ylcarbamate**

A solution of **10** (107 mg) in DCM (1.5 mL) was cooled to 0$^o$C and to it was added diethylaminosulfur trifluoride (52 uL). The reaction was stirred for 30 min at 0$^o$C. Then was added ice-cold 5% w/v $NaHCO_3$ and the two phases were stirred for 15 min at RT. The phases were separated and the aqueous layer was extracted with DCM (3 x 1 mL). Organic layers were dried over $Na_2SO_4$, and the solvent was removed in vacuo to give 81 mg of a colorless oil which was used without further purification

**10-(((4-(Aminomethyl)benzyl)oxy)fluorophosphoryl)decyl but-3-yn-1-ylcarbamate (11)**

Crude 10-(((4-(Aminomethyl)benzyl)oxy)fluorophosphoryl)decyl but-3-yn-1-ylcarbamate (81 mg) was dissolved in 33% TFA in DCM. After 1 h, the solvent was removed under vacuum, and the pale-yellow oily residue was precipitated in water,

frozen, and lyophilized to give a fluffy white solid. The solid was reconstituted with methanol and purified by preparative LC to yield 72 mg of white solid after lyophilization (yield = 73%): **$^{1}$H NMR** (500 MHz, $CDCl_3$) δ 7.47 (s, 4H), 5.21 (d, *J* = 9 Hz, 2H), 4.09 (s, 2H), 4.03 (t, *J* = 6.8 Hz, 2H), 3.35 (s, 1H), 3.29 (t, *J* = 6.75, 2H), 2.39 (td, *J* = 3, 7 Hz, 2H), 2.10 (t, *J* = 2.8 Hz, 1H), 1.92–2.02 (m, 2H), 1.56–1.73 (m, 5H), 1.38–1.46 (br, 2H), 1.25–1.38 (br, 10H); **$^{13}$C NMR** (125 MHz, $CDCl_3$) δ 133.2, 128.9, 128.5, 67.6, 67.5, 42.6, 39.3, 29.9, 29.8, 29.1, 28.9, 28.7, 28.6, 25.5, 21.5, 21.4, 19.3; **HRMS** $[M+H]^+$ *m/z* 455.2469 (calcd.), 455.2469 (found).

*Biological Materials and Equipment*

Valacyclovir hydrochloride, acyclovir, and AEBSF were purchased from Sigma-Aldrich (St. Louis, MO) and used without further purification. FP-PEG-biotin and FP-TAMRA were prepared by Dr. Hao Xu according to previously reported procedures.[48,50] Recombinant BPHL was prepared and generously gifted by Dr. Longsheng Lai. Pooled human intestinal S9 was purchased from Sekisui XenoTech (Lawrence, KS). SDS-PAGE Tris-glycine running buffer (10x), loading buffer (2x), NuPAGE™ reducing agent (10x), and polyacrylamide gels (8 x 8 x 0.1 cm) were purchased from ThermoFisher (Waltham, MA). For cell culture experiments, all media and supplements were purchased from ThermoFisher. Phosphate-buffered saline pH 7.4 (PBS) was purchased from Gibco (ThermoFisher).

*Cell Culture*

The human colon carcinoma cell line Caco-2 (ATCC, HTB-37) was passaged at least six times and grown two weeks post-confluence in Dulbecco's

Minimum Essential Medium with 10% heat-inactivated fetal bovine serum, 1% penicillin-streptomycin and glutamine in 5% $CO_2$ at 37°C. After washing with ice-cold PBS (pH 7.4), cells were harvested by scraping and immediately homogenized by probe sonication on ice. Crude lysates were first spun at 9000 *g* for 20 min, yielding the S9 fraction which was further spun at 100000 *g* for 1 h. The supernatant was used as the cytosolic fraction (S100), while the pellet was resuspended in PBS with 0.1% v/v Triton X-100 and used as the membrane fraction (P100). Protein concentrations were determined by BCA assay, after which aliquots of lysate were stored at -80°C until use.

*Animals*

Animal studies were conducted in accordance with the Guide for the Care and Use of Laboratory Animals as adopted and promulgated by the U.S. National Institutes of Health. *Bphl*-KO mice (pure C57BL/6 strain) were a generous gift from the Institut Clinique de la Souris (Illkirch Cedex, France) and were validated by genotyping. Gender-matched mice (pure C57BL/6 strain), 8–10 weeks old, were used in all the following procedures. The mice were kept in temperature-controlled housing with a 12/12-h light/dark cycle and received a standard diet and water *ad libitum* as provided by the Unit for Laboratory Animal Medicine, University of Michigan, Ann Arbor, MI.

*Lysate Preparation*

One WT and one KO mouse, both male, were sacrificed by cervical dislocation and immediately dissected. The liver and jejunal segment were excised and rinsed in ice-cold PBS to remove blood and bowel remnants. Both tissues

were cut into smaller pieces by razor and Dounce homogenized on ice. Crude lysates were spun 20 min at 9,000 x *g* and 4 °C, and the supernatant S9 fractions were centrifuged for another 60 min at 100,000 x *g* and 4 °C. The supernatant was used as the soluble fraction (S100), and the pellet was resuspended in PBS with 0.1% Triton X-100 and used as the membrane fraction (P100). Lysates were aliquoted and stored at –80 °C until use.

*VACV Activation Probe Inhibition Assay*

Caco-2 lysate or Bphl-KO mouse jejunum/liver lysate (all 1 mg/mL) in PBS (pH 7.4) or rBPHL (0.2 µg/mL) in PBS with 0.1% w/v bovine serum albumin (BSA) was pretreated with inhibitors or vehicle at RT at least 30 min prior to reaction initiation. Reactions were preheated at 37°C for 3 to 5 min, at which point VACV was added to a final concentration of 1 mM to initiate the reaction. At 5, 10, and 15 min post-initiation, aliquots of the reaction were quenched in two to four volumes of chilled organic solvent (acetonitrile or methanol) with 0.1% v/v trifluoroacetic acid (TFA). Precipitated protein was pelleted at 14000 *g* for 5 min, with the supernatant analyzed on Agilent 1100 Series HPLC equipped with a reverse-phase Zorbax Eclipse XDB-C18 column (4.6 x 150 mm, 3.5 µm particle size). A binary solvent gradient from 2% to 90% MeCN in dd$H_2O$ (both with 0.1% TFA) with 1.0 mL/min flow rate was used for separation with UV-based detection at 254 nm. External standards were used to determine the linear range of VACV and ACV while relative peak areas were used to calculate hydrolytic activity. To account for chemical hydrolysis of VACV, control reactions without enzyme were also assayed.

*Optimization of In-Gel Probe Labeling Conditions*

Caco-2 lysate (1 mg/mL) in PBS (pH 7.4) was incubated with AMB-FP-TAMRA (5 or 0.5 μM) at RT. At predetermined time points, an aliquot of the reaction was quenched in 1.25 volumes of 2x SDS loading buffer and 0.25 volumes of 0.5 M dithiothreitol. After heating to 90°C for 10 min, 15 μL per sample was electrophoresed in a Tris-glycine buffer system 226 V for 45 to 50 min. BenchMark™ Fluorescent Protein Standard (Invitrogen) was used for crude molecular weight determination. Gels were scanned on a Typhoon 9200 variable mode imager (Amersham) using 580 nm bandpass emission filter for TAMRA.

*In-Gel Probe Target Comparison in Caco-2*

Caco-2 lysate (1 mg/mL) in PBS (pH 7.4) was pretreated with inhibitor (FP-PEG-biotin or AMB-FP-alk) or vehicle at RT at least 30 min prior to labeling. FP-TAMRA (2 or 5 μM) or AMB-FP-TAMRA (5 or 10 μM) was added and allowed to label lysates for 30 min, at which point the reaction was quenched with 1.25 volumes of 2x SDS loading buffer and 0.25 volumes of 0.5 M dithiothreitol. After heating to 90°C for 10 min, 15 μL per sample was electrophoresed in a Tris-glycine buffer system 226 V for 45 to 50 min. BenchMark™ Fluorescent Protein Standard (Invitrogen) was used for crude molecular weight determination. Gels were scanned on a Typhoon 9200 variable mode imager (Amersham) using 580 nm bandpass emission filter for TAMRA.

*In-Gel Probe Target Comparison in Cell/Tissue Lysates*

FP-TAMRA (5 μM) or AMB-FP-TAMRA (10 μM) was incubated in either Caco-2 S100, Caco-2 P100, Capan-2 S9, mouse liver S100, mouse jejunal S100,

or human intestinal S9 (all 1 $mg \cdot mL^{-1}$) at RT. After 30 min, the reactions were quenched in 1.25 volumes of SDS loading buffer and 0.25 volumes of dithiothreitol (50 mM). Samples were heated to 90 °C for 10 min, and 15 µL per sample were electrophoresed on a 4–20% crosslinker gradient gel at 226 V for 50 min. BenchMark™ Fluorescent Protein Standard (ThermoFisher) was used for approximate molecular weight determination. Gels were scanned using a 580 nm bandpass emission filter for TAMRA fluorescence.

## References


1. Huttunen KM, Raunio H, Rautio J. Prodrugs--from Serendipity to Rational Design. *Pharmacol Rev*. 2011;63(3):750-771. doi:10.1124/pr.110.003459

2. Dammann HG, Burkhardt F, Wolf N. Enteric coating of aspirin significantly decreases gastroduodenal mucosal lesions. *Aliment Pharmacol Ther*. 1999;13(8):1109-1114. doi:10.1046/j.1365-2036.1999.00588.x

3. Gupta S, Kesarla R, Omri A. Formulation strategies to improve the bioavailability of poorly absorbed drugs with special emphasis on self-emulsifying systems. *ISRN Pharm*. 2013;2013:1-16. doi:10.1155/2013/848043

4. Sohi H, Sultana Y, Khar RK. Taste masking technologies in oral pharmaceuticals: recent developments and approaches. *Drug Dev Ind Pharm*. 2004;30(5):429-448. doi:10.1081/DDC-120037477

5. Ratnaparkhi P, Jyoti GP, Mukesh. Sustained release oral drug delivery system - an overview. *Int J Pharma Res Rev IJPRR*. 2013;2(23):11-21.

6. Rautio J, Meanwell NA, Di L, Hageman MJ. The expanding role of prodrugs in contemporary drug design and development. *Nat Rev Drug Discov*. 2018;17(8):559-587. doi:10.1038/nrd.2018.46

7. FDA F and DA. Guidance for Industry: Applications Covered by Section 505(b)(2). *Guidance*. 1999;505(October):1-12. http://www.fda.gov/cder/guidance/index.htm. Accessed August 18, 2019.

8. Clas S-D, Sanchez RI, Nofsinger R. Chemistry-enabled drug delivery (prodrugs): recent progress and challenges. *Drug Discov Today*. 2014;19(1):79-87. doi:10.1016/j.drudis.2013.08.014

9. Ram PR, Priyanka P, Shreekrishna L, Saroj S. Prodrug as a novel approach of drug delivery - a review. *J Drug Deliv Ther*. 2015;5(3):5-9.

10. Wu KM. A new classification of prodrugs: Regulatory perspectives. *Pharmaceuticals*. 2009;2(3):77-81. doi:10.3390/ph2030077

11. Tirkkonen T, Laine K. Drug interactions with the potential to prevent prodrug activation as a common source of irrational prescribing in hospital inpatients. *Clin Pharmacol Ther*. 2004;76(6):639-647. doi:10.1016/j.clpt.2004.08.017

12. Zhang C, Xu Y, Zhong Q, et al. In vitro evaluation of the inhibitory potential of pharmaceutical excipients on human carboxylesterase 1A and 2. *PLoS*

*One*. 2014;9(4). doi:10.1371/journal.pone.0093819

13. Harper TW, Brassil PJ. Reaction phenotyping: Current industry efforts to identify enzymes responsible for metabolizing drug candidates. *AAPS J*. 2008;10(1):200-207. doi:10.1208/s12248-008-9019-6

14. Di L. Reaction phenotyping to assess victim drug-drug interaction risks. *Expert Opin Drug Discov*. 2017;12(11):1105-1115. doi:10.1080/17460441.2017.1367280

15. Zhang Y, Fonslow BR, Shan B, Baek M-C, Yates JR. Protein Analysis by Shotgun/Bottom-up Proteomics. 2013. doi:10.1021/cr3003533

16. Saghatelian A, Cravatt BF. Assignment of protein function in the postgenomic era. *Nat Chem Biol*. 2005;1(3):129. doi:10.1038/nchembio0805-130

17. Cravatt BF, Wright AT, Kozarich JW. Activity-Based Protein Profiling: From Enzyme Chemistry to Proteomic Chemistry. *Annu Rev Biochem*. 2008;77(1):383-414. doi:10.1146/annurev.biochem.75.101304.124125

18. Liu Y, Patricelli MP, Cravatt BF. Activity-based protein profiling: The serine hydrolases. *Proc Natl Acad Sci*. 1999;96(26):14694-14699. doi:10.1073/pnas.96.26.14694

19. van Rooden EJ, Bakker AT, Overkleeft HS, van der Stelt M. Activity-Based Protein Profiling. *eLS*. 2018:1-9. doi:10.1002/9780470015902.a0023406

20. Wang K, Yang T, Wu Q, Zhao X, Nice EC, Huang C. Chemistry-based functional proteomics for drug target deconvolution. *Expert Rev Proteomics*. 2012;9(3):293-310. doi:10.1586/epr.12.19

21. Jeffery DA, Bogyo M. Chemical proteomics and its application to drug discovery. *Curr Opin Biotechnol*. 2003;14(1):87-95. doi:10.1016/S0958-1669(02)00010-1

22. Bantscheff M, Scholten A, Heck AJR. Revealing promiscuous drug-target interactions by chemical proteomics. *Drug Discov Today*. 2009;14(21-22):1021-1029. doi:10.1016/j.drudis.2009.07.001

23. Xu H, Majmudar JD, Davda D, et al. Substrate-Competitive Activity-Based Profiling of Ester Prodrug Activating Enzymes. *Mol Pharm*. 2015;12(9):3399-3407. doi:10.1021/acs.molpharmaceut.5b00414

24. Liederer BM, Borchardt RT. Enzymes involved in the bioconversion of ester-based prodrugs. *J Pharm Sci*. 2006;95(6):1177-1195. doi:10.1002/jps.20542

25. Sun Z, Murry DJ, Sanghani SP, et al. Methylphenidate is stereoselectively hydrolyzed by human carboxylesterase CES1A1. *J Pharmacol Exp Ther*. 2004;310(2):469-476. doi:10.1124/jpet.104.067116

26. Pindel E V., Kedishvili LNY, Abraham TL, et al. Purification and cloning of a human liver carboxylesterase that catalyzes the hydrolysis of cocaine and heroin. *FASEB J*. 1997;11(9):14769-14775.

27. Imai T, Ohura K. The Role of Intestinal Carboxylesterase in the Oral Absorption of Prodrugs. *Curr Drug Metab*. 2011;11(9):793-805. doi:10.2174/138920010794328904

28. Laizure SC, Parker RB, Herring VL, Hu ZY. Identification of carboxylesterase-dependent dabigatran etexilate hydrolysis. *Drug Metab Dispos*. 2014;42(2):201-206. doi:10.1124/dmd.113.054353

29. Shi D, Yang J, Yang D, et al. Anti-Influenza Prodrug Oseltamivir Is Activated by Carboxylesterase Human Carboxylesterase 1, and the Activation Is Inhibited by Antiplatelet Agent Clopidogrel. *J Pharmacol Exp Ther*. 2006;319(3):1477-1484. doi:10.1124/jpet.107.120030

30. Danks MK, Morton CL, Krull EJ, et al. Comparison of activation of CPT-11 by rabbit and human carboxylesterases for use in enzyme/prodrug therapy. *Clin Cancer Res*. 1999;5(4):917-924.

31. Kim I, Chu XY, Kim S, Provoda CJ, Lee KD, Amidon GL. Identification of a human valacyclovirase: Biphenyl hydrolase-like protein as valacyclovir hydrolase. *J Biol Chem*. 2003;278(28):25348-25356. doi:10.1074/jbc.M302055200

32. Beauchamp LM, Orr GF, De Miranda P, Burnette T, Krenitsky TA. Amino acid ester prodrugs of acyclovir. *Antivir Chem Chemother*. 1992;3(3):157-164. doi:10.1177/095632029200300305

33. Ganapathy ME, Huang W, Wang H, Ganapathy V, Leibach FH. Valacyclovir: A substrate for the intestinal and renal peptide transporters PEPT1 and PEPT2. *Biochem Biophys Res Commun*. 1998;246(2):470-475. doi:10.1006/bbrc.1998.8628

34. Balimane P V., Tamai I, Guo A, et al. Direct evidence for peptide transporter (PepT1)-mediated uptake of a nonpeptide prodrug, valacyclovir. *Biochem Biophys Res Commun*. 1998;250(2):246-251. doi:10.1006/bbrc.1998.9298

35. Lai L, Xu Z, Zhou J, Lee K-D, Amidon GL. Molecular Basis of Prodrug Activation by Human Valacyclovirase, an a-Amino Acid Ester Hydrolase. *J Biol Chem*. 2008;283(14):9318-9327. doi:10.1074/jbc.M709530200

36. Kim I, Song X, Vig BS, et al. A novel nucleoside prodrug-activating enzyme: substrate specificity of biphenyl hydrolase-like protein. *Mol Pharm*. 2004;1(2):117-127. doi:10.1021/mp0499757

37. Kim I, Crippen GM, Amidon GL. Structure and specificity of a human valacyclovir activating enzyme: a homology model of BPHL. *Mol Pharm*. 2004;1(6):434-446. doi:10.1021/mp049959+

38. Sun J, Dahan A, Walls ZF, Lai L, Lee KD, Amidon GL. Specificity of a prodrug-activating enzyme hVACVase: The leaving group effect. *Mol Pharm*. 2010;7(6):2362-2368. doi:10.1021/mp100300k

39. Sun J, Dahan A, Amidon GL. Enhancing the intestinal absorption of molecules containing the polar guanidino functionality: A double-targeted prodrug approach. *J Med Chem*. 2010;53(2):624-632. doi:10.1021/jm9011559

40. Dahan A, Khamis M, Agbaria R, Karaman R. Targeted prodrugs in oral drug delivery: the modern molecular biopharmaceutical approach. *Expert Opin Drug Deliv*. 2012;9(8):1001-1013. doi:10.1517/17425247.2012.697055

41. Kim I. A Novel Prodrug Activating Enzyme: Identification and Characterization of BPHL. *Dr Thesis*. 2004. doi:10.1016/B978-012397720-5.50034-7

42. Hu Y, Epling D, Shi J, et al. Effect of biphenyl hydrolase-like (BPHL) gene disruption on the intestinal stability, permeability and absorption of valacyclovir in wildtype and Bphl knockout mice. *Biochem Pharmacol*. 2018;156(August):147-156. doi:10.1016/j.bcp.2018.08.018

43. Patricelli MP, Giang DK, Stamp LM, Burbaum JJ. Direct visualization of serine hydrolase activities in complex proteomes using fluorescent active site-directed probes. *Proteomics*. 2001;1(9):1067-1071. doi:10.1002/1615-9861(200109)1:9<1067::AID-PROT1067>3.0.CO;2-4

44. Bachovchin DA, Ji T, Li W, et al. Superfamily-wide portrait of serine hydrolase inhibition achieved by library-versus-library screening. *Proc Natl Acad Sci U S A*. 2010;107(49):20941-20946. doi:10.1073/pnas.1011663107

45. Lai L. Structure and Function of a Prodrug Activating Enzyme Valacyclovir Hydrolase. *Dr Thesis*. 2006. doi:10.1017/S0165115300023299

46. Middleton WJ. New Fluorinating Reagents. Dialkylaminosulfur Fluorides. *J Org Chem*. 1975;40(5):574-578. doi:10.1021/jo00893a007

47. Burger A, Anderson JJ. Monoesters and Ester-amidates of Aromatic Phosphonic Acids. *J Am Chem Soc*. 1957;79(13):3575-3579. doi:10.1021/ja01570a073

48. Xu H, Sabit H, Amidon GL, Showalter HDH. An improved synthesis of a fluorophosphonate-polyethylene glycol-biotin probe and its use against competitive substrates. *Beilstein J Org Chem*. 2013;9:89-96. doi:10.3762/bjoc.9.12

49. McKenna CE, Higa MT, Cheung NH, McKenna MC. The facile dealkylation of phosphonic acid dialkyl esters by bromotrimethylsilane. *Tetrahedron Lett*. 1977;18(2):155-158. doi:10.1016/S0040-4039(01)92575-4

50. Kidd D, Liu Y, Cravatt BF. Profiling serine hydrolase activities in complex proteomes. *Biochemistry*. 2001;40(13):4005-4015. doi:10.1021/bi002579j

51. Strelow JM. A Perspective on the Kinetics of Covalent and Irreversible Inhibition. *J Biomol Screen*. 2017;22(1):3-20. doi:10.1177/1087057116671509

52. Worek F, Thiermann H, Szinicz L, Eyer P. Kinetic analysis of interactions between human acetylcholinesterase, structurally different organophosphorus compounds and oximes. *Biochem Pharmacol*. 2004;68(11):2237-2248. doi:10.1016/j.bcp.2004.07.038

53. Adibekian A, Martin BR, Chang JW, et al. Confirming target engagement for reversible inhibitors in vivo by kinetically tuned activity-based probes. *J Am Chem Soc*. 2012;134(25):10345-10348. doi:10.1021/ja303400u

54. Sharman J, Pennick M. Lisdexamfetamine prodrug activation by peptidase-mediated hydrolysis in the cytosol of red blood cells. *Neuropsychiatr Dis Treat*. 2014;10:2275-2280. doi:10.2147/NDT.S70382

55. Speers AE, Cravatt BF. Profiling enzyme activities in vivo using click chemistry methods. *Chem Biol*. 2004;11(4):535-546. doi:10.1016/j.chembiol.2004.03.012

56. Harsha HC, Molina H, Pandey A. Quantitative proteomics using stable isotope labeling with amino acids in cell culture. *Nat Protoc*. 2008;3(3):505-516. doi:10.1038/nprot.2008.2

57. Yang Y, Yang X, Verhelst SHL. Comparative analysis of click chemistry mediated activity-based protein profiling in cell lysates. *Molecules*. 2013;18(10):12599-12608. doi:10.3390/molecules181012599

58. Bachovchin DA, Brown SJ, Rosen H, Cravatt BF. Identification of selective inhibitors of uncharacterized enzymes by high-throughput screening with fluorescent activity-based probes. *Nat Biotechnol*. 2009;27(4):387-394. doi:10.1038/nbt.1531

59. Bachovchin DA, Koblan LW, Wu W, et al. A high-throughput, multiplexed assay for superfamily-wide profiling of enzyme activity. *Nat Chem Biol*. 2014;10(8):656-663. doi:10.1038/nchembio.1578

60. Bachovchin DA, Mohr JT, Speers AE, et al. Academic cross-fertilization by public screening yields a remarkable class of protein phosphatase methylesterase-1 inhibitors. *Proc Natl Acad Sci U S A*. 2011;108(17):6811-6816. doi:10.1073/pnas.1015248108

61. Wilk S, Orlowski M. Inhibition of Rabbit Brain Prolyl Endopeptidase by N-Benzyloxycarbonyl-Prolyl-Prolinal, a Transition State Aldehyde Inhibitor. *J Neurochem*. 1983;41(1):69-75. doi:10.1111/j.1471-4159.1983.tb11815.x

62. Hett EC, Xu H, Geoghegan KF, et al. Rational Targeting of Active-Site

Tyrosine Residues Using Sulfonyl Fluoride Probes. 2015. doi:10.1021/cb5009475

63. M. Vorobiev S, Janet Huang Y, Seetharaman J, et al. Human Retinoblastoma Binding Protein 9, a Serine Hydrolase Implicated in Pancreatic Cancers. *Protein Pept Lett*. 2012;19(2):194-197. doi:10.2174/092986612799080356

64. Woitach JT, Zhang M, Niu CH, Thorgeirsson SS. A retinoblastoma-binding protein that affects cell-cycle control and confers transforming ability. *Nat Genet*. 1998;19(4):371-374. doi:10.1038/1258

65. Shields DJ, Niessen S, Murphy EA, et al. RBBP9: A tumor-associated serine hydrolase activity required for pancreatic neoplasia. *Proc Natl Acad Sci*. 2010;107(5):2189-2194. doi:10.1073/pnas.0911646107

66. Vorobiev SM, Su M, Seetharaman J, et al. Crystal structure of human retinoblastoma binding protein 9. *Proteins Struct Funct Bioinforma*. 2009;74(2):526-529. doi:10.1002/prot.22278

67. Simon GM, Cravatt BF. Activity-based proteomics of enzyme superfamilies: Serine hydrolases as a case study. *J Biol Chem*. 2010;285(15):11051-11055. doi:10.1074/jbc.R109.097600

68. Hidalgo IJ, Li J. Carrier-mediated transport and efflux mechanisms of Caco-2 cells. *Adv Drug Deliv Rev*. 1996;22(1-2):53-66. doi:10.1016/S0169-409X(96)00414-0

69. Sambuy Y, De Angelis I, Ranaldi G, Scarino ML, Stammati A, Zucco F. The Caco-2 cell line as a model of the intestinal barrier: influence of cell and culture-related factors on Caco-2 cell functional characteristics. *Cell Biol Toxicol*. 2005;21(1):1-26. doi:10.1007/s10565-005-0085-6

70. Imai, Teruko; Masumi, Imoto; Sakamoto, Hisae; Hashimoto M. Identification of esterases expressed in Caco-2 cells and effects of their hydrolyzing activity in predicting human intestinal absorption. *Drug Metab Dispos*. 2005;33(8):1185-1190. doi:10.1124/dmd.105.004226.tion

71. Imai T, Taketani M, Shii M, Hosokawa M, Chiba K. Substrate specificity of carboxylesterase isozymes and their contribution to hydrolase activity in human liver and small intestine. *Drug Metab Dispos*. 2006;34(10):1734-1741. doi:10.1124/dmd.106.009381

72. Hosokawa M. Structure and catalytic properties of carboxylesterase isozymes involved in metabolic activation of prodrugs. *Molecules*. 2008;13(2):412-431. doi:10.3390/molecules13020412

73. Bar-Even A, Noor E, Savir Y, et al. The moderately efficient enzyme: Evolutionary and physicochemical trends shaping enzyme parameters. *Biochemistry*. 2011;50(21):4402-4410. doi:10.1021/bi2002289

74. Yang B, Hu Y, Smith DE. Impact of peptide transporter 1 on the intestinal

absorption and pharmacokinetics of valacyclovir after oral dose escalation in wild-type and PepT1 knockout mice. *Drug Metab Dispos*. 2013;41(10):1867-1874. doi:10.1124/dmd.113.052597

75. Hidalgo IJ, Raub TJ, Borchardt RT. Characterization of the Human Colon Carcinoma Cell Line (Caco-2) as a Model System for Intestinal Epithelial Permeability. *Gastroenterology*. 1989;96(2):736-749. doi:10.1016/S0016-5085(89)80072-1

76. Inoue M, Morikawa M, Tsuboi M, Sugiura M. Species Difference and Characterization of Intestinal Esterase on the Hydrolizing Activity of Ester-Type Drugs. *Jpn J Pharmacol*. 1979;29(1):9-16. doi:10.1254/jjp.29.9

77. Taketani M, Shii M, Ohura K, Ninomiya S, Imai T. Carboxylesterase in the liver and small intestine of experimental animals and human. *Life Sci*. 2007;81(11):924-932. doi:10.1016/j.lfs.2007.07.026

78. Puente XS, Lopez-Otin C. Cloning and Expression Analysis of a Novel Human Serine Hydrolase with Sequence Similarity to Prokaryotic Enzymes Involved in the Degradation of Aromatic Compounds. *J Biol Chem*. 1995;270(21):12926-12932. doi:10.1074/jbc.270.21.12926

79. Debbage PL, Griebel J, Ried M, Gneiting T, DeVries A, Hutzler P. Lectin intravital perfusion studies in tumor-bearing mice: Micrometer- resolution, wide-area mapping of microvascular labeling, distinguishing efficiently and inefficiently perfused microregions in the tumor. *J Histochem Cytochem*. 1998;46(5):627-639. doi:10.1177/002215549804600508

# CHAPTER III

## Identification and Validation of Candidate VACV PAEs by cABPP

### Introduction

Despite the well-established uses of cABPP for inhibitor profiling, substrate-based cABPP is not as commonplace. One reason may be the kinetic considerations that must be accounted for to observe competition. Reversible ligands and inhibitors already require more careful optimization of reaction conditions to observe competition than do covalent inhibitors; the added factor of enzymatic turnover makes substrate competition even more sensitive to reaction conditions since substrate concentrations are steadily decreasing. The kinetic behavior of covalent inhibitors can be described by both a reversible binding component, $K_I$, and a covalent inactivation component, $k_{inact}$,[51] analogous to the Michaelis-Menten kinetic parameters $K_M$ and $k_{cat}$, respectively (Figure 3.1). Non-specific organophosphonate inhibitors tend to have low binding affinity (i.e. high $K_I$) but rapidly inactivate their target upon binding (i.e. high $k_{inact}$).[52] Consequently, high substrate concentrations or substrates with low $K_M$ and/or low $k_{cat}$ are advantageous when detection of competition is desired. Alternatively, probes with lower $k_{inact}$ are similarly useful in this regard.[53]

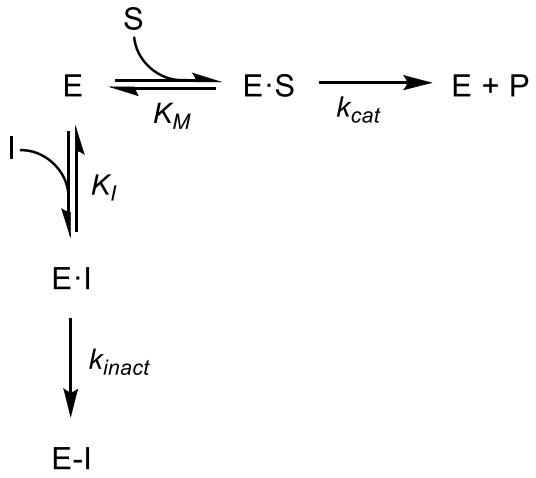


Figure 3.1. Mechanistic model of competitive irreversible inhibition.

In single-binding interactions, substrate and covalent inhibitor compete for free enzyme resulting in either substrate occupancy, whose equilibrium is described by the concentration $K_M$, or inhibitor occupancy, described by the analogous concentration $K_I$. The second step is the irreversible conversion to product, which for substrates leads to product and regenerates the enzyme, described by the rate constant $k_{cat}$. For covalent inhibitors, the enzyme is part of the product, a covalent complex with the inhibitor, and is not regenerated, which is kinetically described the by the analogous rate constant $k_{inact}$.

In addition to optimizing reaction conditions, another challenge in substrate cABPP is presented by the turnover byproducts, which, if allowed to accumulate, can themselves compete with probe labeling, confounding the results if only gel readout is used. After controlling for this, validation is still required to confirm that the enzymes engaged by the substrate are turning them over, not simply being inhibited. These considerations are minor, however, given the simplicity and speed with which cABPP elucidates the number and identity of candidate enzymes with the sought-after activity. For prodrugs whose activating enzyme is not readily determined by cursory reaction phenotyping methods, e.g. lisdexamfetamine,[54] cABPP could vitally aid in this effort.

Among the most useful technological developments of ABPP in the field of drug discovery was its extension to *in vivo* or *in situ* applications by appending click

chemistry functionalities, especially azides and alkynes, to ABPs.[55] Such low-molecular weight and biologically inert moieties enhance the cell permeability and stability of ABPs and enable target identification and selectivity/potency evaluation in more physiologically relevant systems such as intact cells or preclinical organisms. Moreover, the relatively small azide and alkyne functionalities minimally alter the physicochemical properties and binding affinities of ABPs, especially those derived directly from pharmacological inhibitors. When combined with stable isotope labeling methods like SILAC,[56] in which cells are grown in media supplemented with isotopologic amino acids, thus incorporating labels by normal metabolic protein turnover, click-based ABPP is a powerful tool for MS-based identification, and quantitation of even subtle changes in enzyme activity directly within cells—a boon for pharmacological characterization of both enzymes and their modulators in pharmaceutical research and development.

While most biotinylated ABPs are chemically stable, the biotinylated version of AMB-FP, which was able to be synthesized in small quantities (~1 mg), was not stable during storage for reasons that have not been explored. To circumvent this, AMB-FP-alkyne was treated under standard click-CuAAC conditions, with biotin-$(PEG)_3$-azide in organic solvent to pre-generate a biotinylated probe for use in cABPP-MS experiments. Unfortunately, this probe was also unstable in storage, so AMB-FP-alkyne itself was employed in MS-based cABPP experiments. This required extra handling steps, including a desalting step, a click chemistry step, and a precipitation clean-up step, all of which were likely to increase the variability of results of a competitive experiment that was already highly variable due to the

aforementioned sensitivity to kinetic endpoints. We thus used stable isotope labeling using amino acids in cell culture (SILAC) to mitigate this issue, which was a major advantage in using cultured cells for the protein source instead of *ex vivo* tissue samples. Briefly, one cell population is grown in normal media (“light” cells) while another is grown in media containing heavier Arg and Lys isotopologs (“heavy” cells), which are essential amino acids, unable to be synthesized by the cell otherwise. After several rounds of division, the cellular proteome is labeled in its entirety with the respective Arg and Lys. After lysis and treatment with variable or control conditions, the heavy and light samples can be combined in a 1:1 ratio, such that all subsequent handling steps affect both samples equally. This minimizes these extraneous sources of variability, enabling more faithful detection of the effect of the experimental variable itself. To control for potential baseline differences in protein abundance or activity levels between cell populations, treatment and control conditions are applied to both heavy and light proteomes in a reciprocal manner.

In addition to kinetic optimization, adaptation of the gel-based cABPP protocol to an MS-friendly format required the proper selection of sample clean-up techniques and redissolution buffers. An acetone quench/wash step was critical to providing a well-defined endpoint to the competition reaction while simultaneously removing excess probe. Subsequently, a redissolution buffer with high urea and ammonium bicarbonate concentrations was used to dissolve the sample pellets with bath sonication and heating to prepare for solution-phase click chemistry. Next, the removal of urea to provide favorable CuAAC reaction conditions was

accomplished by desalting spin columns. SDS, which also impedes CuAAC,[57] is not efficiently removed by size-exclusion desalting columns when above its critical micellar concentration and was thus omitted from the redissolution buffer. These modifications were critical to translating the gel-based cABPP workflow to an MS-compatible format that could also incorporate CuAAC. The use of MS-based cABPP with substrates is not described in the literature, let alone for the identification of PAEs.

After identifying three candidate VACV PAEs via cABPP-MS, selective inhibitors were used to validate their activity directly in Caco-2 lysates. Only emetine, a selective inhibitor of RBBP9,[58,59] showed any effect, abolishing 95% of VACV activation in Caco-2 S100 at selective concentrations. At the same concentration, emetine only inhibited 17% of VACV hydrolysis by rBPHL. An emetine-competitive ABPP-MS assay was also performed in Caco-2 S100 to ensure that emetine does not inhibit other SHs at 1 mM. Thus, the near-total inhibition of VACV activation in the presence of selective emetine concentrations suggests that RBBP9 may contribute more to gut wall activation of VACV than rBPHL. In addition to identifying RBBP9 as the second likely presystemic PAE for VACV, these findings have revealed the first known substrate of RBBP9.

## Results

*In-Gel Kinetic Optimization of cABPP*

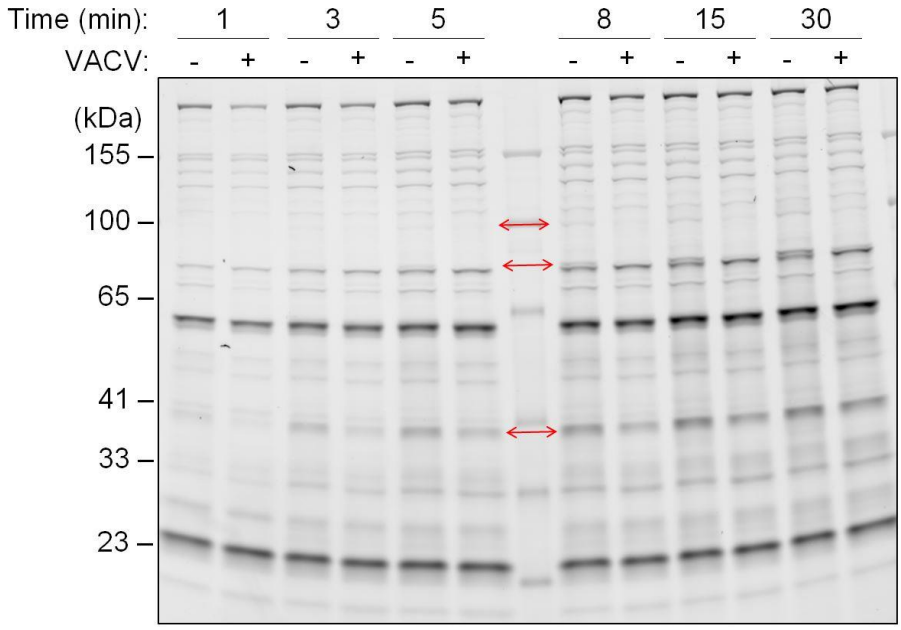


Figure 3.2. Optimization of competition time via gel-based cABPP.

A fluorescent gel scan of VACV-competitive labeling of Caco-2 S100 by AMB-FP-TAMRA (5 µM) at timepoints from 1 to 30 min. Red arrows show VACV-sensitive bands.

Saturating concentrations of VACV (20 mM) were used to compete against AMB-FP-TAMRA labeling in Caco-2 S100, with reactions stopped at various timepoints from 1 to 30 min. Three bands, whose molecular weights were interpolated to 100, 85, and 40 kDa (Figure 3.2, red arrows), were visibly sensitive to VACV, but each one displayed maximal competition at a different timepoint, highlighting the diverse reactivities within the serine hydrolome. The 8 min timepoint was chosen for subsequent studies based on the observation of competition for all three bands, which was confirmed by integration. The experiment was then repeated with 8 min competition using freshly prepared Caco-2 S100 and P100 fractions, resulting the in the detection of an additional VACV-

sensitive band near 25 kDa (Figure 3.3, red arrows). The P100 fraction displayed one 100 kDa band that was more active in the presence of VACV, but none that were less active after VACV treatment, consistent with prior data from our lab which showed around 90% of intestinal VACV activation occurred in the soluble proteome (not shown). These data demonstrate the utility of substrate-based cABPP and the ease with which preliminary screens can be carried out to determine its feasibility for PAE identification on a case-specific basis.

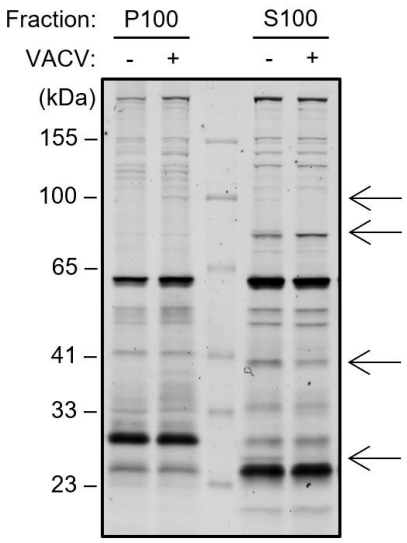


Figure 3.3. Gel-based cABPP with VACV in freshly prepared Caco-2 lysates.

Representative fluorescent gel scan of 20 mM VACV-competitive labeling by AMB-FP-TAMRA (5 μM) in freshly prepared Caco-2 P100 and S100. Black arrows show VACV-sensitive bands.

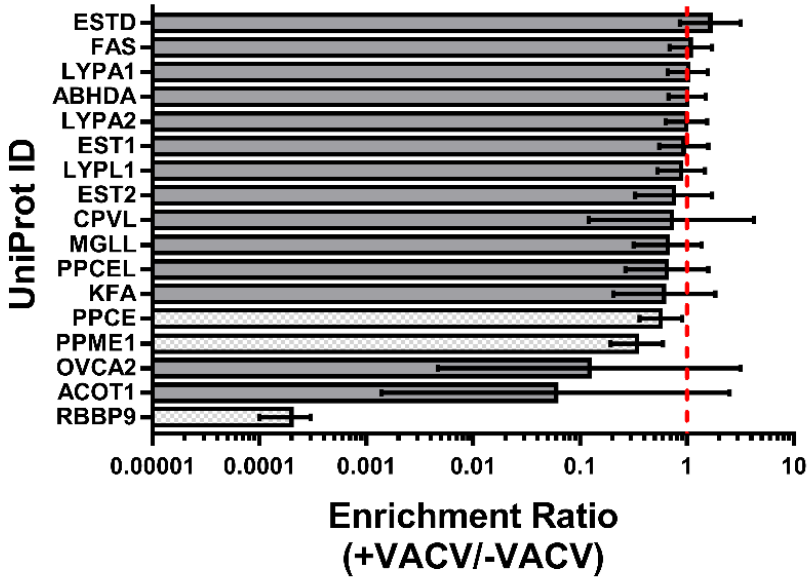


Figure 3.4. VACV cABPP-SILAC in Caco-2 S100.

SILAC enrichment ratios from VACV-competitive ABPP in Caco-2 S100 using 20 mM VACV and 20 μM AMB-FP-alkyne. Results are shown as geometric mean with geometric SD factors (n = 3–4). Checkered bars denote enzymes whose mean and SD factor product is less than one ("hits").

Three SHs with reduced labeling in the presence of VACV were detected by LC-MS/MS (Figure 3.4, checkered bars): RBBP9, PPME1, and PPCE. The MWs predicted from the primary sequences of these candidate VACV PAEs were within 1–4 kDa of the MWs observed in-gel, except for the 100 kDa band. These discrepancies could be due to post-translational modifications or alternative splicing. Notably, RBBP9 labeling was completely inhibited by VACV incubation, essentially undetectable in all treatment samples. Such results were representative of prior non-SILAC cABPP-MS experiments in Caco-2 S100, wherein RBBP9 was not detected after VACV competition.

*In Vitro Validation of RBBP9 Activation of VACV*

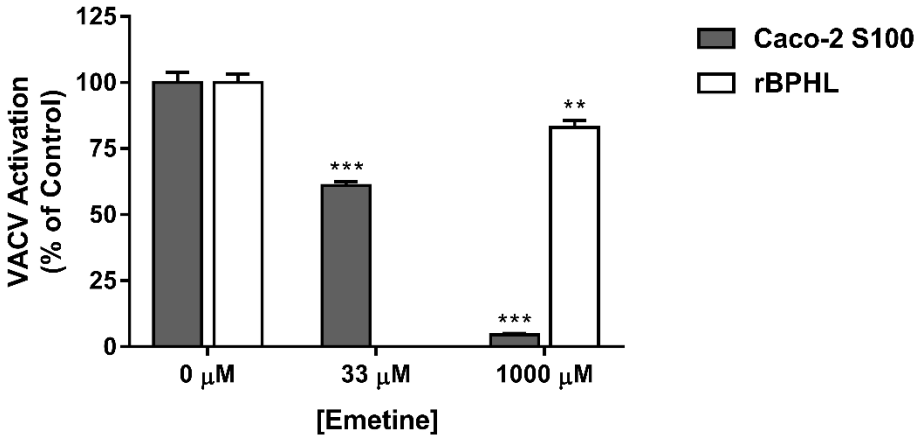


Figure 3.5. Validation of RBBP9 as VACV PAE by emetine inhibition.

Inhibition of VACV activation in Caco-2 S100 and rBPHL by selective RBBP9 inhibitor emetine at two concentrations. Emetine was not assayed against rBPHL at 33 μM. Results are shown as mean ± SD (n = 3). ***p* < .01 and ****p* < .001 by unpaired *t*-test as compared to respective controls at 0 μM.

To validate the VACV PAEs found by MS-based cABPP, selective inhibitors for all three hits were purchased and tested in Caco-2 S100. ABL127, a selective inhibitor of PPME1 with an $IC_{50}$ of 6–12 nM ($K_i$ not determined),[60] produced no detectable inhibition of VACV activation at 100 nM; neither did selective PPCE inhibitor *N*-benzyloxycarbonyl-L-prolyl-L-prolinal at 10 nM, ten times its $K_i$ of 1 nM.[61] Emetine, a commercially available natural product alkaloid found in ipecac syrup, was recently found to selectively inhibit RBBP9 at concentrations up to 33 μM,[59] with gel-based ABPP showing selectivity up to 1 mM in certain RBBP9-doped proteomes.[58] At 33 μM, roughly four times the $IC_{50}$ of 7.8 μM ($K_i$ not determined), emetine inhibited ~40% of VACV activation in Caco-2 S100 (Figure 3.5). At 1 mM, emetine abolished VACV activation (~95%), confirming RBBP9's VACV activation. Because emetine selectivity was established using FP-based assays that cannot test BPHL, the same assay was employed with rBPHL to rule out its inhibition by

emetine, and only 17% inhibition was observed. Based on these data, RBBP9 appears to contribute more to VACV activation than does BPHL in Caco-2 S100. Notably, VACV represents the first reported substrate of RBBP9, synthetic or otherwise.

*Emetine Target Identification by cABPP-SILAC*

| Uniprot ID | Enrichment Ratio (SD Factor) |
|---|---|
| CPVL | 0.295 (3.16) |
| LYPA2 | 0.410 (1.41) |
| PPME1 | 0.474 (1.13) |

Table 3.1. Targets from emetine cABPP-SILAC assay.

A list of SH enzymes in Caco-2 S100 whose labeling by AMB-FP-alkyne (20 μM) was significantly reduced in the presence of 1 mM emetine.

To more confidently conclude from emetine inhibition data that RBBP9 is a VACV PAE, we performed a cABPP-MS assay with 1 mM emetine in Caco-2 S100 (Table 3.1). Prior studies of emetine selectivity were carried out in other cell and tissue lysates, but not in Caco-2. The results revealed three targets of emetine: lysophospholipase 2 (LYPA2), protein phosphatase methylesterase 1 (PPME1), and vitellogenic-like carboxypeptidase (CPVL). Of them, LYPA2 and CPVL were not shown to be targets of VACV by cABPP-MS. On the other hand, PPME1 was shown to be a target of VACV but was subsequently shown not to activate VACV when ABL127 incubation did not alter its hydrolysis rate in lysates. In conclusion, emetine, at the 1 mM concentration used for validation, does not target any potential VACV PAEs in Caco-2 S100, confirming that RBBP9 is indeed activating VACV.

## Discussion

Optimizing one cABPP assay for MS-based readout led to the identification of a new VACV PAE without any *a priori* knowledge, demonstrating the true power of the broad survey enabled by ABPs compounded by state-of-the-art proteomic MS instrumentation and software. Validating the hits after their identification also obviated the need for special controls to address the confounding factor of product inhibition. The validation yielded negative results for the enzymes PPCE and PPME1, suggesting that they are merely binding partners of VACV and not its PAEs. Emetine itself has been well characterized for selectivity within the SH family by ABPP. In conjunction with the observation that AEBSF abolishes VACV activation in Caco-2, it is highly likely that the inhibition of VACV activation by emetine is almost solely the result of RBBP9 inhibition. However, it must be noted there are a handful of reports of sulfonyl fluoride inhibition of non-SH enzymes,[62] so the inhibition of non-SH enzymes by emetine in Caco-2, though unlikely, cannot be definitively ruled out. Though well-characterized inhibitors were used in this study, another potential validation method would be immunoprecipitating the proteins of interest, entailing the use of well-characterized antibodies instead.

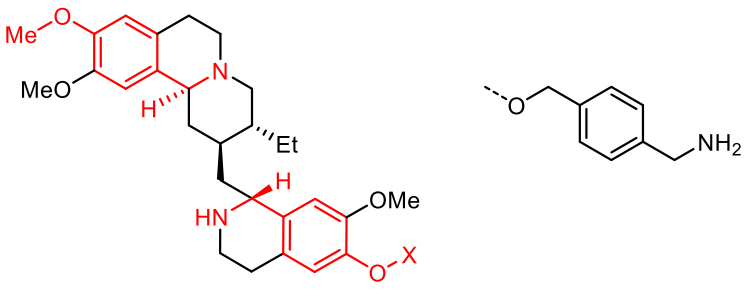


Scheme 3.1. Comparison of emetine and AMB moiety.

Structure of emetine (X = Me) and cephaeline (X = H) with AMB-like motifs highlighted in red (*left*) and an O-substituted AMB moiety drawn as a rotamer emphasizing its similarity (*right*).

A closer look at the structures of the AMB moiety and emetine reveals structural similarities that could explain the affinity of AMB-FP probes for RBBP9: an isomer of the AMB motif in which the positions of the oxygen and methylene group are interchanged is embedded twice within the structure of emetine with conformational restriction of the amino group (Scheme 3.1). In addition, the 6'-*O*-desmethyl analog of emetine, cephaeline, is 3-fold less potent towards RBBP9.[59]

The newly discovered VACV activating enzyme, RBBP9, has been studied in recent years with respect to cellular function, but repeated attempts to find a substrate for it, endogenous or synthetic, have failed.[63] Named for its discovery as the ninth protein to bind the retinoblastoma tumor suppressor protein (*Rb*), this ubiquitously expressed protein was shown to be mandatory for suppression of the TGF-β antiproliferative pathway *in vivo*.[64] This, in combination with its expression in several carcinoma cell lines and significantly elevated activity in pancreatic ductal adenocarcinoma samples,[65] has led to the emergence of RBBP9 as a possible cancer drug target. Structurally, RBBP9 is ~21 kDa with a classic α/β hydrolase superfamily fold.[66] Regarding primary structure, RBBP9 is quite distinct from other human proteins, with the closest being monoacylglyceride lipase (gene: *MGLL*) and, interestingly, BPHL, sharing ~15% sequence identity.[63] The relative similarity to human BPHL may be a coincidence, but the overall uniqueness of the RBBP9 sequence suggests that there may be an opportunity for selectively targeting it. Furthermore, the homology between the human and mouse orthologs of RBBP9 is high (~90%),[67] suggesting that a murine preclinical model may

accurately reflect the *in vivo* disposition of therapeutics primarily metabolized by RBBP9, especially if murine and human expression profiles are similar.

## Methods

*Biological Materials and Equipment*

Valacyclovir hydrochloride, acyclovir, and emetine dihydrochloride were purchased from Sigma-Aldrich (St. Louis, MO) and used without further purification. AMB-FP-alkyne and AMB-FP-TAMRA were prepared as described in the preceding sections. FP-PEG-biotin and FP-TAMRA were prepared by Dr. Hao Xu according to previously reported procedures.[48,50] Recombinant BPHL was prepared and generously gifted by Dr. Longsheng Lai. Recombinant RBBP9 was purchased from Novus Biologicals (Littleton, CO). For biological experiments (cell culture and gel electrophoresis), gels, buffers, and reagents/reagent kits were purchased from ThermoFisher (Waltham, MA). All compositional percentages are reported as v/v unless otherwise noted. Recombinant protein reactions were prepared in low protein-binding plasticware. Gels were electrophoresed on an XCell SureLock Mini-Cell electrophoresis system (ThermoFisher) with a PowerPac power supply adapter from Bio-Rad (Hercules, CA). Fluorescent gels were scanned on a Typhoon 9200 flatbed imager (Amersham, Boston, MA) and integrated using ImageJ software (NIH, Bethesda, MD). Analytical high-performance liquid chromatography (HPLC) was performed on an Agilent 1100 HPLC (Agilent, Santa Clara, CA) equipped with a reverse-phase Zorbax Eclipse XDB-C18 column (4.6 x 150 mm, 3.5 μm). The pH of phosphate-buffered saline (PBS) used in all experiments was 7.4 unless otherwise noted.

*Cell Culture*

The human colon carcinoma cell line Caco-2 (ATCC HTB37) was passaged at least six times and grown two weeks post-confluence in Dulbecco's Minimum Essential Medium supplemented with 10% heat-inactivated fetal bovine serum, 1% penicillin-streptomycin and glutamine in 5% $CO_2$ at 37 °C. Stable isotope-labeled Caco-2 cells were instead grown in lysine- and arginine-deficient SILAC-DMEM supplemented with 100 µg/mL "heavy" Arg ($^{13}C_6$, $^{15}N_4$, +10 Da) and Lys ($^{13}C_6$, $^{15}N_4$, +8 Da) or "light" Arg and Lys. After washing with ice-cold PBS, cells were harvested by scraping and immediately homogenized by probe sonication on ice. Crude lysates were first spun at 9,000 *g* for 20 min, yielding the S9 fraction, which was further spun at 100,000 *g* for 1h. The supernatant was used as the cytosolic fraction (S100), while the pellet was resuspended in PBS with 0.1% Triton X-100 and used as the membrane fraction (P100). No protease inhibitors were used as this would interfere with subsequent studies of esterases. Protein concentrations were determined by BCA assay, after which lysates were aliquoted and stored at -80 °C until use.

*In-Gel Kinetic Optimization of cABPP*

For kinetic optimization, Caco-2 S100 in PBS (1 mg/mL) was pretreated with VACV (20 mM) or vehicle for 5 min at RT, then incubated with AMB-FP-TAMRA (5 µM) at RT. At 1, 3, 5, 8, 15, and 30 min post-initiation, aliquots were quenched in 1.25 volumes of SDS loading buffer and 0.25 volumes of 0.5 M dithiothreitol. Samples were heated to 90 °C for 10 min, and 15 µL per sample were electrophoresed on a 4–20% crosslinker gradient gel at 226 V for 50 min.

BenchMark™ Fluorescent Protein Standard (ThermoFisher) was used for approximate molecular weight determination. Gels were scanned using a 580 nm bandpass emission filter for TAMRA fluorescence.

After optimization, freshly prepared Caco-2 S100 and P100 fractions (both 1 mg/mL) were pretreated with VACV (20 mM) or vehicle for 5 min at RT then incubated with AMB-FP-TAMRA (5 μM) at RT. After 8 min, aliquots were quenched in 1.25 volumes of SDS loading buffer and 0.25 volumes of 0.5 M dithiothreitol and subjected to the same electrophoresis and analysis as for kinetic optimization experiments.

*VACV Target Identification by cABPP-SILAC*

Quadruplicate heavy and light Caco-2 S100 fractions (2 mg/mL, 1 mg total) were pretreated with VACV (20 mM) or vehicle for 2 min, followed by addition of AMB-FP-alkyne (20 μM). After 4 min, VACV-treated heavy (light) and untreated light (heavy) reactions were combined by quenching in the same aliquot of ice-cold acetone (4 mL). After chilling to -20 °C for 30 min, proteins were pelleted at 1,320 g for 10 min. The pellet was washed twice more by sonication in fresh acetone and spun down again. After decanting and air-drying, the cleaned pellet was dissolved in 700 μL of PBS containing 8 M urea and 0.1 M ammonium bicarbonate with heating to 40 °C as needed.

Samples were exchanged into 700 μL PBS using Zeba desalting spin columns (ThermoFisher). To each sample was then added tris(2-carboxyethyl)phosphine (TCEP, 1 mM), tris[(1-benzyl-1H-1,2,3-triazol-4-yl)methyl]amine (100 mM), CuSO4 (1 mM), and biotin-(PEG)3 azide (100 mM),

resulting in immediate formation of a blueish-hued precipitate. The click reaction proceeded for 1.5 h at RT, at which point samples were diluted with 4 mL MeOH, 0.7 mL CHCl3, and 1.5 mL water, vortexed, and centrifuged 10 min at 1,300 g to separate aqueous and organic phases. Both phases were discarded, leaving behind the pellet, which was rinsed twice more by sonicating in an additional 4 mL MeOH and centrifuging.

The biotinylated pellet was dissolved in 700 µL PBS containing 20 mg/mL SDS, 6 M urea, and 50 mM ammonium bicarbonate. Samples were then diluted to 10 mL in PBS and incubated with 50 µL of prewashed (3 x 1 mL PBS) streptavidin-agarose beads (ThermoFisher) for 1.5 h at RT with shaking. Beads were then collected by centrifugation for 2 min at 600 g and washed in PBS with 20 mg/mL SDS and 6 M urea (5 x 700 µL), water with 6 M urea (3 x 800 µL), and PBS (2 x 800 µL). After transferring to low-protein binding microcentrifuge tubes, successive on-bead reduction and alkylation were carried out with iodoacetamide (25 mM, 30 min, RT, dark) and TCEP (10 mM, 30 min, RT), respectively, in PBS with 2 M urea. On-bead digestion was performed overnight with 2 µg SOLu Trypsin (Sigma) in PBS at RT. Beads were spun down at 600 g for 1 min, and the supernatant was transferred onto Oasis C18 solid-phase extraction cartridges (Waters, Milford, MA) for desalting. Tryptic peptides were eluted in 1 mL 50% MeCN/water with 0.1% TFA and concentrated to dryness on a vacuum centrifuge. Before analysis, samples were reconstituted in 60 µL water with 0.1% TFA.

*Emetine Target Identification by cABPP-SILAC*

Duplicate heavy and light Caco-2 S100 fractions (2 mg/mL, 1 mg total) were pretreated with emetine dihydrochloride (1 mM) or vehicle for 2 min, followed by addition of AMB-FP-alkyne (20 μM). After 4 min, VACV-treated heavy (light) and untreated light (heavy) reactions were combined by quenching in the same aliquot of ice-cold acetone (4 mL). All subsequent steps are identical to those reported in the previous subsection (“Identification of VACV Targets by cABPP-MS”).

*Mass Spectrometry and Data Analysis*

Analysis was performed on a TripleTOF 5600 + mass spectrometer (AB Sciex, Framingham, MA) coupled with an Eksigent 2D plus LC system (Eksigent Technologies, Dublin, CA). A trap-elute configuration was used in the LC separation. It consisted of a trapping column (ChromXP C18-CL, 120 Å, 5 μm, 10 × 0.3 mm, Eksigent Technologies, Dublin, CA) and an analytical column (ChromXP C18-CL, 120 Å, 150 × 0.3 mm, 5 μm, Eksigent Technologies, Dublin, CA). The mobile phase A was water containing 0.1% formic acid and mobile phase B was acetonitrile containing 0.1% formic acid. The sample was first loaded and cleaned on the trapping column with the mobile phase A delivered at 10 μL/min for 3 min before being separated on the analytical column with a gradient elution at 5 μL/min for 90 min. The gradient setting was: 0–68 min, 3%–30% B; 68–73 min, 30%–40% B; 73–75 min, 40%–80% B; 75–78 min, 80% B; 78–79 min, 80%–3% B; 79–90 min, 3% B. A blank injection after each sample was used to prevent carryover.

The mass spectrometer was operated in positive ion mode with ion spray voltage floating at 5500 v, ion source gas 1 at 28 psi, gas 2 at 16 psi, curtain gas

at 25 psi and source temperature at 280 °C. A data-dependent acquisition method was used for data acquisition. It consisted of a 250 ms TOF-MS scan from 400 to 1250 Da, followed by MS/MS scans in high sensitivity mode from 100 to 1500 Da for the top 30 precursor ions from the TOF-MS scan (50 ms accumulation time, 10 ppm mass tolerance, charge state from +2 to +5, rolling collision energy, and dynamic accumulation). Former precursor ions were excluded from MS/MS scan for 15 s.

The proteomics data were analyzed using MaxQuant software (version 1.6.2.6, Max Planck Institute of Biochemistry, Germany). The UniProt human proteome AUP000005640 which includes both canonical and isoform protein sequences was used as the peptide search reference. Multiplicity was set as 2 with 13C615N2-Lys and 13C615N4-Arg as heavy labels. “Trypsin/P” was set as the digestion enzyme. Peptide lengths were between 7 and 25 residues with up to two missed cleavage sites allowed. Cys carbamidomethylation was set as a fixed modification. Variable modifications included N-terminal acetylation and Met oxidation. Up to 5 modifications per peptide were allowed. Mass tolerance for precursor was 0.07 Da for the first search and 0.006 Da for the main search, while the tolerance for fragment ions was 40 ppm. A false discovery rate (FDR) of 0.01 was used as the cutoff for both peptide and protein identification.

For VACV-competitive ABPP, the enrichment ratio was calculated as the geometric mean of the ratios of SH intensities in treated samples to those of control samples. If one of the two intensity values in a SILAC pair was zero, it was treated as one instead for calculation purposes. If both intensities were zero (i.e. the SH

was not detected in either sample of a SILAC pair), the undefined value was excluded from calculations. SHs with more than one undefined value were excluded. SHs were considered hits if the product of their mean ratio and SD factor was less than one whereas SHs were excluded if the product was greater than 10.

For emetine-competitive ABPP, the enrichment ratio was calculated identically. If one of the two intensity values in a SILAC pair was zero, it was treated as one instead for calculation purposes. If both intensities were zero (i.e. the SH was not detected in either sample of a SILAC pair), the SH was excluded from consideration because only two SILAC pairs per SH, one in each direction, were assayed. SHs for which both SILAC ratios were less than one were considered targets of emetine. Data acquisition was performed by Dr. Jian Shi.

*In Vitro Validation of RBBP9 Activation of VACV*

Caco-2 S100 (1 mg/mL) or purified recombinant hBPHL (0.2 μg/mL) in PBS in triplicate was incubated with emetine (0.33 or 1 mM) for 5 min at 37 °C. Reactions were initiated by the addition of VACV (1 mM) and were quenched 10 min after initiation in four volumes of MeOH with 0.1% TFA. Proteins were pelleted for 5 min at 14,000 g, followed by analysis of the supernatant via HPLC. A binary solvent gradient from 2% to 90% acetonitrile in water (both with 0.1% TFA) with 1.0 mL/min flow rate was used for separation. Analytes were detected by absorbance at 254 nm. Relative peak areas were used to calculate hydrolytic activity. Non-enzymatic control reactions were used to account for chemical hydrolysis.

## References


1. Huttunen KM, Raunio H, Rautio J. Prodrugs--from Serendipity to Rational Design. *Pharmacol Rev*. 2011;63(3):750-771. doi:10.1124/pr.110.003459

2. Dammann HG, Burkhardt F, Wolf N. Enteric coating of aspirin significantly decreases gastroduodenal mucosal lesions. *Aliment Pharmacol Ther*. 1999;13(8):1109-1114. doi:10.1046/j.1365-2036.1999.00588.x

3. Gupta S, Kesarla R, Omri A. Formulation strategies to improve the bioavailability of poorly absorbed drugs with special emphasis on self-emulsifying systems. *ISRN Pharm*. 2013;2013:1-16. doi:10.1155/2013/848043

4. Sohi H, Sultana Y, Khar RK. Taste masking technologies in oral pharmaceuticals: recent developments and approaches. *Drug Dev Ind Pharm*. 2004;30(5):429-448. doi:10.1081/DDC-120037477

5. Ratnaparkhi P, Jyoti GP, Mukesh. Sustained release oral drug delivery system - an overview. *Int J Pharma Res Rev IJPRR*. 2013;2(23):11-21.

6. Rautio J, Meanwell NA, Di L, Hageman MJ. The expanding role of prodrugs in contemporary drug design and development. *Nat Rev Drug Discov*. 2018;17(8):559-587. doi:10.1038/nrd.2018.46

7. FDA F and DA. Guidance for Industry: Applications Covered by Section 505(b)(2). *Guidance*. 1999;505(October):1-12. http://www.fda.gov/cder/guidance/index.htm. Accessed August 18, 2019.

8. Clas S-D, Sanchez RI, Nofsinger R. Chemistry-enabled drug delivery (prodrugs): recent progress and challenges. *Drug Discov Today*. 2014;19(1):79-87. doi:10.1016/j.drudis.2013.08.014

9. Ram PR, Priyanka P, Shreekrishna L, Saroj S. Prodrug as a novel approach of drug delivery - a review. *J Drug Deliv Ther*. 2015;5(3):5-9.

10. Wu KM. A new classification of prodrugs: Regulatory perspectives. *Pharmaceuticals*. 2009;2(3):77-81. doi:10.3390/ph2030077

11. Tirkkonen T, Laine K. Drug interactions with the potential to prevent prodrug activation as a common source of irrational prescribing in hospital inpatients. *Clin Pharmacol Ther*. 2004;76(6):639-647. doi:10.1016/j.clpt.2004.08.017

12. Zhang C, Xu Y, Zhong Q, et al. In vitro evaluation of the inhibitory potential of pharmaceutical excipients on human carboxylesterase 1A and 2. *PLoS*

*One*. 2014;9(4). doi:10.1371/journal.pone.0093819

13. Harper TW, Brassil PJ. Reaction phenotyping: Current industry efforts to identify enzymes responsible for metabolizing drug candidates. *AAPS J*. 2008;10(1):200-207. doi:10.1208/s12248-008-9019-6

14. Di L. Reaction phenotyping to assess victim drug-drug interaction risks. *Expert Opin Drug Discov*. 2017;12(11):1105-1115. doi:10.1080/17460441.2017.1367280

15. Zhang Y, Fonslow BR, Shan B, Baek M-C, Yates JR. Protein Analysis by Shotgun/Bottom-up Proteomics. 2013. doi:10.1021/cr3003533

16. Saghatelian A, Cravatt BF. Assignment of protein function in the postgenomic era. *Nat Chem Biol*. 2005;1(3):129. doi:10.1038/nchembio0805-130

17. Cravatt BF, Wright AT, Kozarich JW. Activity-Based Protein Profiling: From Enzyme Chemistry to Proteomic Chemistry. *Annu Rev Biochem*. 2008;77(1):383-414. doi:10.1146/annurev.biochem.75.101304.124125

18. Liu Y, Patricelli MP, Cravatt BF. Activity-based protein profiling: The serine hydrolases. *Proc Natl Acad Sci*. 1999;96(26):14694-14699. doi:10.1073/pnas.96.26.14694

19. van Rooden EJ, Bakker AT, Overkleeft HS, van der Stelt M. Activity-Based Protein Profiling. *eLS*. 2018:1-9. doi:10.1002/9780470015902.a0023406

20. Wang K, Yang T, Wu Q, Zhao X, Nice EC, Huang C. Chemistry-based functional proteomics for drug target deconvolution. *Expert Rev Proteomics*. 2012;9(3):293-310. doi:10.1586/epr.12.19

21. Jeffery DA, Bogyo M. Chemical proteomics and its application to drug discovery. *Curr Opin Biotechnol*. 2003;14(1):87-95. doi:10.1016/S0958-1669(02)00010-1

22. Bantscheff M, Scholten A, Heck AJR. Revealing promiscuous drug-target interactions by chemical proteomics. *Drug Discov Today*. 2009;14(21-22):1021-1029. doi:10.1016/j.drudis.2009.07.001

23. Xu H, Majmudar JD, Davda D, et al. Substrate-Competitive Activity-Based Profiling of Ester Prodrug Activating Enzymes. *Mol Pharm*. 2015;12(9):3399-3407. doi:10.1021/acs.molpharmaceut.5b00414

24. Liederer BM, Borchardt RT. Enzymes involved in the bioconversion of ester-based prodrugs. *J Pharm Sci*. 2006;95(6):1177-1195. doi:10.1002/jps.20542

25. Sun Z, Murry DJ, Sanghani SP, et al. Methylphenidate is stereoselectively hydrolyzed by human carboxylesterase CES1A1. *J Pharmacol Exp Ther*. 2004;310(2):469-476. doi:10.1124/jpet.104.067116

26. Pindel E V., Kedishvili LNY, Abraham TL, et al. Purification and cloning of a human liver carboxylesterase that catalyzes the hydrolysis of cocaine and heroin. *FASEB J*. 1997;11(9):14769-14775.

27. Imai T, Ohura K. The Role of Intestinal Carboxylesterase in the Oral Absorption of Prodrugs. *Curr Drug Metab*. 2011;11(9):793-805. doi:10.2174/138920010794328904

28. Laizure SC, Parker RB, Herring VL, Hu ZY. Identification of carboxylesterase-dependent dabigatran etexilate hydrolysis. *Drug Metab Dispos*. 2014;42(2):201-206. doi:10.1124/dmd.113.054353

29. Shi D, Yang J, Yang D, et al. Anti-Influenza Prodrug Oseltamivir Is Activated by Carboxylesterase Human Carboxylesterase 1, and the Activation Is Inhibited by Antiplatelet Agent Clopidogrel. *J Pharmacol Exp Ther*. 2006;319(3):1477-1484. doi:10.1124/jpet.107.120030

30. Danks MK, Morton CL, Krull EJ, et al. Comparison of activation of CPT-11 by rabbit and human carboxylesterases for use in enzyme/prodrug therapy. *Clin Cancer Res*. 1999;5(4):917-924.

31. Kim I, Chu XY, Kim S, Provoda CJ, Lee KD, Amidon GL. Identification of a human valacyclovirase: Biphenyl hydrolase-like protein as valacyclovir hydrolase. *J Biol Chem*. 2003;278(28):25348-25356. doi:10.1074/jbc.M302055200

32. Beauchamp LM, Orr GF, De Miranda P, Burnette T, Krenitsky TA. Amino acid ester prodrugs of acyclovir. *Antivir Chem Chemother*. 1992;3(3):157-164. doi:10.1177/095632029200300305

33. Ganapathy ME, Huang W, Wang H, Ganapathy V, Leibach FH. Valacyclovir: A substrate for the intestinal and renal peptide transporters PEPT1 and PEPT2. *Biochem Biophys Res Commun*. 1998;246(2):470-475. doi:10.1006/bbrc.1998.8628

34. Balimane P V., Tamai I, Guo A, et al. Direct evidence for peptide transporter (PepT1)-mediated uptake of a nonpeptide prodrug, valacyclovir. *Biochem Biophys Res Commun*. 1998;250(2):246-251. doi:10.1006/bbrc.1998.9298

35. Lai L, Xu Z, Zhou J, Lee K-D, Amidon GL. Molecular Basis of Prodrug Activation by Human Valacyclovirase, an a-Amino Acid Ester Hydrolase. *J Biol Chem*. 2008;283(14):9318-9327. doi:10.1074/jbc.M709530200

36. Kim I, Song X, Vig BS, et al. A novel nucleoside prodrug-activating enzyme: substrate specificity of biphenyl hydrolase-like protein. *Mol Pharm*. 2004;1(2):117-127. doi:10.1021/mp0499757

37. Kim I, Crippen GM, Amidon GL. Structure and specificity of a human valacyclovir activating enzyme: a homology model of BPHL. *Mol Pharm*. 2004;1(6):434-446. doi:10.1021/mp049959+

38. Sun J, Dahan A, Walls ZF, Lai L, Lee KD, Amidon GL. Specificity of a prodrug-activating enzyme hVACVase: The leaving group effect. *Mol Pharm*. 2010;7(6):2362-2368. doi:10.1021/mp100300k

39. Sun J, Dahan A, Amidon GL. Enhancing the intestinal absorption of molecules containing the polar guanidino functionality: A double-targeted prodrug approach. *J Med Chem*. 2010;53(2):624-632. doi:10.1021/jm9011559

40. Dahan A, Khamis M, Agbaria R, Karaman R. Targeted prodrugs in oral drug delivery: the modern molecular biopharmaceutical approach. *Expert Opin Drug Deliv*. 2012;9(8):1001-1013. doi:10.1517/17425247.2012.697055

41. Kim I. A Novel Prodrug Activating Enzyme: Identification and Characterization of BPHL. *Dr Thesis*. 2004. doi:10.1016/B978-012397720-5.50034-7

42. Hu Y, Epling D, Shi J, et al. Effect of biphenyl hydrolase-like (BPHL) gene disruption on the intestinal stability, permeability and absorption of valacyclovir in wildtype and Bphl knockout mice. *Biochem Pharmacol*. 2018;156(August):147-156. doi:10.1016/j.bcp.2018.08.018

43. Patricelli MP, Giang DK, Stamp LM, Burbaum JJ. Direct visualization of serine hydrolase activities in complex proteomes using fluorescent active site-directed probes. *Proteomics*. 2001;1(9):1067-1071. doi:10.1002/1615-9861(200109)1:9<1067::AID-PROT1067>3.0.CO;2-4

44. Bachovchin DA, Ji T, Li W, et al. Superfamily-wide portrait of serine hydrolase inhibition achieved by library-versus-library screening. *Proc Natl Acad Sci U S A*. 2010;107(49):20941-20946. doi:10.1073/pnas.1011663107

45. Lai L. Structure and Function of a Prodrug Activating Enzyme Valacyclovir Hydrolase. *Dr Thesis*. 2006. doi:10.1017/S0165115300023299

46. Middleton WJ. New Fluorinating Reagents. Dialkylaminosulfur Fluorides. *J Org Chem*. 1975;40(5):574-578. doi:10.1021/jo00893a007

47. Burger A, Anderson JJ. Monoesters and Ester-amidates of Aromatic Phosphonic Acids. *J Am Chem Soc*. 1957;79(13):3575-3579. doi:10.1021/ja01570a073

48. Xu H, Sabit H, Amidon GL, Showalter HDH. An improved synthesis of a fluorophosphonate-polyethylene glycol-biotin probe and its use against competitive substrates. *Beilstein J Org Chem*. 2013;9:89-96. doi:10.3762/bjoc.9.12

49. McKenna CE, Higa MT, Cheung NH, McKenna MC. The facile dealkylation of phosphonic acid dialkyl esters by bromotrimethylsilane. *Tetrahedron Lett*. 1977;18(2):155-158. doi:10.1016/S0040-4039(01)92575-4

50. Kidd D, Liu Y, Cravatt BF. Profiling serine hydrolase activities in complex proteomes. *Biochemistry*. 2001;40(13):4005-4015. doi:10.1021/bi002579j

51. Strelow JM. A Perspective on the Kinetics of Covalent and Irreversible Inhibition. *J Biomol Screen*. 2017;22(1):3-20. doi:10.1177/1087057116671509

52. Worek F, Thiermann H, Szinicz L, Eyer P. Kinetic analysis of interactions between human acetylcholinesterase, structurally different organophosphorus compounds and oximes. *Biochem Pharmacol*. 2004;68(11):2237-2248. doi:10.1016/j.bcp.2004.07.038

53. Adibekian A, Martin BR, Chang JW, et al. Confirming target engagement for reversible inhibitors in vivo by kinetically tuned activity-based probes. *J Am Chem Soc*. 2012;134(25):10345-10348. doi:10.1021/ja303400u

54. Sharman J, Pennick M. Lisdexamfetamine prodrug activation by peptidase-mediated hydrolysis in the cytosol of red blood cells. *Neuropsychiatr Dis Treat*. 2014;10:2275-2280. doi:10.2147/NDT.S70382

55. Speers AE, Cravatt BF. Profiling enzyme activities in vivo using click chemistry methods. *Chem Biol*. 2004;11(4):535-546. doi:10.1016/j.chembiol.2004.03.012

56. Harsha HC, Molina H, Pandey A. Quantitative proteomics using stable isotope labeling with amino acids in cell culture. *Nat Protoc*. 2008;3(3):505-516. doi:10.1038/nprot.2008.2

57. Yang Y, Yang X, Verhelst SHL. Comparative analysis of click chemistry mediated activity-based protein profiling in cell lysates. *Molecules*. 2013;18(10):12599-12608. doi:10.3390/molecules181012599

58. Bachovchin DA, Brown SJ, Rosen H, Cravatt BF. Identification of selective inhibitors of uncharacterized enzymes by high-throughput screening with fluorescent activity-based probes. *Nat Biotechnol*. 2009;27(4):387-394. doi:10.1038/nbt.1531

59. Bachovchin DA, Koblan LW, Wu W, et al. A high-throughput, multiplexed assay for superfamily-wide profiling of enzyme activity. *Nat Chem Biol*. 2014;10(8):656-663. doi:10.1038/nchembio.1578

60. Bachovchin DA, Mohr JT, Speers AE, et al. Academic cross-fertilization by public screening yields a remarkable class of protein phosphatase methylesterase-1 inhibitors. *Proc Natl Acad Sci U S A*. 2011;108(17):6811-6816. doi:10.1073/pnas.1015248108

61. Wilk S, Orlowski M. Inhibition of Rabbit Brain Prolyl Endopeptidase by N-Benzyloxycarbonyl-Prolyl-Prolinal, a Transition State Aldehyde Inhibitor. *J Neurochem*. 1983;41(1):69-75. doi:10.1111/j.1471-4159.1983.tb11815.x

62. Hett EC, Xu H, Geoghegan KF, et al. Rational Targeting of Active-Site

Tyrosine Residues Using Sulfonyl Fluoride Probes. 2015. doi:10.1021/cb5009475

63. M. Vorobiev S, Janet Huang Y, Seetharaman J, et al. Human Retinoblastoma Binding Protein 9, a Serine Hydrolase Implicated in Pancreatic Cancers. *Protein Pept Lett*. 2012;19(2):194-197. doi:10.2174/092986612799080356

64. Woitach JT, Zhang M, Niu CH, Thorgeirsson SS. A retinoblastoma-binding protein that affects cell-cycle control and confers transforming ability. *Nat Genet*. 1998;19(4):371-374. doi:10.1038/1258

65. Shields DJ, Niessen S, Murphy EA, et al. RBBP9: A tumor-associated serine hydrolase activity required for pancreatic neoplasia. *Proc Natl Acad Sci*. 2010;107(5):2189-2194. doi:10.1073/pnas.0911646107

66. Vorobiev SM, Su M, Seetharaman J, et al. Crystal structure of human retinoblastoma binding protein 9. *Proteins Struct Funct Bioinforma*. 2009;74(2):526-529. doi:10.1002/prot.22278

67. Simon GM, Cravatt BF. Activity-based proteomics of enzyme superfamilies: Serine hydrolases as a case study. *J Biol Chem*. 2010;285(15):11051-11055. doi:10.1074/jbc.R109.097600

68. Hidalgo IJ, Li J. Carrier-mediated transport and efflux mechanisms of Caco-2 cells. *Adv Drug Deliv Rev*. 1996;22(1-2):53-66. doi:10.1016/S0169-409X(96)00414-0

69. Sambuy Y, De Angelis I, Ranaldi G, Scarino ML, Stammati A, Zucco F. The Caco-2 cell line as a model of the intestinal barrier: influence of cell and culture-related factors on Caco-2 cell functional characteristics. *Cell Biol Toxicol*. 2005;21(1):1-26. doi:10.1007/s10565-005-0085-6

70. Imai, Teruko; Masumi, Imoto; Sakamoto, Hisae; Hashimoto M. Identification of esterases expressed in Caco-2 cells and effects of their hydrolyzing activity in predicting human intestinal absorption. *Drug Metab Dispos*. 2005;33(8):1185-1190. doi:10.1124/dmd.105.004226.tion

71. Imai T, Taketani M, Shii M, Hosokawa M, Chiba K. Substrate specificity of carboxylesterase isozymes and their contribution to hydrolase activity in human liver and small intestine. *Drug Metab Dispos*. 2006;34(10):1734-1741. doi:10.1124/dmd.106.009381

72. Hosokawa M. Structure and catalytic properties of carboxylesterase isozymes involved in metabolic activation of prodrugs. *Molecules*. 2008;13(2):412-431. doi:10.3390/molecules13020412

73. Bar-Even A, Noor E, Savir Y, et al. The moderately efficient enzyme: Evolutionary and physicochemical trends shaping enzyme parameters. *Biochemistry*. 2011;50(21):4402-4410. doi:10.1021/bi2002289

74. Yang B, Hu Y, Smith DE. Impact of peptide transporter 1 on the intestinal

absorption and pharmacokinetics of valacyclovir after oral dose escalation in wild-type and PepT1 knockout mice. *Drug Metab Dispos*. 2013;41(10):1867-1874. doi:10.1124/dmd.113.052597

75. Hidalgo IJ, Raub TJ, Borchardt RT. Characterization of the Human Colon Carcinoma Cell Line (Caco-2) as a Model System for Intestinal Epithelial Permeability. *Gastroenterology*. 1989;96(2):736-749. doi:10.1016/S0016-5085(89)80072-1

76. Inoue M, Morikawa M, Tsuboi M, Sugiura M. Species Difference and Characterization of Intestinal Esterase on the Hydrolizing Activity of Ester-Type Drugs. *Jpn J Pharmacol*. 1979;29(1):9-16. doi:10.1254/jjp.29.9

77. Taketani M, Shii M, Ohura K, Ninomiya S, Imai T. Carboxylesterase in the liver and small intestine of experimental animals and human. *Life Sci*. 2007;81(11):924-932. doi:10.1016/j.lfs.2007.07.026

78. Puente XS, Lopez-Otin C. Cloning and Expression Analysis of a Novel Human Serine Hydrolase with Sequence Similarity to Prokaryotic Enzymes Involved in the Degradation of Aromatic Compounds. *J Biol Chem*. 1995;270(21):12926-12932. doi:10.1074/jbc.270.21.12926

79. Debbage PL, Griebel J, Ried M, Gneiting T, DeVries A, Hutzler P. Lectin intravital perfusion studies in tumor-bearing mice: Micrometer- resolution, wide-area mapping of microvascular labeling, distinguishing efficiently and inefficiently perfused microregions in the tumor. *J Histochem Cytochem*. 1998;46(5):627-639. doi:10.1177/002215549804600508

# CHAPTER IV

## *In Vitro, Ex Vivo,* and *In Situ* Characterization of RBBP9 Activity

### Introduction

After the discovery of RBBP9 as a VACV PAE and the assignment of VACV as its first substrate, the next step was to characterize the substrate-enzyme interaction and investigate how this activity compared to that of BPHL. First was to examine the binding stoichiometry of VACV to RBBP9 by gel-based cABPP $IC_{50}$ determination to evaluate the applicability of the Michaelis-Menten model in further studies. Afterwards, a steady-state Michaelis-Menten model was derived from reaction velocity of RBBP9 VACV activation at eight VACV concentrations. This would provide an estimate of the catalytic efficiency of RBBP9, which can then be compared to that of BPHL for initial insight. The overall goal was to determine the relevance and estimate the relative contribution of RBBP9 presystemic VACV activation to the disposition of VACV *in vivo*, which would ideally be extrapolated from an *in vitro* model. *In vitro* models are highly desirable in the pharmaceutical industry for their simplicity, reproducibility, throughput, cost, and ethical advantages over *in vivo* models. However, their usefulness hinges on the strength of their correlation to *in vivo* metrics since they ultimately serve to predict important drug properties.

Caco-2 cells, from which RBBP9 was identified as another PAE of VACV, have long been regarded as an *in vitro* model of enterocytes in studies of intestinal

drug absorption. They are well-known for expressing several clinically relevant transporters, including peptide transporter 1, PEPT1, organic anion transporting polypeptide 2B1, OATP2B1, breast cancer resistance protein, BCRP, and P-glycoprotein, P-gp.[68] Additionally, roughly two weeks after reaching confluence, Caco-2 cells differentiate into polarized cells with tight junctions, structurally resembling microvilli.[69] However, with ester-bearing agents in particular, caution must be used in interpreting study results obtained from Caco-2 cells due to the differential expression patterns of CES isozymes as compared to actual human enterocytes.[70] Specifically, CES1 is abundantly expressed in Caco-2 cells but is undetectable in the small intestine while CES2, which is the predominant isoform in the small intestine, is only expressed at low levels in Caco-2 cells. This is significant if one considers the remarkably different substrate specificities of the two isoforms, whereby CES1 prefers large acyl groups and small alcohol groups and CES2 prefers the opposite.[71] Furthermore, RBBP9 has not been characterized to date in Caco-2 cells at the expression, abundance, or activity level.

Thus, it was imperative that our results from VACV assays in Caco-2 with emetine inhibition be tested in another model that more convincingly approximates human *in vivo* conditions. Rodent models are well-characterized for several classes of therapeutic compounds and are universally utilized as preclinical species. Both rats and mice are known to highly express CES2 in the small intestine with CES1 essentially undetectable, similar to the human expression profile.[72] Mice are also strongly preferred for the generation of gene-silenced knockout organisms, which are vital in cases where no specific probes or chemical

modulators exist for a gene product, such as BPHL. Fortunately, *Bphl*-knockout (KO) mice were available for study, making reaction phenotyping of VACV with respect to both BPHL and RBBP9 feasible. First, lysates were prepared from the jejuna and livers of both WT and KO mice. The VACV activation in each of the four lysates was assayed with and without emetine. Finally, single-pass intestinal perfusions (SPIPs) of VACV were performed in WT mice with and without emetine pre-perfusion; unfortunately, KO mice were not old enough for inclusion at the time of study. Evaluation of VACV and ACV levels in the portal blood were carried out after 5 min of VACV perfusion to obtain a snapshot of presystemic activation.

Results from the $IC_{50}$ determination of VACV by gel-ABPP showed single-binding stoichiometry, which justified kinetic characterization by Michaelis-Menten experiments. Overall affinity was ten-fold lower than BPHL, but catalytic efficiency was roughly half of BPHL. In spite of this, studies in WT and KO mouse lysates showed that RBBP9 could be activating VACV to a much greater extent than BPHL in the gut wall while the two were roughly equal activators of VACV in the liver. Perfusion data revealed that RBBP9 is involved in presystemic activation of VACV as a statistically significant difference in activation was observed with and without emetine.

## Results

*$IC_{50}$ Determination of VACV vs. RBBP9 by Gel-Based ABPP*

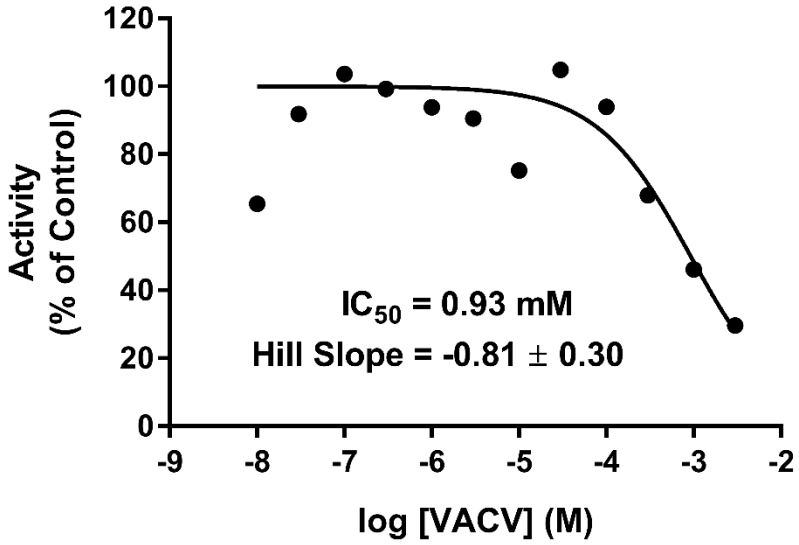


Figure 4.1. VACV $IC_{50}$ determination in rRBBP9.

Concentration-response curve by gel-based cABPP of rRBBP9 with VACV and AMB-FP-TAMRA. Response was measured as fluorescent intensity. Data points were fitted to the Hill equation with a fixed slope of one by nonlinear least squares regression.

One common application of gel-based ABPP in inhibitor profiling is the determination of $IC_{50}$ values, where it is most useful for enzymes with no assigned substrates. Gel-based activity readouts are facile and rapid, with higher throughput than chromatographic methods, though not truly high-throughput in nature. This provides a fast way to estimate inhibitor potency or substrate affinity. A major shortcoming of the approach is that time-dependent probe inhibition results in an $IC_{50}$ that changes depending on the competition time chosen for the assay, requiring some measure of optimization as with other cABPP assays.

After optimizing the VACV-RBBP9 competition time at high VACV concentrations, the competition was performed with 11 concentrations of VACV spanning 10 nM to 3 mM and one control reaction without VACV. Above 3 mM

VACV, the pH of the buffer begins to be affected by a nontrivial amount (>0.5 units), so these were not tested. After plotting the activities against VACV concentrations and fitting the Hill equation by nonlinear least-squares regression, the $IC_{50}$ was estimated to be 0.93 mM (Figure 4.1). The coefficient of determination ($R^2$) of 0.67 indicates an acceptable fit that was substantially lowered by the variability at low VACV concentrations. This supported the single-binding stoichiometry of the RBBP9-VACV interaction, justifying the application of the Michaelis-Menten model for studying reaction kinetics.

*Steady-State Michaelis-Menten Kinetic Assay*

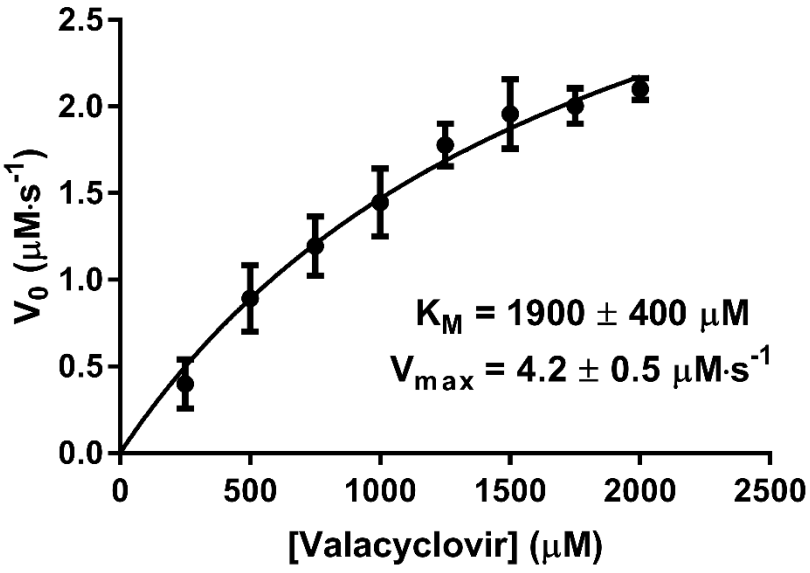


Figure 4.2. Michaelis-Menten kinetics of RBBP9 VACV activation.

Plot of initial reaction velocity versus substrate concentration. Each data point represents the mean ± SD of three independent determinations. All 24 points were fitted to the steady-state Michaelis-Menten equation using nonlinear least squares regression. Parameters are shown with standard error.

To compare the VACV hydrolytic activities of RBBP9 and BPHL, the first step was to perform a kinetic characterization of RBBP9 activity. The steady-state Michaelis-

Menten model is often used for modeling single-substrate reactions. Based on the good approximation when using the Hill equation with a slope of one to estimate the $IC_{50}$ of VACV against AMB-FP-TAMRA labeling of RBBP9, the assumption of a single-substrate reaction is likely valid and justifies the use of this model.

By plotting the initial reaction velocities of VACV hydrolysis by RBBP9 at 8 concentrations from 250 to 2000 μM against the VACV concentration and fitting the Michaelis-Menten equation by nonlinear least-squares regression, the $V_{max}$ and $K_M$ were estimated to be 4.2 $\mu M \cdot s^{-1}$ and 1.9 mM, respectively, translating to a $k_{cat}$ of 193 $s^{-1}$, and a catalytic efficiency, $k_{cat} \cdot K_M^{-1}$, of 104 $mM^{-1} \cdot s^{-1}$ (Figure 4.2). This is an average value relative to the distribution of known enzyme catalytic efficiencies[73] but is comparable to the catalytic efficiency of 223 $mM^{-1} \cdot s^{-1}$ obtained for BPHL,[31] which is higher mainly due to its greater affinity for VACV ($K_M$ = 0.19 mM).

*Half-Life Determination of Valyl-Gemcitabine in rRBBP9*

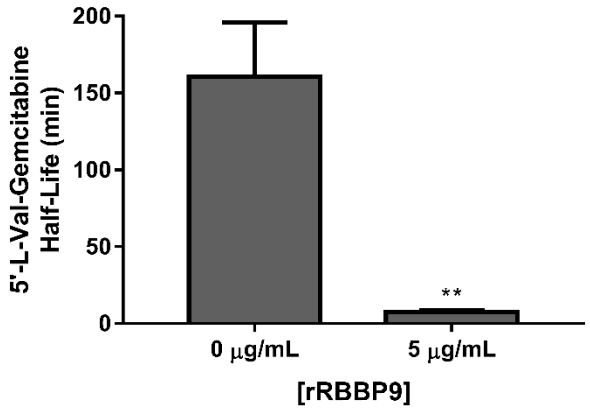


Figure 4.3. Half-life determination of 5'-L-Val-gemcitabine in rRBBP9.

The in vitro half-life of 5'-L-Val-gemcitabine was determined in rRBBP9 at 37 °C with data presented as mean ± SD (n = 3). $^{**}p < .01$ as determined by unpaired *t*-test.

The immediate availability of 5'-L-Val-gemcitabine prompted us to test whether it, too, was a substrate of RBBP9 in the same way that it is a substrate of BPHL, which has been shown to be specific for α-amino acid esterases. The half-life of the prodrug in 5 $\mu g \cdot mL^{-1}$ rRBBP9 at 37 °C was calculated to be 20-fold lower than the half-life in buffer at the same temperature (8 vs. 160 min), demonstrating that it is very likely a substrate (Figure 4.3). Further investigations into the substrate specificity of RBBP9 are warranted.

*VACV Hydrolysis Assay with Emetine in Mouse Tissue Lysates*

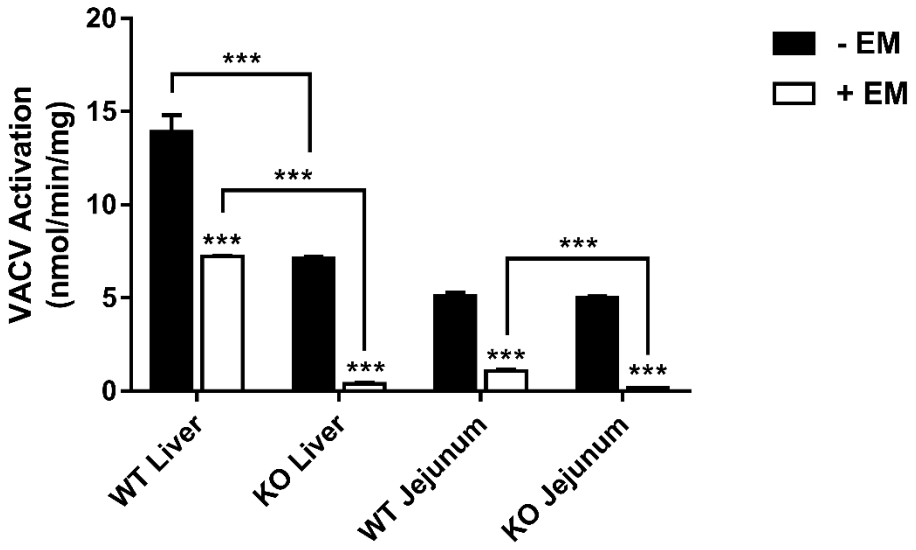


Figure 4.4. Emetine inhibition of VACV activation in WT and Bphl-KO mouse tissue lysates.

VACV hydrolytic activity in various mouse tissue lysates with and without emetine (1 mM). Data are presented as mean ± SD of three technical replicates. ***$p < .001$ by unpaired *t*-test as compared to control of same tissue type or as noted by brackets.

Due to the fact that Caco-2 cells may not be representative of the human intestinal mucosa specifically with respect to ester-based drugs, we sought to establish preliminary proof of relevance in mice, whose RBBP9 ortholog is highly identical (>90%) to humans and whose Bphl-KO variant was accessible for our

experiments. Experiments in soluble tissue lysates of the liver and jejunum from both WT and KO mice with and without emetine yielded estimates of the contribution of each enzyme to presystemic VACV activation (Figure 4.4).

Comparison of VACV hydrolysis in WT and KO lysates of the same tissue without emetine revealed the likely proportion of BPHL-dependent activation in that tissue. In the liver, KO lysates show roughly half the activity of WT, while jejunal KO samples were roughly equal in activity to the WT samples, implying that BPHL contributes significantly to hepatic activation of VACV but may be trivial with respect to intestinal activation.

On the other hand, comparison of KO tissue lysate activities in the presence and absence of emetine revealed the likely proportion of RBBP9-dependent activation in that tissue. In both KO liver and jejunum samples, addition of emetine resulted in the near-total elimination of VACV activation, strongly implying that RBBP9 is the only presystemic VACV PAE in Bphl-KO mice. The difference between KO samples with and without emetine, when added to the same difference between WT samples, almost reconstitutes the entire activity of WT samples without emetine, signifying that RBBP9 and BPHL are essentially the only two presystemic VACV PAEs.

*Single-Pass Intestinal Perfusions with and without Emetine*

| Group | [ACV] (μM) | [VACV] (μM) | [ACV + VACV] (μM) | % Activated |
|---|---|---|---|---|
| - EM (n = 6) | 5.0 ± 1.1 | 1.8 ± 0.5 | 6.8 ± 1.6 | 73.8 ± 2.3 |
| + EM (n = 8) | 1.3 ± 0.2** | 1.0 ± 0.2 | 2.2 ± 0.3** | 58.4 ± 4.5* |

Table 4.1. Results of single-pass intestinal perfusions of VACV in WT mice.

Results of single-pass intestinal perfusions of VACV (1 mM) in WT mice with and without emetine (EM) pre-perfusion presented as mean ± SEM. The sample numbers listed represent biological replicates in each group. *$p < .05$, ** $p < .01$ by Welch's unequal variance unpaired *t*-test.

SPIP studies are often carried out to study absorptive processes of drug candidates in isolation in a physiologically relevant system. Additionally, SPIP can be used to presystemic metabolism that takes place in the intestinal lumen by analyzing metabolite levels in the outlet perfusate. To assess presystemic metabolism taking place within the gut wall, however, sampling of the portal vein blood is required, which is the approach we chose to assess BPHL and RBBP9 first-pass activity. With regards to analysis, a tradeoff exists between accuracy and analyzability due to the terminal nature of non-cannulated portal vein sampling: choosing a sampling timepoint that is too early results in analyte levels that could be below the limit of detection, while one that is too late captures a snapshot of metabolism that is convoluted by hepatic and systemic metabolism, distribution, and elimination. Emetine, which was historically used for its emetic effect to expel ingested poisons, is thought not to cause the same effect in rodents, and consistent with this notion, no emesis or GI disturbance was observed in our studies.

Because our approach utilized UPLC analysis instead of the more sensitive LC-MS/MS, the concentration of VACV in the perfusion buffer was high (1 mM), taking advantage of the extremely high-capacity mouse PepT1 transporter that exclusively mediates intestinal VACV uptake.[74] The high VACV concentration thus

enabled the selection of a relatively quick 5 min sampling timepoint. The extended pre-perfusion of emetine (60 min) was informed by preliminary experiments to ensure the free intracellular emetine concentration is as high as possible prior to the addition of VACV. KO mice could not be used as they were not of sufficient age at the time of study, so only WT mice were used (six control mice, eight treatment mice).

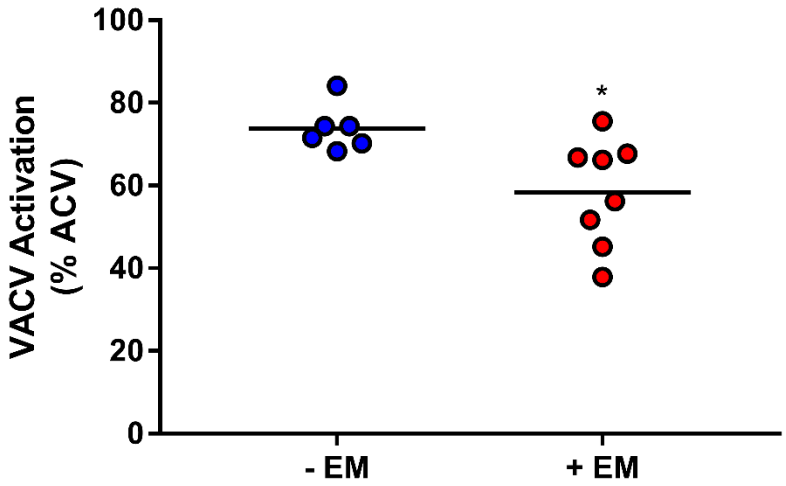


Figure 4.5. Single-pass intestinal perfusions of VACV in WT mice.

Single-pass intestinal perfusion of VACV (1 mM) for 5 min in WT mice with and without emetine (EM) pre-perfusion. Portal vein blood was assayed for ACV and VACV by UPLC. Each data point represents the proportion of parent drug ACV detected in individual mice, with the group mean denoted by horizontal bars. *p < 0.05 by Welch's unequal variance unpaired t-test.

Emetine pre-perfusion resulted in a statistically significant ($p$ < .05) decrease in pre-systemic VACV activation from 74 ± 2% to 58 ± 5%, representing a ~22% relative decrease in activation and a ~50% increase in unactivated prodrug levels (Figure 4.5). Interestingly, the amount of ACV detected was also significantly reduced ($p$ < .01, Table 4.1) in the treatment group (1.3 ± 0.2 μM vs. 5.0 ± 1.1 μM), but the amount of VACV detected was not significantly different (1.0 ± 0.2 μM, treatment vs. 1.8 ± 0.5 μM, control).

## Discussion

After validating the VACV hydrolytic activity of RBBP9 in Caco-2 lysates using the selective inhibitor emetine, the next step was to characterize the activity and establish relevance in mice with the goal of gathering evidence for clinical relevance. Caco-2 cells are heterogeneous, and genetic drift can lead to cell subpopulations with considerably different genotypes after repeated passaging.[75] Furthermore, Caco-2 cell esterases, such as CES1 and CES2, are at levels that are not representative of human enterocytes.[70] Mice, on the other hand, better approximate humans in terms of presystemic ester metabolism.[72,76,77] In addition, we had access to *Bphl*-KO mice for some of the experiments, allowing us to individually study the contributions of the two known VACV PAEs, BPHL and RBBP9.

To characterize the activity, gel-based ABPP $IC_{50}$ studies of VACV against RBBP9 were performed to validate that the reaction was indeed a single-substrate reaction with only one enzyme binding site to justify application of the steady state Michaelis-Menten kinetic model for subsequent characterization. The estimated Hill slope magnitude of 0.81 was reasonably close to one, confirming the single-binding stoichiometry, which was expected given the crystal structure of RBBP9 revealing one active site.[66] The Michaelis-Menten experiments yielded a Michaelis constant that was about tenfold below that of BPHL, though the turnover number was roughly five times that of BPHL, giving a catalytic efficiency that was just under half the value for BPHL. This indicates that RBBP9 is likely a lower affinity VACV hydrolase with a higher capacity and thus lower likelihood of saturation.

Upon scrutiny of the *ex vivo* experiments, it was confirmed that RBBP9 is likely the primary VACV PAE in the small intestine based on the observation that emetine, which selectively inhibits RBBP9, nearly completely extinguishes VACV hydrolysis in both WT and KO soluble jejunum lysates, with slight residual activity seen in the WT samples. The difference between baseline activities of WT and KO jejunal lysates was very little, further suggesting a diminutive contribution to VACV activation by BPHL in the tissue. In the liver lysates, the WT samples showed roughly equal contributions by both enzymes, given about half the activity remained after addition of emetine. In both tissues of the KO mice, emetine incubation nearly totally inhibited VACV activation, demonstrating that RBBP9 is likely the only other presystemic activating of enzyme upon deletion of BPHL. These activity data with respect to BPHL corroborate previously published results showing the tissue expression levels of BPHL in mice, in which 3–8 times the expression was detected in the liver than in any of the three segments of the small intestine.[42] The same expression pattern is also seen in humans.[78]

In the follow-up *in vivo* experiments, emetine pre-perfusion significantly decreased presystemic intestinal VACV activation as monitored in the portal vein blood. Activation was calculated as the proportion of parent drug to total drug species (VACV and ACV), normalizing for any potential differences in VACV uptake or permeability that could be caused by emetine, e.g. by inhibition of PepT1. The long pre-perfusion of emetine was meant to deliver sufficiently high intracellular concentrations of emetine to effect RBBP9 inhibition, though this could not be ensured. The considerable residual activation seen in the emetine-treated

group could be due to intracellular concentrations of emetine that are well below the *in vitro* concentrations that were used in the tissue lysate experiments or the significant activity of BPHL in the liver, which would be reflected in the data due to the 5 min sampling time being much longer than the 15 s blood circulation time in mice.[79] In conclusion, the data obtained from SPIP experiments indicate that neither RBBP9 nor BPHL, individually, is obligatory for the presystemic conversion of VACV to ACV *in vivo*.

From these findings, it is clear that RBBP9 and BPHL in tandem, mediate the presystemic activation of VACV *in vivo*, with RBBP9-dominant activation in enterocytes and equally shared activation in the liver. Both BPHL and RBBP9 are highly identical between mouse and human orthologs, with BPHL also showing similar expression patterns between mouse and humans, ultimately suggestive of a similar VACV activation profile in humans. What remains to be studied, with respect to drug and prodrug development in particular, are the relative activity factors and substrate specificities of mouse, rat, and higher preclinical species enzymes as compared to the human enzymes to aid in preclinical model selection and allometric scaling/dose prediction. This would also empirically assist the rational design of RBBP9-targeted prodrugs, which could be further supported by computer-aided design. Additionally, genetic polymorphisms should be examined from individual genetic data, and the consequently discovered mutants should be generated and assayed for activity to appreciate the pharmacogenetic risks of developing agents activated or metabolized by RBBP9. Finally, other ester-based

agents might be assayed for activation/metabolism by RBBP9 to determine what potential drug-drug interactions exist.

## Methods

*Materials and Equipment*

AMB-FP-TAMRA was synthesized according to procedures reported previously herein (Chapter II). All gels, buffers, and reagent/reagent kits were purchased from ThermoFisher. All compositional percentages are reported as v/v unless otherwise noted. Purified recombinant hRBBP9 was purchased from Novus Biologicals (Littleton, CO). Gels were electrophoresed on an XCell SureLock Mini-Cell electrophoresis system (ThermoFisher) with a PowerPac power supply adapter from Bio-Rad. Fluorescent gels were scanned on a Typhoon 9200 flatbed imager (Amersham) and integrated using ImageJ software (NIH, Bethesda, MD). Analytical high-performance liquid chromatography (HPLC) was performed on an Agilent 1100 HPLC (Agilent, Santa Clara, CA) equipped with a reverse-phase Zorbax Eclipse XDB-C18 column (Agilent, 4.6 x 150 mm, 3.5 µm). The pH of phosphate-buffered saline (PBS) used in all experiments was 7.4 unless otherwise noted.

*$IC_{50}$ Determination of VACV vs. RBBP9 by Gel-based ABPP*

Purified recombinant RBBP9 in PBS (5 µg·mL$^{-1}$) was pretreated with one of 11 concentrations of VACV (0.01–3,000 µM) or vehicle for 2 min at RT, then labeled with AMB-FP-TAMRA (5 µM) at RT. After 5 min of labeling, aliquots were quenched in 1.25 volumes of SDS loading buffer and 0.25 volumes of 0.5 M dithiothreitol. Samples were heated to 90 °C for 10 min, and 15 µL per sample (30 ng total protein) were electrophoresed on a 4–20% crosslinker gradient gel at 226 V for 50 min. Gels were scanned using a 580 nm bandpass emission filter for

TAMRA fluorescence and integrated on ImageJ software (National Institutes of Health, Bethesda, MD). The fluorescence intensities were normalized to the control (vehicle) and plotted against log [VACV]. The points were fitted to the two-parameter Hill equation by nonlinear least-squares regression on Prism software (GraphPad, La Jolla, CA) with the $IC_{50}$ and Hill slope thus estimated.

*Steady-State Michaelis-Menten Kinetic Assay*

Purified recombinant hRBBP9 (0.5 $\mu g \cdot mL^{-1}$) in PBS was incubated with eight concentrations of VACV (0.25–2 mM) at 37 °C in triplicate. Reactions were quenched after 2 min in four volumes MeOH with 0.1% TFA and pelleted for 5 min at 14,000 *g*. The supernatant was analyzed by HPLC using a binary solvent gradient from 2–90% acetonitrile/water (both with 0.1% TFA) at a 1.0 $mL \cdot min^{-1}$ flow rate. Analytes were detected by absorbance at 254 nm. Relative peak areas were used to calculate hydrolytic activity. Non-enzymatic control reactions were used to account for chemical hydrolysis. Initial reaction velocities were fitted to the steady-state Michaelis-Menten equation by nonlinear least-squares regression in Prism 8.0 (GraphPad, La Jolla, CA). Protein concentrations were used as nominally labeled by the vendor in calculations of $k_{cat}$.

*Half-Life Determination of Valyl-Gemcitabine in rRBBP9*

Triplicate solutions of rRBBP9 (5 $\mu g \cdot mL^{-1}$) in PBS or plain PBS were incubated with 5'-L-valyl-gemcitabine (1 mM) at 37 °C for 15 min, with aliquots quenched at 5, 10, and 15 min in four volumes MeOH with 0.1% TFA. After pelleting for 5 min at 14,000 *g*, the supernatant was analyzed by HPLC using a binary solvent gradient from 2–90% acetonitrile in water (both with 0.1% TFA) at a

1.0 mL·min$^{-1}$ flow rate. Analytes were detected by absorbance at 254 nm. Relative peak areas were used to calculate half-life by fitting the quantity of prodrug remaining to a first-order exponential decay equation.

*Animals*

Animal studies were conducted in accordance with the Guide for the Care and Use of Laboratory Animals as adopted and promulgated by the U.S. National Institutes of Health. *Bphl*-KO mice (pure C57BL/6 strain) were a generous gift from the Institut Clinique de la Souris (Illkirch Cedex, France) and were validated by genotyping. Gender-matched mice (pure C57BL/6 strain), 8–10 weeks old, were used in all the following procedures. The mice were kept in temperature-controlled housing with a 12/12-h light/dark cycle and received a standard diet and water *ad libitum* as provided by the Unit for Laboratory Animal Medicine, University of Michigan, Ann Arbor, MI.

*Lysate Preparation*

One WT and one KO mouse, both male, were sacrificed by cervical dislocation and immediately dissected. The liver and jejunal segment were excised and rinsed in ice-cold PBS to remove blood and bowel remnants. Both tissues were cut into smaller pieces by razor and Dounce homogenized on ice. Crude lysates were spun 20 min at 9,000 x *g* and 4 °C, and the supernatant S9 fractions were centrifuged for another 60 min at 100,000 x *g* and 4 °C. The supernatant was used as the soluble fraction (S100), and the pellet was resuspended in PBS with 0.1% Triton X-100 and used as the membrane fraction (P100). Lysates were

aliquoted and stored at –80 °C until use. Animal dissection and organ harvesting were performed by Dr. Yongjun Hu.

*VACV Hydrolysis Assay with Emetine in Mouse Tissue Lysates*

Triplicate mouse tissue lysate S100 fractions (1 $mg \cdot mL^{-1}$) in PBS were incubated with emetine (1 mM) for 5 min at 37 °C. Reactions were initiated by the addition of VACV (1 mM) and were quenched 10 min after initiation in four volumes of MeOH with 0.1% TFA. Proteins were pelleted for 5 min at 14,000 *g*, followed by analysis of the supernatant via HPLC. A binary solvent gradient from 2% to 90% acetonitrile in water (both with 0.1% TFA) with 1.0 $mL \cdot min^{-1}$ flow rate was used for separation. Analytes were detected by absorbance at 254 nm. External standards of VACV and ACV were used to calculate hydrolytic activity. Non-enzymatic control reactions were used to account for chemical hydrolysis.

*Single-Pass Intestinal Perfusions with and without Emetine*

Mice were sedated and anesthetized by pentobarbital sodium injection prior to incision of the peritoneal cavity and cannulation of the small intestine. The perfusion solution contained 1 mM VACV ± 1 mM emetine in a pH 6.0 buffer containing 145 mM NaCl, 0.5 mM $MgCl_2$, 1 mM $NaH_2PO_4$, 1 mM $CaCl_2$, 3 mM KCl, 5 mM glucose, and 5 mM MES. The pre-perfusion solutions with and without emetine were composed identically except without VACV. Emetine (or vehicle) pre-perfusion solution was perfused through the cannulated intestinal segment for 60 min at 0.1 $mL \cdot min^{-1}$ in a 31 °C perfusion chamber, followed by a 5 min perfusion of the perfusion solution containing VACV with (or without) emetine. After this,

~200 µL of portal blood was collected into a tube containing EDTA. This blood was centrifuged at 3,000 *g* for 4 min at 4 °C and a 50 µL sample of plasma collected.

To the 50 µL plasma sample was then added 200 µL of ice-cold ACN containing 5 µM caffeine as an internal standard. The sample was then vortexed by hand and placed in the -20 °C freezer until all samples were collected. At this point, the sample was vortexed at 1500 rpm for 5 min and then centrifuged at 17,000 *g* for 10 min at 4 °C. 200 µL of supernatant was transferred to a new tube and dried in a SpeedVac concentrator with heating at 45 °C for 1 h. The dried sample was then reconstituted in 80 µL water with 0.1% TFA, vortexed for 5 min at 1500 rpm, and bath sonicated for 5 min. The resulting solution was then centrifuged at 17,000 *g* for 10 min at 4 °C, of which 15 µL supernatant was analyzed by UPLC.

The analytes were separated at 40 °C on an Acquity HSS T3 column (2.1 x 100 mm), fitted with an HSS T3 VanGuard precolumn (2.1 x 5 mm). The mobile phase flow rate was 0.5 $mL \cdot min^{-1}$ and the same gradient was used as on 7/9/2019 (100% water at 0 min, 90% water + 10% ACN at 5 min, 90% water + 10% ACN at 5.25 min, 30% water + 70% ACN at 7 min, 100% water at 8 min). The detection wavelengths for caffeine, VACV, and ACV were 275, 254, and 284 nm, respectively. The percentages of activated drug ($\frac{[ACV]}{[ACV]+[VACV]}$) and unactivated drug ($\frac{[VACV]}{[ACV]+[VACV]}$) were calculated. Sample collection, data acquisition, and data analysis were performed by Brian Thompson. Experimental design and sample processing were carried out by Vikram Shenoy and Brian Thompson.

## References


1. Huttunen KM, Raunio H, Rautio J. Prodrugs--from Serendipity to Rational Design. *Pharmacol Rev*. 2011;63(3):750-771. doi:10.1124/pr.110.003459

2. Dammann HG, Burkhardt F, Wolf N. Enteric coating of aspirin significantly decreases gastroduodenal mucosal lesions. *Aliment Pharmacol Ther*. 1999;13(8):1109-1114. doi:10.1046/j.1365-2036.1999.00588.x

3. Gupta S, Kesarla R, Omri A. Formulation strategies to improve the bioavailability of poorly absorbed drugs with special emphasis on self-emulsifying systems. *ISRN Pharm*. 2013;2013:1-16. doi:10.1155/2013/848043

4. Sohi H, Sultana Y, Khar RK. Taste masking technologies in oral pharmaceuticals: recent developments and approaches. *Drug Dev Ind Pharm*. 2004;30(5):429-448. doi:10.1081/DDC-120037477

5. Ratnaparkhi P, Jyoti GP, Mukesh. Sustained release oral drug delivery system - an overview. *Int J Pharma Res Rev IJPRR*. 2013;2(23):11-21.

6. Rautio J, Meanwell NA, Di L, Hageman MJ. The expanding role of prodrugs in contemporary drug design and development. *Nat Rev Drug Discov*. 2018;17(8):559-587. doi:10.1038/nrd.2018.46

7. FDA F and DA. Guidance for Industry: Applications Covered by Section 505(b)(2). *Guidance*. 1999;505(October):1-12. http://www.fda.gov/cder/guidance/index.htm. Accessed August 18, 2019.

8. Clas S-D, Sanchez RI, Nofsinger R. Chemistry-enabled drug delivery (prodrugs): recent progress and challenges. *Drug Discov Today*. 2014;19(1):79-87. doi:10.1016/j.drudis.2013.08.014

9. Ram PR, Priyanka P, Shreekrishna L, Saroj S. Prodrug as a novel approach of drug delivery - a review. *J Drug Deliv Ther*. 2015;5(3):5-9.

10. Wu KM. A new classification of prodrugs: Regulatory perspectives. *Pharmaceuticals*. 2009;2(3):77-81. doi:10.3390/ph2030077

11. Tirkkonen T, Laine K. Drug interactions with the potential to prevent prodrug activation as a common source of irrational prescribing in hospital inpatients. *Clin Pharmacol Ther*. 2004;76(6):639-647. doi:10.1016/j.clpt.2004.08.017

12. Zhang C, Xu Y, Zhong Q, et al. In vitro evaluation of the inhibitory potential of pharmaceutical excipients on human carboxylesterase 1A and 2. *PLoS*

*One*. 2014;9(4). doi:10.1371/journal.pone.0093819

13. Harper TW, Brassil PJ. Reaction phenotyping: Current industry efforts to identify enzymes responsible for metabolizing drug candidates. *AAPS J*. 2008;10(1):200-207. doi:10.1208/s12248-008-9019-6

14. Di L. Reaction phenotyping to assess victim drug-drug interaction risks. *Expert Opin Drug Discov*. 2017;12(11):1105-1115. doi:10.1080/17460441.2017.1367280

15. Zhang Y, Fonslow BR, Shan B, Baek M-C, Yates JR. Protein Analysis by Shotgun/Bottom-up Proteomics. 2013. doi:10.1021/cr3003533

16. Saghatelian A, Cravatt BF. Assignment of protein function in the postgenomic era. *Nat Chem Biol*. 2005;1(3):129. doi:10.1038/nchembio0805-130

17. Cravatt BF, Wright AT, Kozarich JW. Activity-Based Protein Profiling: From Enzyme Chemistry to Proteomic Chemistry. *Annu Rev Biochem*. 2008;77(1):383-414. doi:10.1146/annurev.biochem.75.101304.124125

18. Liu Y, Patricelli MP, Cravatt BF. Activity-based protein profiling: The serine hydrolases. *Proc Natl Acad Sci*. 1999;96(26):14694-14699. doi:10.1073/pnas.96.26.14694

19. van Rooden EJ, Bakker AT, Overkleeft HS, van der Stelt M. Activity-Based Protein Profiling. *eLS*. 2018:1-9. doi:10.1002/9780470015902.a0023406

20. Wang K, Yang T, Wu Q, Zhao X, Nice EC, Huang C. Chemistry-based functional proteomics for drug target deconvolution. *Expert Rev Proteomics*. 2012;9(3):293-310. doi:10.1586/epr.12.19

21. Jeffery DA, Bogyo M. Chemical proteomics and its application to drug discovery. *Curr Opin Biotechnol*. 2003;14(1):87-95. doi:10.1016/S0958-1669(02)00010-1

22. Bantscheff M, Scholten A, Heck AJR. Revealing promiscuous drug-target interactions by chemical proteomics. *Drug Discov Today*. 2009;14(21-22):1021-1029. doi:10.1016/j.drudis.2009.07.001

23. Xu H, Majmudar JD, Davda D, et al. Substrate-Competitive Activity-Based Profiling of Ester Prodrug Activating Enzymes. *Mol Pharm*. 2015;12(9):3399-3407. doi:10.1021/acs.molpharmaceut.5b00414

24. Liederer BM, Borchardt RT. Enzymes involved in the bioconversion of ester-based prodrugs. *J Pharm Sci*. 2006;95(6):1177-1195. doi:10.1002/jps.20542

25. Sun Z, Murry DJ, Sanghani SP, et al. Methylphenidate is stereoselectively hydrolyzed by human carboxylesterase CES1A1. *J Pharmacol Exp Ther*. 2004;310(2):469-476. doi:10.1124/jpet.104.067116

26. Pindel E V., Kedishvili LNY, Abraham TL, et al. Purification and cloning of a human liver carboxylesterase that catalyzes the hydrolysis of cocaine and heroin. *FASEB J*. 1997;11(9):14769-14775.

27. Imai T, Ohura K. The Role of Intestinal Carboxylesterase in the Oral Absorption of Prodrugs. *Curr Drug Metab*. 2011;11(9):793-805. doi:10.2174/138920010794328904

28. Laizure SC, Parker RB, Herring VL, Hu ZY. Identification of carboxylesterase-dependent dabigatran etexilate hydrolysis. *Drug Metab Dispos*. 2014;42(2):201-206. doi:10.1124/dmd.113.054353

29. Shi D, Yang J, Yang D, et al. Anti-Influenza Prodrug Oseltamivir Is Activated by Carboxylesterase Human Carboxylesterase 1, and the Activation Is Inhibited by Antiplatelet Agent Clopidogrel. *J Pharmacol Exp Ther*. 2006;319(3):1477-1484. doi:10.1124/jpet.107.120030

30. Danks MK, Morton CL, Krull EJ, et al. Comparison of activation of CPT-11 by rabbit and human carboxylesterases for use in enzyme/prodrug therapy. *Clin Cancer Res*. 1999;5(4):917-924.

31. Kim I, Chu XY, Kim S, Provoda CJ, Lee KD, Amidon GL. Identification of a human valacyclovirase: Biphenyl hydrolase-like protein as valacyclovir hydrolase. *J Biol Chem*. 2003;278(28):25348-25356. doi:10.1074/jbc.M302055200

32. Beauchamp LM, Orr GF, De Miranda P, Burnette T, Krenitsky TA. Amino acid ester prodrugs of acyclovir. *Antivir Chem Chemother*. 1992;3(3):157-164. doi:10.1177/095632029200300305

33. Ganapathy ME, Huang W, Wang H, Ganapathy V, Leibach FH. Valacyclovir: A substrate for the intestinal and renal peptide transporters PEPT1 and PEPT2. *Biochem Biophys Res Commun*. 1998;246(2):470-475. doi:10.1006/bbrc.1998.8628

34. Balimane P V., Tamai I, Guo A, et al. Direct evidence for peptide transporter (PepT1)-mediated uptake of a nonpeptide prodrug, valacyclovir. *Biochem Biophys Res Commun*. 1998;250(2):246-251. doi:10.1006/bbrc.1998.9298

35. Lai L, Xu Z, Zhou J, Lee K-D, Amidon GL. Molecular Basis of Prodrug Activation by Human Valacyclovirase, an a-Amino Acid Ester Hydrolase. *J Biol Chem*. 2008;283(14):9318-9327. doi:10.1074/jbc.M709530200

36. Kim I, Song X, Vig BS, et al. A novel nucleoside prodrug-activating enzyme: substrate specificity of biphenyl hydrolase-like protein. *Mol Pharm*. 2004;1(2):117-127. doi:10.1021/mp0499757

37. Kim I, Crippen GM, Amidon GL. Structure and specificity of a human valacyclovir activating enzyme: a homology model of BPHL. *Mol Pharm*. 2004;1(6):434-446. doi:10.1021/mp049959+

38. Sun J, Dahan A, Walls ZF, Lai L, Lee KD, Amidon GL. Specificity of a prodrug-activating enzyme hVACVase: The leaving group effect. *Mol Pharm*. 2010;7(6):2362-2368. doi:10.1021/mp100300k

39. Sun J, Dahan A, Amidon GL. Enhancing the intestinal absorption of molecules containing the polar guanidino functionality: A double-targeted prodrug approach. *J Med Chem*. 2010;53(2):624-632. doi:10.1021/jm9011559

40. Dahan A, Khamis M, Agbaria R, Karaman R. Targeted prodrugs in oral drug delivery: the modern molecular biopharmaceutical approach. *Expert Opin Drug Deliv*. 2012;9(8):1001-1013. doi:10.1517/17425247.2012.697055

41. Kim I. A Novel Prodrug Activating Enzyme: Identification and Characterization of BPHL. *Dr Thesis*. 2004. doi:10.1016/B978-012397720-5.50034-7

42. Hu Y, Epling D, Shi J, et al. Effect of biphenyl hydrolase-like (BPHL) gene disruption on the intestinal stability, permeability and absorption of valacyclovir in wildtype and Bphl knockout mice. *Biochem Pharmacol*. 2018;156(August):147-156. doi:10.1016/j.bcp.2018.08.018

43. Patricelli MP, Giang DK, Stamp LM, Burbaum JJ. Direct visualization of serine hydrolase activities in complex proteomes using fluorescent active site-directed probes. *Proteomics*. 2001;1(9):1067-1071. doi:10.1002/1615-9861(200109)1:9<1067::AID-PROT1067>3.0.CO;2-4

44. Bachovchin DA, Ji T, Li W, et al. Superfamily-wide portrait of serine hydrolase inhibition achieved by library-versus-library screening. *Proc Natl Acad Sci U S A*. 2010;107(49):20941-20946. doi:10.1073/pnas.1011663107

45. Lai L. Structure and Function of a Prodrug Activating Enzyme Valacyclovir Hydrolase. *Dr Thesis*. 2006. doi:10.1017/S0165115300023299

46. Middleton WJ. New Fluorinating Reagents. Dialkylaminosulfur Fluorides. *J Org Chem*. 1975;40(5):574-578. doi:10.1021/jo00893a007

47. Burger A, Anderson JJ. Monoesters and Ester-amidates of Aromatic Phosphonic Acids. *J Am Chem Soc*. 1957;79(13):3575-3579. doi:10.1021/ja01570a073

48. Xu H, Sabit H, Amidon GL, Showalter HDH. An improved synthesis of a fluorophosphonate-polyethylene glycol-biotin probe and its use against competitive substrates. *Beilstein J Org Chem*. 2013;9:89-96. doi:10.3762/bjoc.9.12

49. McKenna CE, Higa MT, Cheung NH, McKenna MC. The facile dealkylation of phosphonic acid dialkyl esters by bromotrimethylsilane. *Tetrahedron Lett*. 1977;18(2):155-158. doi:10.1016/S0040-4039(01)92575-4

50. Kidd D, Liu Y, Cravatt BF. Profiling serine hydrolase activities in complex proteomes. *Biochemistry*. 2001;40(13):4005-4015. doi:10.1021/bi002579j

51. Strelow JM. A Perspective on the Kinetics of Covalent and Irreversible Inhibition. *J Biomol Screen*. 2017;22(1):3-20. doi:10.1177/1087057116671509

52. Worek F, Thiermann H, Szinicz L, Eyer P. Kinetic analysis of interactions between human acetylcholinesterase, structurally different organophosphorus compounds and oximes. *Biochem Pharmacol*. 2004;68(11):2237-2248. doi:10.1016/j.bcp.2004.07.038

53. Adibekian A, Martin BR, Chang JW, et al. Confirming target engagement for reversible inhibitors in vivo by kinetically tuned activity-based probes. *J Am Chem Soc*. 2012;134(25):10345-10348. doi:10.1021/ja303400u

54. Sharman J, Pennick M. Lisdexamfetamine prodrug activation by peptidase-mediated hydrolysis in the cytosol of red blood cells. *Neuropsychiatr Dis Treat*. 2014;10:2275-2280. doi:10.2147/NDT.S70382

55. Speers AE, Cravatt BF. Profiling enzyme activities in vivo using click chemistry methods. *Chem Biol*. 2004;11(4):535-546. doi:10.1016/j.chembiol.2004.03.012

56. Harsha HC, Molina H, Pandey A. Quantitative proteomics using stable isotope labeling with amino acids in cell culture. *Nat Protoc*. 2008;3(3):505-516. doi:10.1038/nprot.2008.2

57. Yang Y, Yang X, Verhelst SHL. Comparative analysis of click chemistry mediated activity-based protein profiling in cell lysates. *Molecules*. 2013;18(10):12599-12608. doi:10.3390/molecules181012599

58. Bachovchin DA, Brown SJ, Rosen H, Cravatt BF. Identification of selective inhibitors of uncharacterized enzymes by high-throughput screening with fluorescent activity-based probes. *Nat Biotechnol*. 2009;27(4):387-394. doi:10.1038/nbt.1531

59. Bachovchin DA, Koblan LW, Wu W, et al. A high-throughput, multiplexed assay for superfamily-wide profiling of enzyme activity. *Nat Chem Biol*. 2014;10(8):656-663. doi:10.1038/nchembio.1578

60. Bachovchin DA, Mohr JT, Speers AE, et al. Academic cross-fertilization by public screening yields a remarkable class of protein phosphatase methylesterase-1 inhibitors. *Proc Natl Acad Sci U S A*. 2011;108(17):6811-6816. doi:10.1073/pnas.1015248108

61. Wilk S, Orlowski M. Inhibition of Rabbit Brain Prolyl Endopeptidase by N-Benzyloxycarbonyl-Prolyl-Prolinal, a Transition State Aldehyde Inhibitor. *J Neurochem*. 1983;41(1):69-75. doi:10.1111/j.1471-4159.1983.tb11815.x

62. Hett EC, Xu H, Geoghegan KF, et al. Rational Targeting of Active-Site

Tyrosine Residues Using Sulfonyl Fluoride Probes. 2015. doi:10.1021/cb5009475

63. M. Vorobiev S, Janet Huang Y, Seetharaman J, et al. Human Retinoblastoma Binding Protein 9, a Serine Hydrolase Implicated in Pancreatic Cancers. *Protein Pept Lett*. 2012;19(2):194-197. doi:10.2174/092986612799080356

64. Woitach JT, Zhang M, Niu CH, Thorgeirsson SS. A retinoblastoma-binding protein that affects cell-cycle control and confers transforming ability. *Nat Genet*. 1998;19(4):371-374. doi:10.1038/1258

65. Shields DJ, Niessen S, Murphy EA, et al. RBBP9: A tumor-associated serine hydrolase activity required for pancreatic neoplasia. *Proc Natl Acad Sci*. 2010;107(5):2189-2194. doi:10.1073/pnas.0911646107

66. Vorobiev SM, Su M, Seetharaman J, et al. Crystal structure of human retinoblastoma binding protein 9. *Proteins Struct Funct Bioinforma*. 2009;74(2):526-529. doi:10.1002/prot.22278

67. Simon GM, Cravatt BF. Activity-based proteomics of enzyme superfamilies: Serine hydrolases as a case study. *J Biol Chem*. 2010;285(15):11051-11055. doi:10.1074/jbc.R109.097600

68. Hidalgo IJ, Li J. Carrier-mediated transport and efflux mechanisms of Caco-2 cells. *Adv Drug Deliv Rev*. 1996;22(1-2):53-66. doi:10.1016/S0169-409X(96)00414-0

69. Sambuy Y, De Angelis I, Ranaldi G, Scarino ML, Stammati A, Zucco F. The Caco-2 cell line as a model of the intestinal barrier: influence of cell and culture-related factors on Caco-2 cell functional characteristics. *Cell Biol Toxicol*. 2005;21(1):1-26. doi:10.1007/s10565-005-0085-6

70. Imai, Teruko; Masumi, Imoto; Sakamoto, Hisae; Hashimoto M. Identification of esterases expressed in Caco-2 cells and effects of their hydrolyzing activity in predicting human intestinal absorption. *Drug Metab Dispos*. 2005;33(8):1185-1190. doi:10.1124/dmd.105.004226.tion

71. Imai T, Taketani M, Shii M, Hosokawa M, Chiba K. Substrate specificity of carboxylesterase isozymes and their contribution to hydrolase activity in human liver and small intestine. *Drug Metab Dispos*. 2006;34(10):1734-1741. doi:10.1124/dmd.106.009381

72. Hosokawa M. Structure and catalytic properties of carboxylesterase isozymes involved in metabolic activation of prodrugs. *Molecules*. 2008;13(2):412-431. doi:10.3390/molecules13020412

73. Bar-Even A, Noor E, Savir Y, et al. The moderately efficient enzyme: Evolutionary and physicochemical trends shaping enzyme parameters. *Biochemistry*. 2011;50(21):4402-4410. doi:10.1021/bi2002289

74. Yang B, Hu Y, Smith DE. Impact of peptide transporter 1 on the intestinal

absorption and pharmacokinetics of valacyclovir after oral dose escalation in wild-type and PepT1 knockout mice. *Drug Metab Dispos*. 2013;41(10):1867-1874. doi:10.1124/dmd.113.052597

75. Hidalgo IJ, Raub TJ, Borchardt RT. Characterization of the Human Colon Carcinoma Cell Line (Caco-2) as a Model System for Intestinal Epithelial Permeability. *Gastroenterology*. 1989;96(2):736-749. doi:10.1016/S0016-5085(89)80072-1

76. Inoue M, Morikawa M, Tsuboi M, Sugiura M. Species Difference and Characterization of Intestinal Esterase on the Hydrolizing Activity of Ester-Type Drugs. *Jpn J Pharmacol*. 1979;29(1):9-16. doi:10.1254/jjp.29.9

77. Taketani M, Shii M, Ohura K, Ninomiya S, Imai T. Carboxylesterase in the liver and small intestine of experimental animals and human. *Life Sci*. 2007;81(11):924-932. doi:10.1016/j.lfs.2007.07.026

78. Puente XS, Lopez-Otin C. Cloning and Expression Analysis of a Novel Human Serine Hydrolase with Sequence Similarity to Prokaryotic Enzymes Involved in the Degradation of Aromatic Compounds. *J Biol Chem*. 1995;270(21):12926-12932. doi:10.1074/jbc.270.21.12926

79. Debbage PL, Griebel J, Ried M, Gneiting T, DeVries A, Hutzler P. Lectin intravital perfusion studies in tumor-bearing mice: Micrometer- resolution, wide-area mapping of microvascular labeling, distinguishing efficiently and inefficiently perfused microregions in the tumor. *J Histochem Cytochem*. 1998;46(5):627-639. doi:10.1177/002215549804600508

# CHAPTER V

## Summary

Prodrugs, latent drug derivatives activated within the body, are an essential tool for overcoming issues with the parent drug that cannot be resolved by formulation or analog generation. The best prodrug solution available will vary significantly depending on case-specific circumstances, but one piece of information is invariably crucial: the prodrug-activating enzyme (PAE) profile. Because a prodrug will not take proper effect until activation, knowing when, where, and how it is activated is central to studying its safety, tolerability, and efficacy. The first step, then, in the study of prodrug candidates should be the identification of PAEs so that one can subsequently study preclinical species orthologs for animal model selection, human pharmacogenetic variants for prediction of interindividual variability, and drug interactions with other drugs, foods, or disease states. An additional benefit is the possibility of targeted prodrugs against a given PAE by empirical or structure-based prodrug design, which could enable tissue- or cell-selective activation of toxic drugs used in chemotherapy or as antibiotics/antivirals. The prodrug strategy is typically used as a late-stage intervention to salvage failing drug candidates instead of taking a large financial loss on the investment, but identification of PAEs and subsequently characterizing them can substantially de-risk early-stage implementation of the prodrug strategy, which may represent a more favorable route to approval.

In spite of the need for PAE identification, many prodrugs are developed without this knowledge, with many instances of PAEs not being identified until several years after prodrug approval. The typical approach to PAE identification uses activity-guided fractionation, which is tedious and time-consuming. Our lab adapted a relatively recent chemical biology technique, known as activity-based protein profiling (ABPP), for faster identification of serine hydrolase (SH) PAEs by modifying the standard fluorophosphonate (FP) activity-based probe (ABP). The prodrug we focused on, valacyclovir (VACV), was approved in 1995, but the PAE biphenyl hydrolase-like protein (BPHL) was not discovered until 2003 in our lab by activity-guided fractionation from Caco-2 cells. This SH was shown by various experiments to not be obligatory for the conversion of VACV to acyclovir (ACV) *in vivo*. The commercially available standard FP ABP did not inhibit VACV activation in Caco-2 lysates, so we set out to modify the probe.

In Chapter 2, we describe the semi-rational design of this novel probe based on the observation that pan-serine protease inhibitor 4-(2-aminoethyl)benzylsulfonyl fluoride (AEBSF) abolished VACV activation in Caco-2 lysates. While direct esterification of the phenolic analog of AEBSF, tyramine, to the phosphonate group in the commercial FP ABP was not fruitful, the isobaric benzylic isomer, 4-(aminomethyl)benzyl alcohol (AMB), was successfully installed using dicyclohexylcarbodiimide in refluxing tetrahydrofuran, yielding novel AMB-FP probes. Both the alkyne and TAMRA versions of the probe were thus synthesized, whereas the biotinylated probe was unstable in storage. These novel ABPs resulted in inhibition of VACV activation at working concentrations in Caco-

2 lysate, but none of them inhibited recombinant human BPHL, suggesting that they were targeting undiscovered VACV PAEs. VACV activation was inhibited in *Bphl* knockout mice jejunum and liver lysates as well, corroborating this finding. After optimization of probe labeling conditions, in-gel visualization revealed that AMB-FP and FP probes were broad-spectrum probes, but that FP reacted with more targets and labeled them faster. Both probes labeled some targets to a greater extent than the other, and a few targets were exclusively labeled by one probe.

In Chapter 3, a competitive ABPP (cABPP) assay with VACV was developed and optimized in-gel to determine the proper time at which competition is best observed. Irreversible inhibitors such as probes reduce the free enzyme population, eventually labeling all available enzyme if present in excess and reducing to zero the signal difference between samples with and without prodrug present. Gel-based cABPP confirmed that the VACV PAEs were only present in the soluble fraction (S100) and not the membrane fraction. Once the ideal timepoint was selected, the cABPP assay was adapted to an MS-compatible format and Caco-2 cells were grown in SILAC media to label all proteins with heavier Arg and Lys isotopologs. In the assay, three SHs were identified as targets of VACV: PPME1, PPCE, and RBBP9. Fortunately, well-characterized selective inhibitors were commercially available for all candidate PAEs. Co-incubation of each inhibitor with VACV in Caco-2 S100 led to the confirmation of only RBBP9 as a VACV PAE. Emetine, the RBBP9-selective inhibitor, was also assayed in an MS-

based cABPP assay and against rBPHL, confirming that no off-target interactions were confounding the results.

In Chapter 4, the activity of RBBP9 was characterized *in vitro* and *in situ* and compared to the data reported for BPHL. Recombinant human RBBP9 was purchased and the $IC_{50}$ of VACV was assayed to show single-binding stoichiometry via fitting of the Hill equation. This justified the kinetic characterization of RBBP9 VACV activation via the Michaelis-Menten model, which demonstrated that the catalytic efficiency of RBBP9 was about half that of BPHL, with tenfold lower affinity for VACV but a roughly fivefold greater turnover rate. Then emetine inhibition was assayed in WT and Bphl-KO mouse jejunum and liver lysates, where the data indicated that RBBP9 and BPHL are essentially the only VACV PAEs in those tissues. In the liver, BPHL and RBBP9 both comprised about half of the total activity each. In the jejunum, which had under 40% of the total liver activity, three-fourths of the activity was attributable to RBBP9. In the knockout tissues, virtually all the activity was due to RBBP9. Subsequently, single-pass intestinal perfusions were carried out in mice with and without emetine pre-perfusion and demonstrated significant reduction in portal vein activation of VACV, resulting in >50% increase in unactivated prodrug levels.

Taken together, all the preceding results imply with high likelihood that RBBP9 is involved in the *in vivo* disposition of oral valacyclovir as a presystemic PAE and plays a pre-eminent role in the gut and a major role in the liver. These two enzymes, in wildtype individuals, are likely to be the only two presystemic VACV PAEs though others are still not able to be definitively ruled out pending

further experiments. Incidentally, VACV represents the first reported substrate of RBBP9 and hopefully can serve as a starting point to discover more substrates, especially endogenous ones. Future directions with respect to this enzyme include the aforementioned studies: characterization of interspecies differences, pharmacogenomic variability, drug interactions, and substrate-activity relationships. Beyond this enzyme, the broader application of cABPP as a tool for PAE identification might be very useful, particularly in cases where rudimentary reaction phenotyping methods cannot identify individual PAEs. This concept extends beyond the SH family and could be useful for PAEs belonging to other hydrolase families and many other mechanistic enzyme subclasses with well-developed suites of ABPs. We hope that the ensuing discoveries, by broadening and deepening the understanding of molecular physiology and de-risking early-stage prodrug ventures, greatly benefit prodrug discovery and development efforts in academia and the pharmaceutical industry.